UNIVERSITEIT GENT

FACULTEIT WETENSCHAPPEN
Vakgroep **Geologie en Bodemkunde**

Analysis and modelling of tree succession on the 1991 Randa rockslide (Switzerland).

Liesbet Van der Burght

Academiejaar 2009–2010

Scriptie voorgelegd tot het behalen van de graad
Van Master in de Geologie

Promotor: Prof. Dr. F. Mostaert
Co-promotor: Dr. M. Stoffel
Leescommissie: Prof. Dr. P. Jacobs, Prof. Dr. J. Nyssen, Prof. Dr. P. Goetghebeur

Judging from the surprised looks on the faces of some people and the moderate enthusiasm of others, this thesis subject might not have been the most logical choice for a Belgian geology student, with only minor background knowledge on Alpine geology and dendrochronology. Personally however, I have always seen studying abroad as a major advantage in many aspects of life, an experience worth to be stimulated. Moreover, I have always been fascinated by the Alpine geology, and even when a couple of months and a lot of interest are most certainly not enough to understand all aspects of it, nor to grasp its full complexity, I found my passion even more awakened and stimulated.
As so, this thesis subject has always seemed a very sensible choice to me, and despite the numerous administrational, meteorological, lingual, and logistic problems, I would most happily make the same choice tomorrow.

I would like to thank my parents and grandmother, I'm sure it wasn't always easy to them to see their only child roam off again, nevertheless they have always been uttermost supportive. A warm and grateful word also to Charlotte and her family in Gasenried, and to Georgette in Stettlen, for indulging and taking care of me, as if I were their own daughter.
Michelle and Markus, thanks for giving me the opportunity to work on this subject and for being an incredible support and motivation, again and again and again! Christof, thanks for the time and effort you put into explaining me statistical methods, all of your suggestions were very much of use. Prof. Mostaert, thanks for your support, critical point of view and honest fascination. A grateful word also goes to Igor, Estelle, Dirk, and Valentin.
And finally, Lina, Oliver, David, Glenn, and Ben, thanks a lot for your support and helping out whenever possible.

Foreword

1 Introduction

1.1 Natural hazards in the Alps

The Alpine geomorphology is moulded by the remains of hazardous events. Landforms resulting from debris flows, rock fall activity, and rock slides are numerous. During recent years, the number of such events seems to increase (Bloetzer et al., 1998). In general however, no systematic data acquisition for these processes exists, whereas especially in this respect it is of importance to understand process characteristics in space and time, in order to structure risk and hazard management. In addition, the acquired data might improve our understanding towards the causes of these processes, and their possible interaction with climatic variations. Having in mind the relevant time span to study these processes, which is rather short, it is of importance to use appropriate dating techniques of high resolution.

In 1991, a rockslide destroyed the hamlet of Unnär Lerch, which is part of Randa, a village in the Swiss canton of Valais. Fortunately, the rockslide made no victims. However, the valley main road, Vispa riverbed, cogwheel trail and some ten stables and holiday chalets were completely destroyed. Some livestock got killed and at several places in Randa up to 50 cm of dust were measured. The atypical nature of the rockslide, that continued in several phases, prevented further damage (Truffer, 1995). Ever since, the scenery of Randa has become dominated by the talus cone, stretching from approximately 1300 to 1500 m a.s.l., as it was decided by the cantonal government to leave the deposit intact in order to use it for scientific research. With time, the rock slide surface stabilised, and afforestation could start. In 1995 a first study conducted on the deposit, showed that pioneer tree species such as larches and birches already managed to colonise distinct regions of the deposit (Gasser, 1995). Figures 1 and 2 give an impression of the rockslide area today.

1.2 Aim of this study

The geomorphology of the Matter Valley, where the village of Randa is situated, is dominated by several rockslide deposits. These and other deposits resulting from hazardous processes are marked on the satellite image of Appendix D (p.99). Only for the historically documented rockslide deposits (which are few, 2 out of 43) (Truffer, 1995), information on the age is known. Therefore, the recently formed deposit in Randa, might lead to a better understanding of rockslide characteristics, and may provide a possibility to determine the age of other similar deposits by means of dendrochronology. No studies whatsoever have been conducted concerning primary succession on rockslide deposits, which gives this study a pioneering status.

Thus, it is the aim of this research to study tree growth and density distribution of various tree species. The most attention will go to larches (*Larix decidua*), birches (*Betula pendula*) and spruces (*Picea abies*), and to mapping of the substratum. By means of counting bud-scale scars and growth rings on larches, as to determine their age, primary succession and colonisation rates will be studied. An attempt will be made to retrieve a reliable age determination for surface stabilisation. The scientific accuracy of the former method is not yet confirmed, and will be tested in this research. Also, we will try

to explain variability in tree height and density by conducting statistical analysis on several environmental parameters.

A precise description of the study site allows the reader to gain insights into regional geography (p.9), and geomorphology (p.10), and underlines the constraints of climate (p.11), soil (p.13), and vegetation (p.13). A large section is devoted to the general Alpine geology (p.15), with specific attention for the Penninicum (p.15), as this is the region were Randa is situated. Also, detailed information on the 1991 rockslide event is given (p.23), with a related appendix containing pictures that manage to transmit the atmosphere of those days rather well (p.103). A few words concern the present research around the scarp area (p.30), conducted by a group of researchers of the *ETHZ*.
Background knowledge on dendrochronological principles (p.33) and primary succession (p.35) was gained and is described in the literature study (p.32). In addition, information on the prevailing tree species is provided (p.36). Further on, a description of a previously conducted vegetational study is presented (p.47), briefly stating the used methods (p.47) and relevant results (p.48).
The methods used in the field, and for sample gathering and preparation are described (p.49), as are the statistical methods used for data processing (p.56).
In the following section, results considering the grain size distribution (p.61), bud-scale scar age determination accuracy (p.62), primary succession and larch colonisation (p.63), tree abundance and density (p.68), and tree growth (p.78) are collected. Finally, the obtained results are discussed and compared with data obtained from other research (p.81). A Dutch abstract is added as well (p.86).

Fig 1. An impression of the eastern boundary of the Randa rockslide deposit and the Vispa river *(LVdB)*.

1.3 Cooperation with Swiss researchers[1]

For this study, cooperation with the university of Berne (*Unibe*) and the *Eidgenössische Technische Hochschule* in Zürich was established. Field work and data analysis were supervised by Dr. Markus Stoffel (*Unibe*), Dr. Michelle Bollschweiler (*Unibe*), and Dr. Christof Bigler (*ETHZ*).

Being the head of the Laboratory of Dendrogeomorphology (Dendrolab) and senior lecturer at the lab since its start, Markus Stoffel is specialised in mass-transfer processes in mountain regions (debris flows, rockfall, snow avalanches, flooding), activity of geomorphic processes and landscape evolution, magnitude–frequency relationship and dynamics of mass movement processes, tree-ring dating of geomorphic processes (dendrogeomorphology, dendroecology), and alpine meteorology (precipitation, threshold exceedances, extreme events, climate change). Fields of specialisation of Michelle Bollschweiler, who is research assistant at the lab since April 2003, are wood anatomy, natural hazards, and study of mass movements (debris flows, floods, lahars, snow avalanches).
The Dendrolab was founded in July 2000 upon the initiative of Markus Stoffel at the University of Fribourg. Since 2009, the Dendrolab is affiliated to the Institute of Geological Sciences at the University of Berne. The Dendrolab is also currently employing three PhD students. In addition, four PhD students from Spain, France, and Austria, as well as a PostDoc from Argentina are currently realising part of their tree-ring analyses at the lab. Eight students are preparing their Master's and Bachelor's thesis under the guidance of different lab members. Therefore, the Dendrolab constitutes one of the largest institutions worldwide focusing on the appraisal of past geomorphic processes and events based on information contained in tree-ring series.
Tree-ring reconstructions of geomorphic processes (such as debris flows, flooding, rockfall, snow avalanches, landslides, erosion) are performed with conifer and broadleaved species. Dating of events is based on the presence of injuries, changes in the anatomical structure of tree rings as well as on abrupt changes in growth. Data obtained are used by local communities and the mandating cantonal authorities for the assessment of frequencies and magnitudes of past events. Besides the application of well-known methods, the members of the lab are also performing fundamental research in order to test new applications and to elaborate better and more efficient techniques for the identification of geomorphological signals in tree-ring series.

The ETH tree-ring laboratory was established in 2006, and is now directed by Dr. Christof Bigler. The lab is part of the Chair of Forest Ecology at *ETH* Zurich.
The research at the lab focuses on dendroecological studies: tree rings are used to study forest dynamics such as regeneration, growth and mortality processes, and the effects of climate and natural disturbances on trees, forests and landscapes are investigated. Our goal is to improve the understanding of ecological processes, particularly in mountain forests, and to use tree rings to develop, improve and validate empirical and process-based models of trees and forest ecosystems. Christof Bigler investigates spatio-temporal processes of stand dynamics of forests, with a particular interest for growth and mortality processes of individual trees and forest stands as well as the impact of natural disturbances (e.g., fire, insect outbreaks and drought) on processes of stand and landscape

[1] *Modified from www.dendrolab.ch and www.ethz.ch*

development. Current projects are climatic and topographic impacts on mortality processes of mountain pine in the Swiss National Park, changes in litter and dead wood loadings following tree mortality of subalpine conifer species in northern Colorado, relationship between growth rates, site characteristics and longevity of trees, influence of site characteristics and climate on tree growth.

Fig 2. Aerial photograph of the study area *(Google Earth, 2010)*.

2 Study site description

2.1 Regional geography

The village of Randa (1406 m a.s.l.) is situated in the Matter Valley, in the Upper Valais (which is the eastern, German speaking part of the canton of Valais). The Valais is situated in the southwest of Switzerland (Fig 3), bordered in the south by France and Italy, in the north by the cantons of Vaud and Berne, and in the east by the cantons of Uri and Ticino (see Appendix A, p.96). According to the SOIUSA classification (Marazzi, 2005), the canton of Valais is clenched between the Bernese, Pennine (or Valais) and Lepontine Alps (see Appendix B, p.97), which results in a very distinct climate. Geomorphologically, it is dominated by the wide, glacial Rhone Valley, stretching from Gletsch (see Appendix A, p.96) in the east to the glacial Lake Geneva in the west, of which several side valleys branch off. One of these is the Visper Valley, stretching from Visp to Stalden, where it splits into the eastern Saaser Valley and the western Matter or Nikolai Valley (see Appendix C, p.98). The valley is named after the river Vispa (fed by its Saaser and Matter branches), that flows into the Rhone near Visp. As the Rhone Valley, it is mainly shaped by glacial and post-glacial processes (Schindler et al., 1993). Travelling through the Matter Valley, passing the main municipality of St. Niklaus (hence the name Nikolai Valley), we arrive at Randa, situated between the villages of Herbriggen and Täsch, some 19 km inward the valley (see Appendix C, p.98). The picturesque chalets of Randa are clenched between the steep mountain flanks of the Dom (4545 m), Bishorn (4153 m), Brunegghorn (3833 m), Nadelhorn (4327 m), Täschhorn (4491 m) and Weisshorn (4506 m), some of the highest mountains of the Alps. The view on the valley is therefore characterised by high altitude differences, up to 3300 m, over short distances (approximately 6 km). The village is built on the debris cones of the Wildibach and Dorfbach, two small, intermittent mountain streams, fed by the melting waters of respectively the Kin and Festi glaciers. Both torrent channels are reworked by debris flows at regular intervals (Bloetzer et al., 1998). Other rather small torrents feeding the Vispa river near Randa, are the ones streaming down the Rosszügji, Schusslauizug, and Bisbach, respectively fed by the melting waters of the Ross, Schmal and Bis glacier.

The 1991 Randa rockslide deposit is situated on the northwest of Randa and covers a horizontal area of 68,25 ha (Truffer, 1995). It stretches from about 1300 m to 1900 m a.s.l.

Fig 3. The canton of Valais, marked red on the map of Switzerland. The black arrow points out the location of Randa *(Wikipedia, 2005)*.

2.2 Geomorphology

The geomorphology of the Randa region mostly results from glacial and post-glacial processes. The valley has got it characteristic shape from glacial erosional processes (Schindler et al, 1993). For geological reasons that will be explained further on, the western valley flanks are considerably steeper than the eastern. The original post-glacial valley form has been modified by several debris cones. Near Randa, those of the previously named Wildi- (Fig 5) and Dorfbach especially catch the eye.

Other commonly seen geomorphic features are zones of sagging. A sagging is a form of settlement independent from the pressure of topping layers, that can often be seen in Alpine valleys or on steep slopes (Burri, 1992). The upper part of the sagging tends to be characterised by a depression, whereas the lower part tends to be characterised by an elevation (see Appendix E, p.100). Geomorphologically, there are some analogies with landslides; the dynamics of both processes however are completely different. Unlike a landslide, a sagging is a slowly developing process (cm to dm per year). Also, part of the rocks undergo a turnover (in this case a rotation round a near-horizontal axe), which is not seen in landslides. Saggings can be found as well in consolidated as unconsolidated rock. Their origin has to be sought in a changing ground water level and / or a change in stress (e.g., when a steep flank loses the support of a glacier). A zone of sagging can be seen just south of the scarp (Fig 4), which acted passive during the rockslide event. If the scarp would have reached slightly higher up into this zone, the cubature would have been a lot larger, since a fairly large instable area would have been entrained (Schindler et al., 1993).

Fig 4. View from the *Europawegbrücke* towards the Weisshorn. Encircled is the instable zone of sagging above the rockslide scarp *(Oliver Fux)*.

Fig 5. Stapled lines mark the shape of the debris cone of the Wildi bach *(LVdB)*.

The most expressed feature clearly is the rockslide deposit to the northwest of the village. Rockslide deposits are generally rather flattened and tend to cover large areas (Erismann & Abele, 2001). Due to its atypical nature however, the Randa rockslide deposit covers a fairly small area, when taking into account the released cubature, and therefore has a rather steep slope (Truffer, 1995).

After the rockslide event it was point of discussion whether to remove or not remove the deposit. The villagers preferred using the rocks for construction sites, ultimately freeing the covered agricultural space, whereas the cantonal government saw a more scientific destination for the deposit. The canton managed to press its ideas, recently however, broaching of the rocks as to use them for construction has started in several regions of the deposit.

Another feature that developed shortly after the rockslide event was the earlier mentioned lake, resulting from the damming of the Vispa. A lake in the driest valley of Switzerland might of course seem appalling on first sight, but the disadvantages for the local people could not outweigh the touristic advantages, and so the bed of the Vispa was cleared again.

2.3 Climate

The Matter Valley is clenched between the Bernese and Pennine Alps, orientated perpendicular to the main chains of both. This explains the continental character of the region, with an extremely low average amount of rainfall, due to the created rain shadow. For Randa, the main chain of the Pennine Alps, which reaches above 4000 m a.s.l. near Zermatt and protects the valley from most external weather influences, is of most importance (Bloetzer et al., 1998).

For the region of the Visper Valleys a difference in mean rainfall between both valleys and from north to south can be observed. Bloetzer et al. (1998) mention an average value of 855 mm, measured for the village of Saas Fee in the east, compared to a mere 710 mm for Zermatt more to the west. As for the north-south distribution, they speak of a tendency towards higher values inward the valley (562 mm for Grächen and 529 mm in Stalden). The mild temperatures and low amount of rainfall in the Nikolai Valley imply short and mild winters, compared to other alpine regions. The valley floor only tends to be snow covered from December until March (Bloetzer et al., 1998).

Because of the higher southern tops, the Matter Valley is less favourable for foehny conditions, as they occur in the Saaser Valley (Bloetzer et al., 1998). The foehn wind is a dry down-slope wind which occurs in the lee side of a mountain chain. It's a rain shadow wind which results from the subsequent adiabatic warming of air which has dropped most of it's water on windward slopes. As a consequence of the different adiabatic lapse rates of moist and dry air, the air on the leeward slopes becomes

warmer than the air at equivalent elevations on the windward slope. Therefore, when these conditions do occur in the Nikolai Valley, they can result in a quick substantial temperature raise. This has a strong influence on the snow covering in the lower valley parts. The distinct climate has an important influence on the growing season, that does not start before June and ends early in October (Stoffel et al, 2005).

Figure 6 shows the average climatic conditions from 1961 to 1990 in Zermatt, the nearest measuring point of the governmental Swiss weather service. Since 2008, a weather station is operative in Randa as well, however due to the recent beginning of measurements, no reliable mean values could be retrieved.

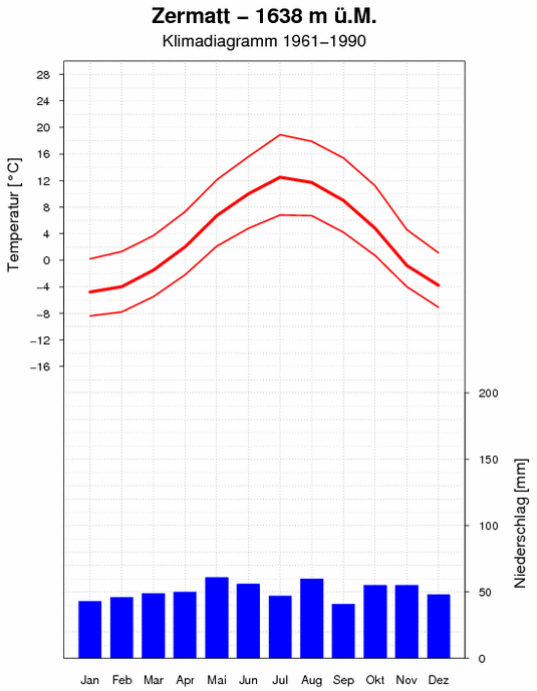

Fig 6. Monthly mean values of maximum, daily mean and minimum temperatures (red), and monthly mean rainfall (blue) *(Meteoschweiz, 2004)*.

It is certainly of importance to underline that in the rockslide area even more specific conditions prevail (compared to the rest of the valley), as could be observed during fieldwork. Due to the size and position of several blocks, (rather small) snowy patches can be found - even at valley floor level - until May. The harsh winters of 2009 and 2010 caused several snow avalanche deposits near the rockslide deposit to prevail in the valley floor until late spring. The scarp area itself repeatedly became snow covered. The large blocks that can be found on the deposit also create large shady and moist areas, much wanted environments for several plant species. In addition, albedo effects of the rock-dominated and vegetation-lacking surface have an important influence on the ranging temperature, that tends to be higher than elsewhere in the valley ground near Randa.

2.4 Soil

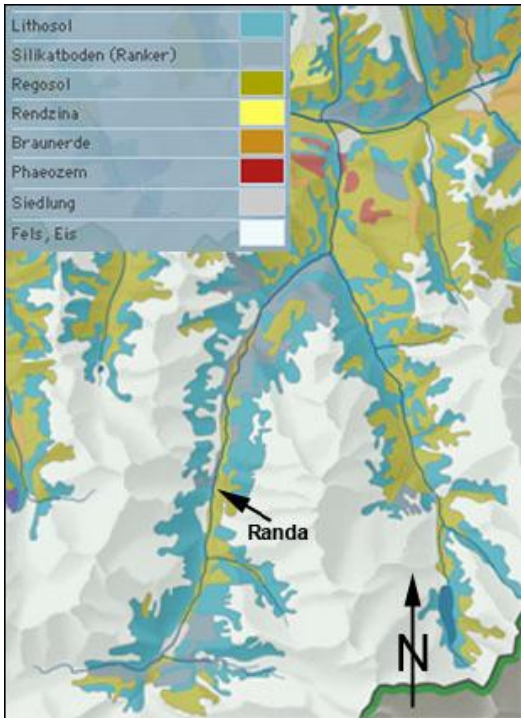

The abundance of silicate rocks in the Matter Valley leads to the establishment of clayey soils, generally with lime deficiency. The influence of the host rock tends to be large where soils are shallow or at dry spots. At sun exposed places we find slightly acidic cambisols (beginning soil formation, weak horizon differentiation), that tend to be rich in humic material. Shady spots show brown podzolic soils, rich in humus. The dry climate and high continentality cause leaching of the soil and a water deficiency during the growing season, which results in a top layer rich in leaf mould. Near Randa, we find mainly podzolic cambisols and silicate regosols (Gasser, 1995), as can also be seen in figure 7.

Fig 7. Map of soil types in the Matter Valley *(Atlas der Schweiz, 2004)*.

2.5 Vegetation

The Valais is the most species rich canton of Switzerland. About 1800 different plant species have been observed. In terms of geographical zonation, the canton is situated at the southern rim of the subtemperate zone, and borders on the submeridional zone (Gasser, 1995). As it is situated in the central region of the Alps, containing the highest peaks, high mountain plants are numerously represented. Due to the previously mentioned lime deficiency, silicate plants are most common. Since the Central Alps were (apart from the highest peaks) fully covered in ice during the ice ages, only few endemic species exist. At higher altitudes, where temperatures are lower and the climate is more continental, we find mainly pines and several *Erica* species, which immediately border on the subalpine woods with larches and Swiss stone pines. Typical for the Valais are the steppe grasses, which seem to suit the dry climate extremely well (Schubbiger-Bossard, 1998).

2.6 Geology

2.6.1 Alpine Geology[2]

The Alps were formed due to the collision of the European and African Plates. During this process several microplates and ocean troughs were formed, that all went through their own distinct evolution. This justifies the division of the Alps in three geological zones or nappe stacks: (1) the External Zone, which is the northern outer rim, that shows only minor deformation, (2) the Internal Zone, showing the strongest deformation, (3) the Eastern and Southern Alpine zones, nearly undeformed and part of the African Plate (the latter having no outcrops in Switzerland, and will therefore not be further discussed) (Fig 8). The common terms used in Switzerland are respectively (1) Helvetic zone or Helveticum, (2)

[2] *Modified from Burri (1992).*

Penninic nappes or Penninicum, and (3) the Austroalpine or Eastern Alpine nappes. Of these nappe stacks, the Penninic nappes have the highest metamorphic grade. They contain highly metamorphic rocks of different palaeogeographic regions. In Switzerland, the boundaries of these geological zones are orientated roughly northeast-southwest (Fig 8). The Helveticum is the area to the north of the Rhone, that stretches far beyond the boundaries of the cantons of Vaud and Berne. The Penninicum is situated south of the Rhone, and as well are the Eastern Alpine nappes. The latter only showing in the Valais, under the form of a klippe or outlier (Fig 9).

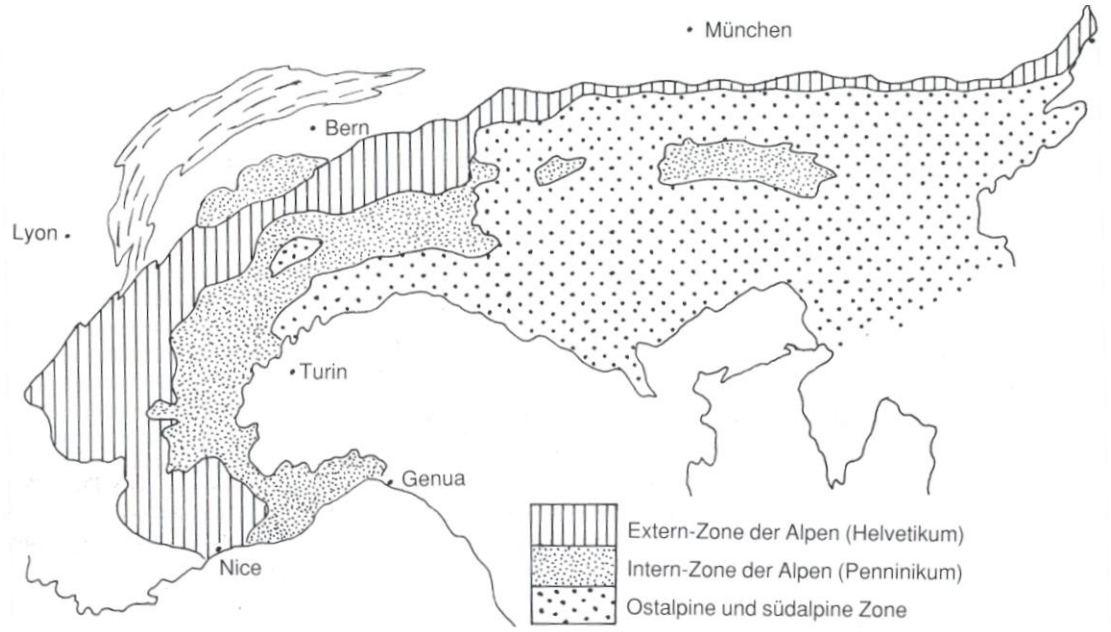

Fig 8. Tectonic units in Switzerland *(Burri, 1992)*.

In the Helvetic Zone, the boundary between the pre-Jurassic basement and the Jurassic sedimentary deposits is rather clear. The sedimentary rocks are arranged in large folds, have been displaced towards the north and are densely packed. Towards the northwest, near the Jura, the Helveticum changes into even more external regions, where the European Plate remains undeformed. In the southeast, the Helveticum is covered by the Penninicum, and the tectonic style changes completely. The basement and sedimentary rocks are deformed together, which results in complex and chaotic structures. In addition, the rather complex geological structures are further moulded by a highly variable topography. The sedimentary rocks of the Eastern Alpine zone, which shows as the rim of the African Plate again a less complex structure, were moved over the Penninicum. The only remaining trace in Switzerland is the outlier of the Dent Blanche nappe.

Figure 10A shows a simplified tectonic image of the pre-Alpine region during the Jurassic. The sedimentary rocks of the Helveticum and the Eastern Alpine zone are deposited on granitic-gneissic basement rocks. The situation is different for the Penninicum at the southern border of the European Plate. The sedimentary rocks partially cover granitic-gneissic continental basement rocks and partially oceanic crust, that had developed between the European and African Plates. At the beginning of the Jurassic these plates were joined into one large continent, Pangaea. This major continent however fell apart and an ocean developed in the future Alpine region, called the Valais Trough. This trough was

bordered with undeep seas and rows of islands. The Penninicum of the Valais Alps will now be discussed in more detail, since this is the region were Randa is situated.

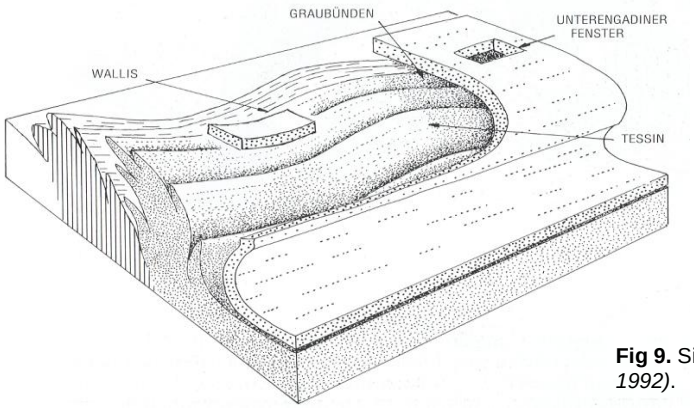

Fig 9. Simplified Alpine tectonics *(Burri, 1992)*.

2.6.1.1 Penninic Palaeogeography[3]

In the Valais Alps, four palaeogeographic domains can be recognised. (1) A zone consisting of rocks that belonged to the former European continental margin, that were subducted and obducted again. (2) A zone consisting of rocks of the continental crust of the Valais Ocean (or Through), also including metamorphosed ophiolites and other sedimentary rocks from this ocean basin. (3) Zones consisting of rocks of the Brianconnais microcontinent. These are rocks from the lower crust, deformed and intruded by Variscan granites, and also sedimentary rocks (graphite-bearing Carboniferous rocks, red sandstones from the Permian period, Triassic evaporites and thin limestones of the Jurassic and Cretaceous). Examples of the Brianconnais Terranes are the Sankt Bernhard and Monte Rosa nappes. (4) A zone consisting of rocks from the former Piemont-Liguria Ocean. These are mainly ophiolites, limestones (metamorphosed into marbles) of the shallower zones and deep marine mudstones. From the Cretaceous onward, the crust of the Piemont-Liguria Ocean subducted at the trenches at the northern edge of the Apulian Plate (see Appendix G, p.102).

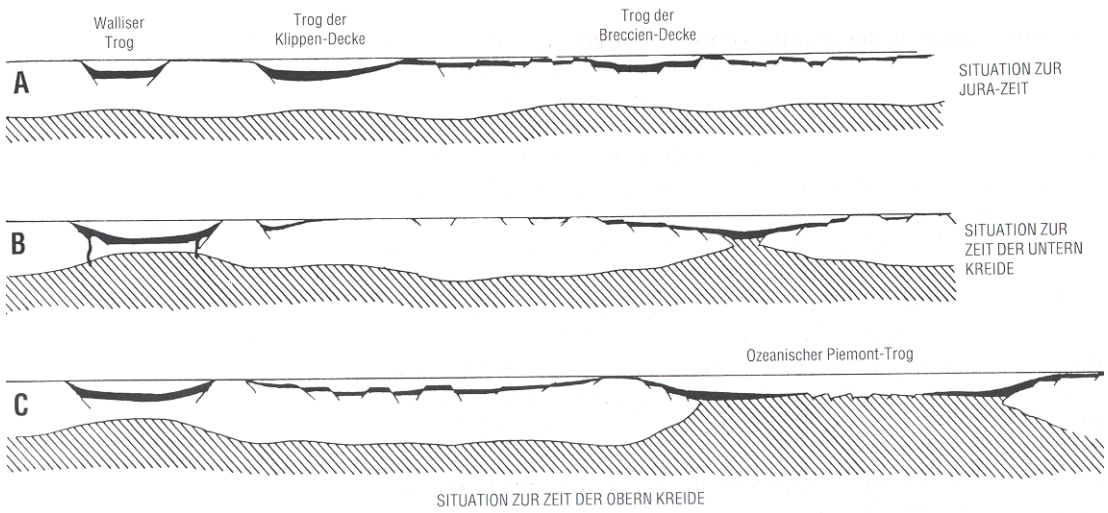

Fig 10. Ocean throughs *(Burri, 1992)*.

[3] *Modified from Burri (1992) and Pfiffner (2009).*

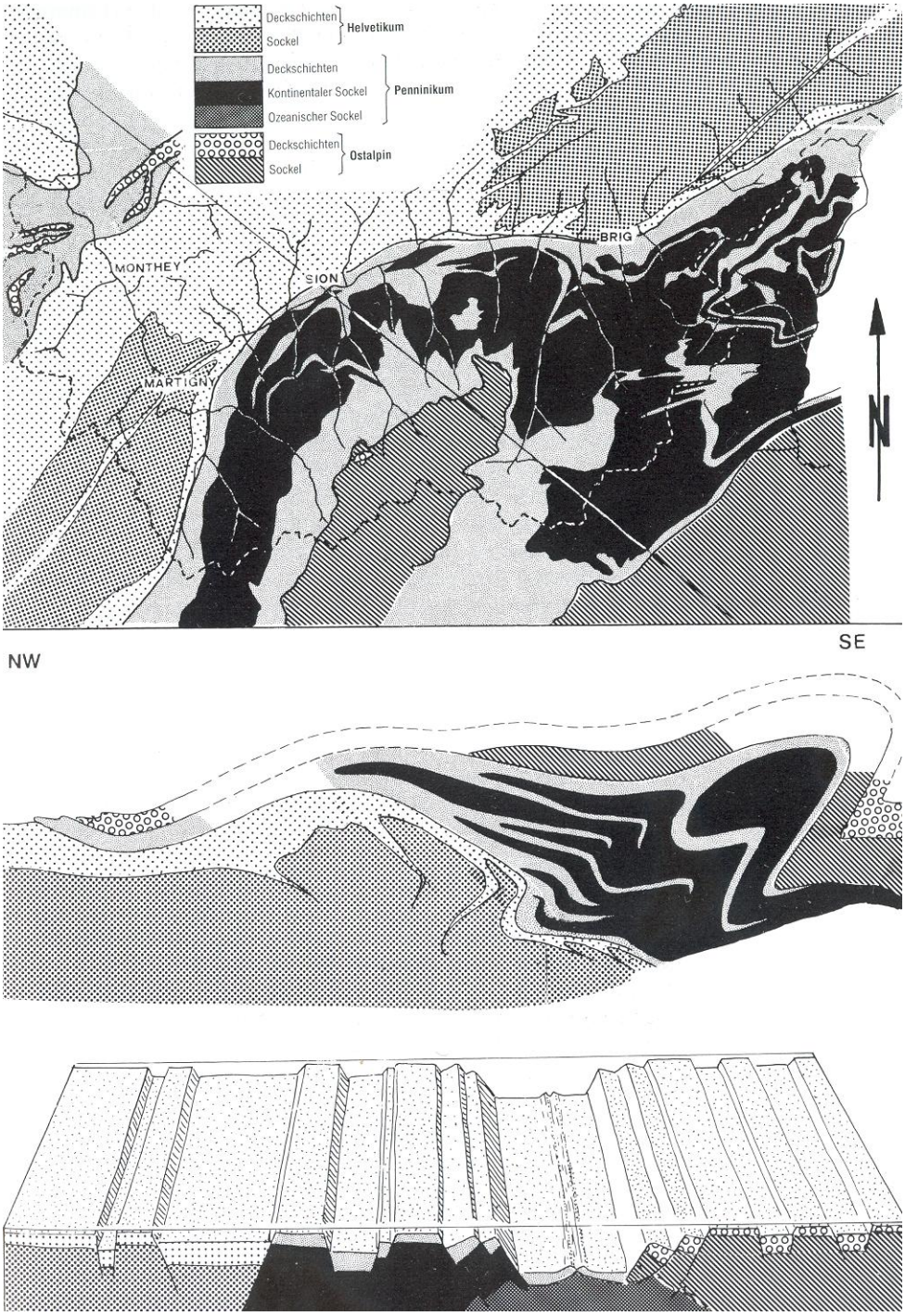

Fig 11. The geology of the Valais Alps represented in a map and profile. The block diagram shows their palaeogeography, uninfluenced by the Alpine folding *(Burri, 1992)*.

2.6.1.2 Penninic basement[4]

The oldest gneissic rocks are metamorphosed older sediments, lava and granite (Fig 13). These are the major components of the basements of the Pontis- and Siviez-Mischabel nappes, as is shown in the palaeogeographical profile of figure 12. Embedded in the gneiss we find large granitic masses. Whenever these are also metamorphosed to gneiss, they are called Randa gneiss (after the village of Randa, where they were first described). Permian sediments were deposited on top of the gneiss and granite. These sediments once consisted of sand and pebbles, can now be seen as sandstone and conglomerates, of very variable thickness. The sediments were intruded by basaltic and rhyolithic magmas.

Fig 12. Randa gneiss *(LVdB)*.

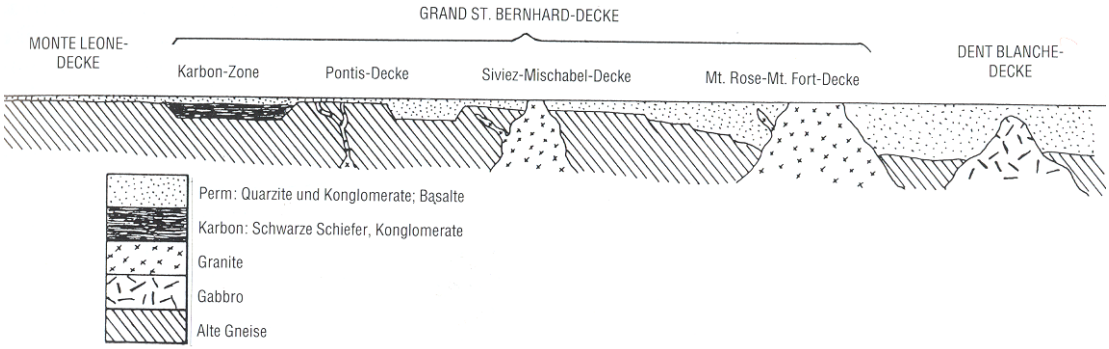

Fig 13. Profile of the Penninic basement, uninfluenced by Alpine folding *(Burri, 1992)*.

2.6.1.3 Penninic sedimentary rocks[5]

In the beginning of the Jurassic, tension caused Pangaea to split, so that long and narrow basins could form. During the Triassic, the region was an undeep sea, where sands were deposit (that were transformed into bright quartzites during the alpine orogeny). Subsidence lead to the deposition of chalk instead of quartz. At the same time, the topography of the region changed and the once uniform zone was divided into several basins, that slowly deepened individually. Given this configuration, enormous deposits could form under the rather shallow waters. These very thick deposits (several hundreds of meters) were named Pontis chalk. Thin deposits formed at the relatively undeep parts between the different basins. Several times under conditions that gave way to the formation of evaporites, such as at the gypsum formations that can now be seen in Nax and Gebidem (see Appendix A, p.96). During the Jurassic, the movement of the continents continued and high rates of sedimentation continually occurred in two separate basins. These were the basins of the *Klippen-*

[4 & 5] *Modified from Burri (1992).*

Decke and the *Breccien-Decke*. Both contain the for the deep sea characteristic chalky and marley sedimentation. The sedimentation in these basins continued into the Tertiary. The extension of the crust continued during the Jurassic and the beginning of the Cretaceous, so that two seas could develop towards the north and south of the two previously mentioned basins. In the north there was the Valais Trough, with very distinct conglomerates: enormous quartzitic blocks (that are assumed to have fallen from cliff coasts). Also some basalts intruded the thinned crust. In the south, the Piemont Trough finally formed the breach between the African and European Plates. The continental crust ended and basalts of a new oceanic crust were formed. A rock typical for the Penninic troughs is *Bündnerschiefer* (also known as *schistes lustrés*).

The chalk and basalts of the Penninicum were metamorphosed into marbles and greenstones. Only the deposits from the *Klippen-* and *Breccien-Decke* were not metamorphosed (see Appendix F, p.101).

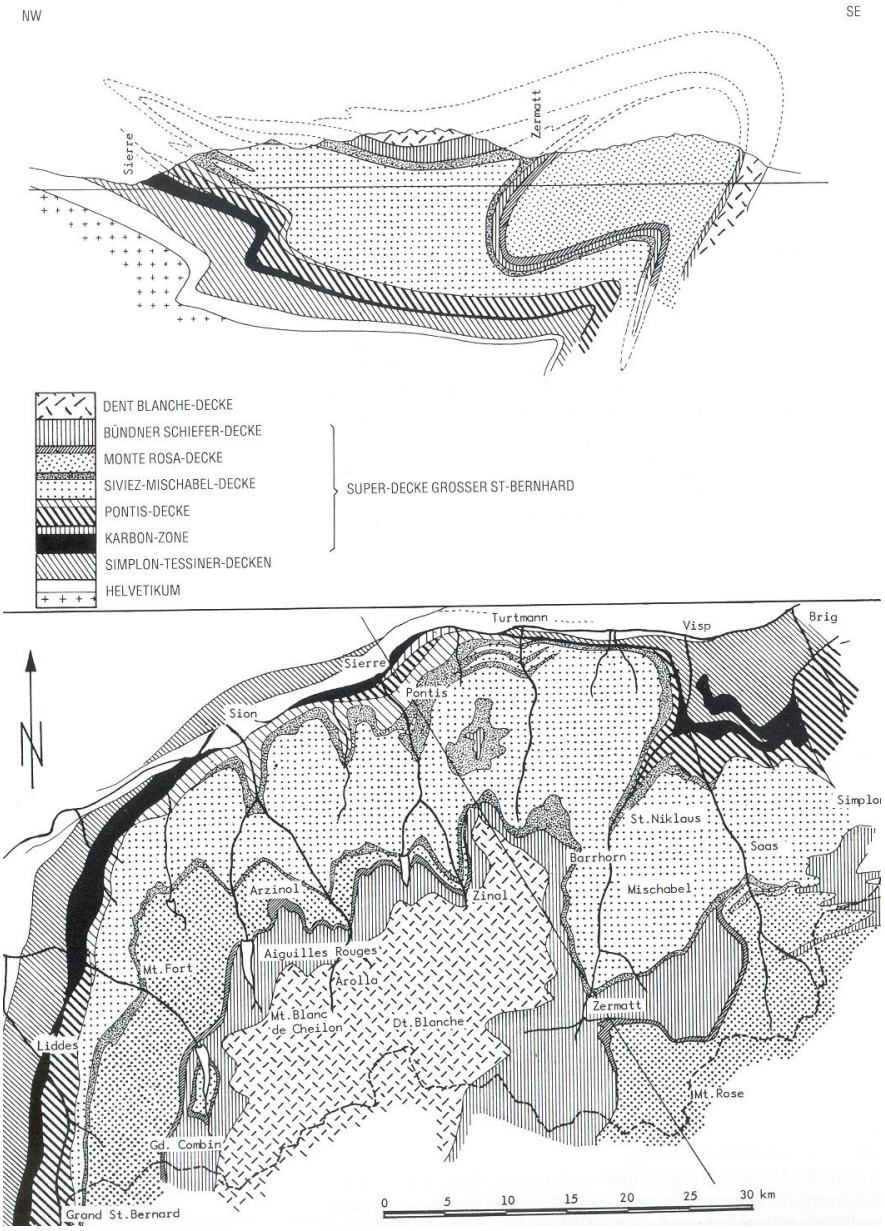

Fig 14. The nappes that build the Walliser Penninicum *(Burri, 1992)*.

2.6.2 Folding[6]

The folding of the Alps started 65 Ma ago in the south and ended 25 Ma in the Molasse basin. The folding process is simplified depicted below by means of six sketches (Fig 15).

1. The situation before the beginning of folding (Early Cretaceous, 145.5 – 99.6 Ma). The pre-Alpine palaeogeographical region is characterised by a succession of throughs, that are separated from one another by shallow seas, islands and microcontinents. These throughs all formed on a continental crust, apart from the Piemont Through which has an oceanic (basaltic) crust.
2. Late Cretaceous (99.6 – 65.5 Ma). The African Plate moves towards the European Plate and the crust deforms. The Piemont Through with its thin oceanic crust disappears under the Eastern Alpine zone. Folding starts in the central regions. The Helveticum is lifted and a continental deposit is formed (the Siderolithicum).
3. The southern part of the European Plate subducts under the Eastern Alpine zone. 40 Ma ago, when the Helveticum was flooded again, the Penninicum might have partially lifted, causing the displacement of the Ultrahelveticum into the Helvetic Basin.
4. Culmination of the Alpine folding 38 Ma ago. The Penninicum is subducted under the Eastern Alpine zone, its complex structures stay intact, and the formations are intensely metamorphosed. At this point the *Klippen-* and *Breccien-Decke* are already displaced, since these do not show signs of the intense metamorphosis.
5. 32 Ma ago, the Helvetic sediments are deposited. Their most southern parts, which form the Simplon-Tessin nappes, are already subducted underneath the Penninicum. In the small sea before the Helvetic uplifted regions, the deposition of flysch (sediments deposited in rapidly narrowing seas in the foreland of developing mountain chains; a rhythmical deposition of breccia, sandstone and schiefer) comes to an end, and the deposition of molasse (sediments deposited in the fore- or backland of developing mountain chains: conglomerates, sandstone, marl and clay) starts.
6. A large deformation causes roll back towards the south, which severely changes the tectonics of the southern chains (*Mischabel Rückfalte*; see Appendix F, p.101). Between 30 and 20 Ma the high peaks (up to 6000 m) of the Alps are lowered by intense erosion. The eroded material is deposit in the Molasse basin. 20 Ma ago the Ultrahelveticum (including the topping *Klippen-* and *Breccien-Decke*) took its final position on the recent molasse deposit.

[6] *Modified from Burri (1992).*

Fig 15. Pictures representing the Alpine folding, as described in section 2.6.2 *(Burri, 1992)*.

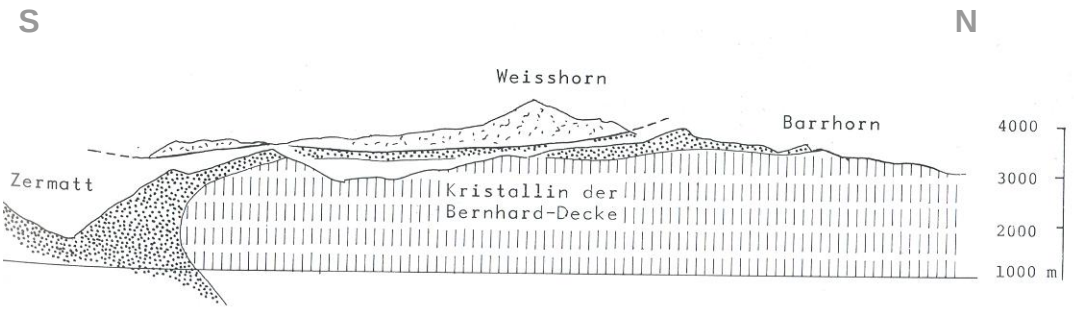

Fig 16. Profile Nikolai Valley: the Bernhard nappe basement (stapled), the Bernard nappe sedimentary units (dotted), and the Dent Blanche nappe gneisses (speckled). The fold towards the south is the *Mischabel Rückfalte (Burri, 1992)*.

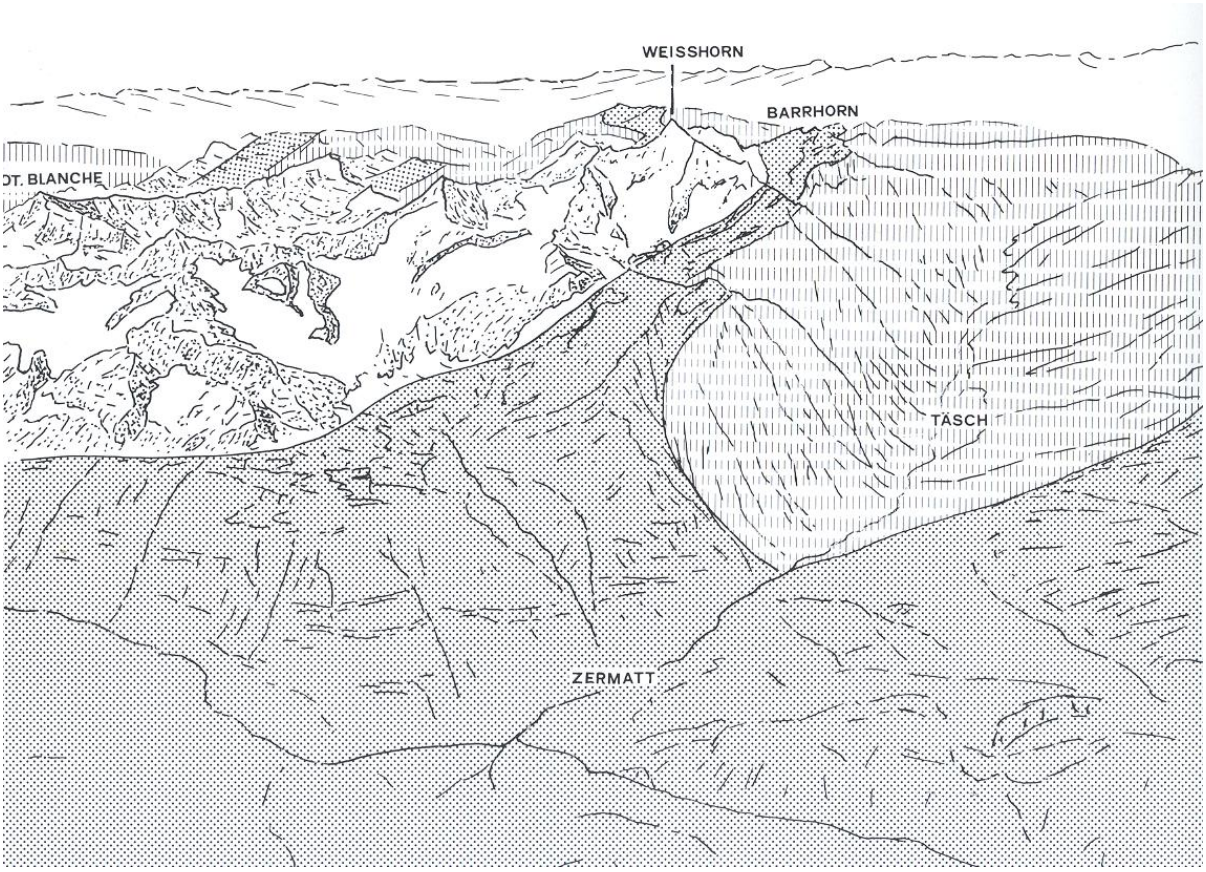

Fig 17. Geology of the Mattertal: the Bernard nappe basement (stapled), the Bernard nappe sedimentary units (dotted), and the Dent Blanche nappe gneisses (speckled). The fold between Täsch and Zermatt is the *Mischabel Rückfalte*. Randa is situated just north of Täsch *(Burri, 1992)*.

2.6.3 Local Geology[7]

The rockslide area is situated in the crystalline core of the penninic Siviez-Mischabel nappes (part of the Saint Bernard nappes, see Fig 14, 16 and 17). The valley flank at the bottom is made up of pale grey slightly schistous augengneiss (from now on referred to as the previously mentioned Randa gneiss), which was thus originally a variscan granite intrusion. Higher up, very schistous brownish weathering paragneiss with layers of amphibolite and flattened granite intrusions can be seen (*Bündnerschiefer,* locally referred to as the A*ltkristallin*). A clear boundary between these two formations slopes from 1850 m a.s.l. at the south of the niche, to 1945 m a.s.l. at the north (Fig 18). This boundary continues as it is in the niche further to the north, but suddenly declines to the south under the influence of the *Mischabel Rückfalte* (see Fig 16, 17, and Appendix F, p.101). The layers are dipping to the west (approx. 25°), which results in rather stable west flanks, compared to those on the east (as was already mentioned in section 2.2). This explains the appearance of numerous rockfall and avalanche deposits and several zones of sagging on the eastern side of the valley.

Structural surveys have shown that near Randa, two sub-parallel systems of schistosity and isoclinal faults have developed under high pressure and temperature, dipping 20 – 40° west-southwest. They are thus dipping niche-inward and therefore certainly don't have a negative influence on its stability. The post-metamorphic (mainly brittle) deformations however, have a very different nature. Since they have been measured and categorised into several systems, it is theoretically possible to define the

Fig 18. Boundary (white line) between the *Altkristallin* and Randa gneiss. The *Altkristallin* tops the Randa gneiss *(LVdB)*.

[7] *Modified from Truffer (1995).*

critically unstable rock masses. However, there are limits to this method. Because the orientation of individual deformations is very scattered, it is hard to place them in categories. Also it is questionable how representative single measurements are for the full image. In addition are spatial distribution, frequency, and especially inclination of the discontinuities strongly influenced by the characteristics of the rock. As so, the rather massive randagneiss is divided in fairly cubic masses, whereas the less competent A*ltkristallin* has a more platy disposition. Another hindering factor is that the pattern of deformation becomes less structured with increasing distance from the Randa gneiss. In general, it can be said that the younger systems of discontinuity clearly have an influence on the stability, but the interrelations are complex.

2.6.4 Rockslide event[8]

Appendix H (p.103) collects pictures made before, during and after the rockslide event, representing the atmosphere of those days.

2.6.4.1 The situation before 1979

Fig 19. The arrow points towards the rock face above the Grossgufer area in 1990 *(Lina Summermatter)*.

An indication of what the area must have looked like can be found in its name, that remained unchanged. Grossgufer is Walliser dialect and means as much as 'heaps of giant rocks'. The name, as well as old pictures and descriptions from inhabitants of Randa, indicate that the forest of mainly high spruces and larches present at that time, had grown on an ancient slope now covered by the rockslide deposit. Since the forest consisted of old and tall trees (also according to inhabitants) we can think of a relatively calm period before 1979, without any important events. There was, however, a central zone of active rockfall present, that had cleared a small couloir in the forest. Also, several locals observed cracks in the rock face (Fig 19 and 20), with widths up to 1.5 m and of unknown depth.

[8] *Modified from Burri (1992).*

2.6.4.2 The rockslide event of 18.4.1991 and its foreplay

In 1979 the Grossgufer forest at the foot of the valley flank was nearly completely destroyed by rockfall activity. From January 1991 on, higher activity was noticed, under the form of continuing smaller rockfall events. On 17 April 1991, large amounts of infiltration water were delivered by the springs at the bottom of the flank, and two large rock plates were forced out of the face in an explosion-like manner. The next day, the first part of the actual rockslide took place from 06:25 till 23:05 local time. According to eyewitnesses, most of the rock masses slid down in their original position, and only a smaller amount was tilted. Apparently the rock below the springs stayed intact. It was only after continued activity during night that the niche reached into the A*ltkristallin* above the Randa gneiss. Just bellow the upper boundary of the Randa gneiss, new springs were sighted the following day. These must have been covered by debris before. The landform resulting of the slide was a very steep, rather atypical fan of large blocks, slightly flattened near its perimeter. Whilst most rockslide deposits have a typical flattened morphology, with large runout, the Randa rockslide must owe its unusual form to the succession of relatively small events over several hours, rather than the release of the complete mass at once. Another consequence of this rather unusual process was that the destructive air blast was not as large as it could have been. Only some nearby trees were uprooted and some stables deroofed. At some locations, up to 50 cm of pale dust were measured. The bed of the Vispa river was dammed over a length of 850 m, and the trail of the local railway, the Matterhorn-Gotthard Bahn (MGB) was destroyed (Fig 21).

2.6.4.3 19.4.1991 – 22.4.1991

A team of geologists set out for a first inspection of the niche area, and installed a dense network of reflectors for distance measuring, fissure monitors, as well as four vibration measuring devices of the Vibroguard type. On 21 April the alarm level was raised again and a nearby construction site for the broaching of the Vispa bed was evacuated. One day later two smaller slides of few 100 000 m^3 each came down, without causing much damage. They were registered at the Zmutt seismological measuring station (to the west of Zermatt, 10 km from the rockslide deposit) with an intensity of 2 – 3 MSK.

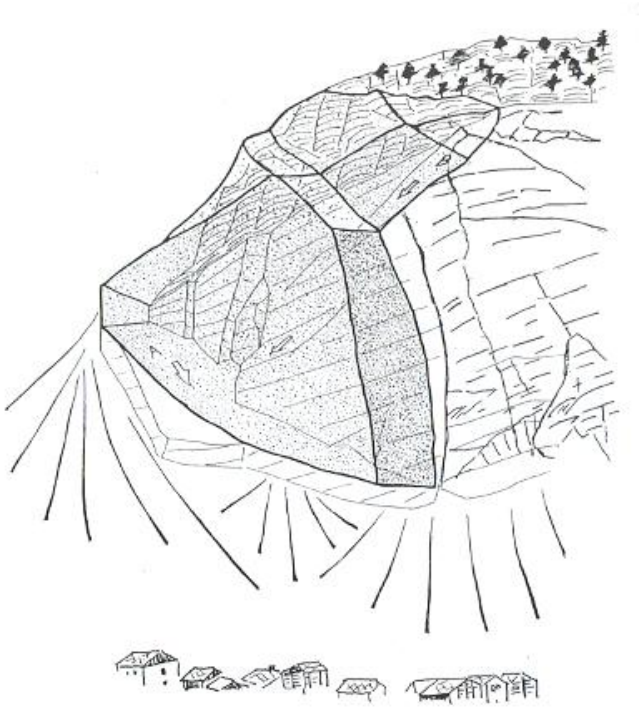

Fig 20. Rock face before the event *(Burri, 1992)*.

2.6.4.4 23.4.1991 – The rockslide event from 09.5.1991

By 23 April twenty fissures were being constantly monitored and fifteen geodetic measuring stations were still active. Up to

this point, the water of the Vispa river could seep through the rockslide deposit and only a small lake was formed south of the deposit. Until 6 May a minor tendency of higher movement was registered at the geodetic stations and most of the fissure monitoring points. Also, a muddy, near-horizontal water jet was observed close to the upper boundary of the Randa gneiss. The next day however, an exponential trend in displacement rates was noticed, which is a classic indication for a rockslide event. The vibrometers also registered more, and stronger signals. Early in the morning of 9 May, the next rockslide event started, with the opening of the fissures, and the generation of several dust and water fountains. By the evening some stations had registered 70 cm of displacement over 11 hours and the alarm was raised. A rockslide followed, with its origin in the A*ltkristallin*, immediately above the springs, spread over 7 hours. This time, only A*ltkristallin* units came down, and again the highest point of the niche was first reached during the night. And this time as well, most of the masses seemed to have slid down in their original upright position and only some tilted. Again a lot of dust was produced

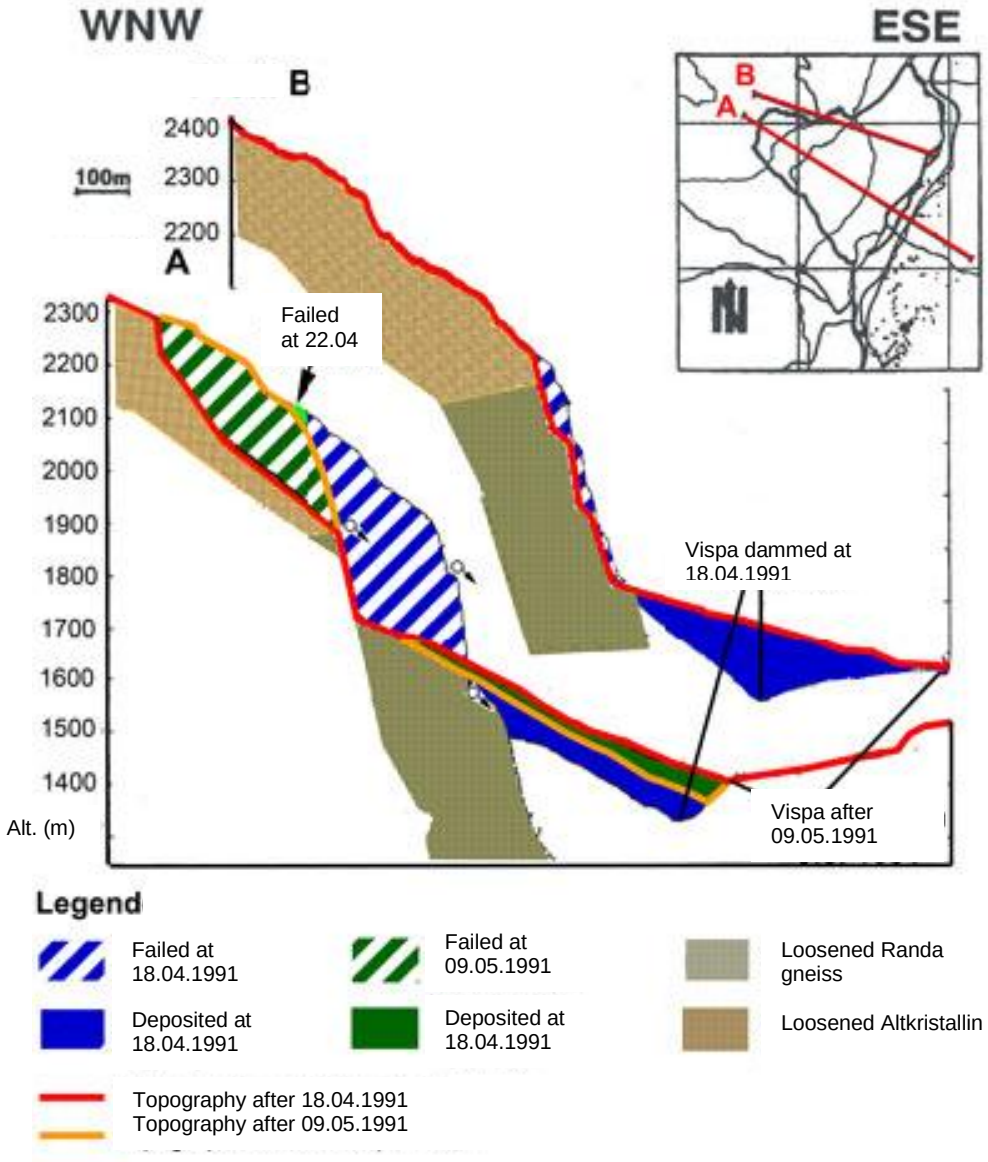

Fig 21. Profile showing the deplaced materials during the succeeding events*(Schindler et al., 1993)*.

and muddy water poured out of the flank near the springs. The dust reached heights of about 1900 m a.s.l. and prevented light and sound from penetrating the valley. This time, the street and MGB trail were blocked over a larger distance, the dam of blocks in the Vispa river bed had become higher and now prevented the water from leaching through (Fig 21).

2.6.4.5 Development since 1991

The partially destroyed measuring network has been re-established and expanded upward as well as to the north, based on the results of previous measurements and expectations. Shortly after the event, the fissure monitors responded depending on their orientation. They acted either stable, opening or closing. Vibro measurements are only made in case of higher alarm level. In spring 1992 a phase of exponential opening was expected again, it did, however, never take place. Today zones of higher risk are localised and charted, as well as possibly threatened parts of the valley. As for the Vispa river, shortly after the event there was the permanent threat of flooding in Randa and of dam breach. In order to prevent more catastrophes the water was pumped, the bed was cleared as soon as possible, and a tunnel was made parallel to the flank, inside the mountain, to discharge extreme water amounts of the Vispa river. In spring and summer, small amounts of infiltration water are constantly pouring out the tunnel opening (Fig 22).

Fig 22. Entrance and exit of the tunnel constructed after the 1991 events *(LVdB)*.

2.6.4.6 Erosion, relaxation processes

Glacial erosion gave the valley its distinct trough shaped form. Near Randa, measurements at the valley floor have placed the basement rock at 1250 – 1300 m a.s.l., so at a depth of 100 – 150 m bellow the valley floor, before the rockslide event. During the most intense period of the Würm glaciation (*Hochwürm* 115 000 – 10 000 a), the level of the glacier surface reached up to 2250 m a.s.l. However, the abrasion range reaches as high up as 2700 m a.s.l., which indicates an earlier, higher

glacier level. The quick retreat of the glaciers, has made the valley floor permanently free of ice at the latest 10 000 years ago. The erosion and retreating ice pressure gave way to relaxation of rock masses. Resulting in a lateral spreading and opening of discontinuities. In the region of Randa, the rocks were already intensely deformed due to tectonic forces, therefore the relaxation caused the activation of existing fracture systems. This improved water circulation and weathering in the flank, and so its stability got further reduced.

2.6.4.7 Hydrogeology

Systematic hydrogeological data are not available previous to the event. Therefore, we have to rely on observations and indications of the villagers. According to several inhabitants, periodical springs were observed from time to time at the base of the future rockslide mass, and smaller springs occurred near the upper limit of the Randa gneiss. These springs were active from April to the end of June. This implies that they were not fed by glaciers (since their melting peak takes place during July and August), and that their origin therefore should be related to the infiltration of melting water of the winter snow and rain, that can easily infiltrate (up to 2530 m a.s.l.) the thin debris layer covering the massive rock. Interestingly enough, the springs seem to react very slowly to short-time processes and hardly react, if at all, to heavy rains after June. These observations were confirmed by rusty coloured discontinuities that were exposed after the rockslide event, indicating that the water infiltrated the rock mass at least to a depth of 200 m (1700 m a.s.l.). This implies that there is no response to short time processes, that the circulation through the rocks is slow and that the storage capacity of the flank is limited.

Fig 23. Spring activity (marked with a white arrow) at the rock scarp on 16/05/2010 *(LVdB)*.

During the second period of fieldwork, from 29 April on, several springs were activated at the upper boundary of the Randa gneiss (Fig 23). The actual springs were covered by debris, but the water could be clearly seen, streaming along the exposed rock face. This is in accordance with the pattern observed before the rockslide, and is a yearly returning phenomenon.

2.6.4.8 Seismicity

Earthquake risk maps indicate the possibility of a 8.7 MSK earthquake once per 1000 years and the possibility of a 9.6 MSK earthquake once per 10 000 years. The risk increases towards the northern part of the valley (Fig 24). The largest historic earthquake in the region took place on 25 July 1855 at 13:00 GMT, with an epicentre between Brig and Visp, and a MSK magnitude of 8 – 9. This earthquake induced high rockfall activity, several smaller rockslide events near St. Niklaus, debris flows and large cracks in the ground. Several houses in St. Niklaus were completely destroyed or severely damaged and the churches of Visp, St. Niklaus, Törbel and Stalden collapsed. However, written records indicated only minor damage near the Grossgufer area. Nevertheless, earthquakes, and especially of such magnitudes are known to have a loosening and weakening effect even on massive rock masses.

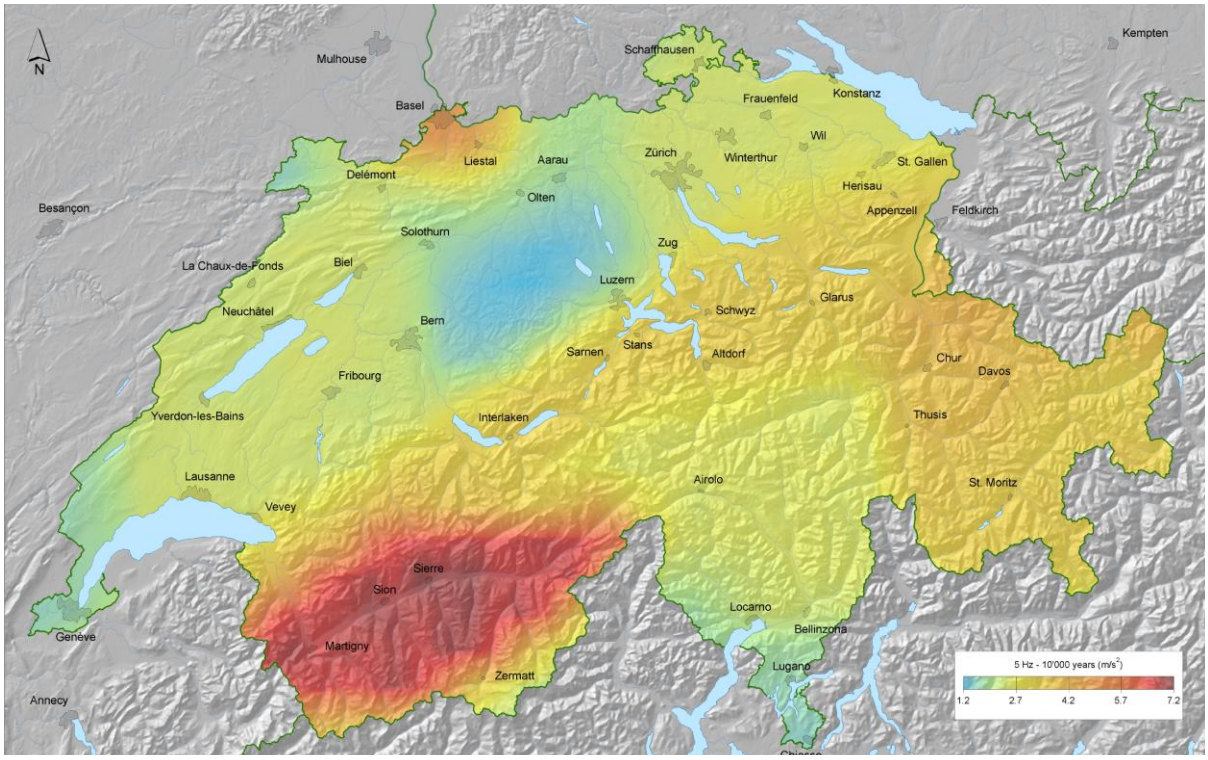

Fig 24. Map depicting the level of horizontal ground motion (in units of the 5% damped acceleration response spectrum at 5Hz frequency) expected to be reached in a period of 10 000 years. The map is calibrated for rock ground conditions, with shear wave velocities of about 1500 m/sec *(www.earthquake.ethz.ch, 2010)*.

2.6.4.9 Cubature, dust, settlement, interstices

By use of detailed topographical maps (1:10 000) the volume of the rock masses before its displacement was estimated on 29.72×10^6 m^3. An aerial survey estimated the volume after deposition to 33.63×10^6 m^3. Unfortunately no photogrammetric measurements could be made after the first event, therefore only visual estimations exist. By estimation, the volume released on 18 April was pinned at 20×10^6 m^3, compared to a mere 10×10^6 m^3 on 9 May (only A*ltkristallin*). The bulking coefficient is

determined as the volume of the deposit divided through the volume of rock mass before displacement and thus equals 1.13. Expected bulking coefficient values for rockslides range from 1.25 to 1.35, so an explanation for the lacking rock volume had to be found. The deposit was studied in detail when the bed of the Vispa river was cleared. Here the deposit consisted of small to very large blocks, loosely packed, with a minor amount of interstitional voids, often filled with clayey material. Its density was estimated on 1.9 – 2 g/cm^3. The amount of dust resulting from the first event was estimated on 200 000 – 500 000 m^3. About the same amount resulted from the second event, although the cubature was only half of that of the first event and the covered distance was clearly less. This is due to the characteristics of the *Altkristallin*, which is much more brittle. The density of the dust was estimated at 0.906 g/cm^3. It's composition was determined at 18% clay, 62% silt and 30% sand.

If this is brought into account a bulking coefficient of 1.14 – 1.145 results, which is still smaller than is expected for a such event. Therefore the settlement has to be taken into account as well. Approximately 140 m of debris is deposited on a valley floor of which the top layer consists of unconsolidated rock (mudflow deposit, covering rock debris, covering moraines). The settlement volume was estimated on 5 – 7% of the rock slide mass. This brings the bulking coefficient to 1.19 –1.215. The porosity of the deposited mass is approximately 25 – 30%, this means that the mountain before the event had about 7 – 15% crack space, which is an unusual high grade of shattering (Fig 25).

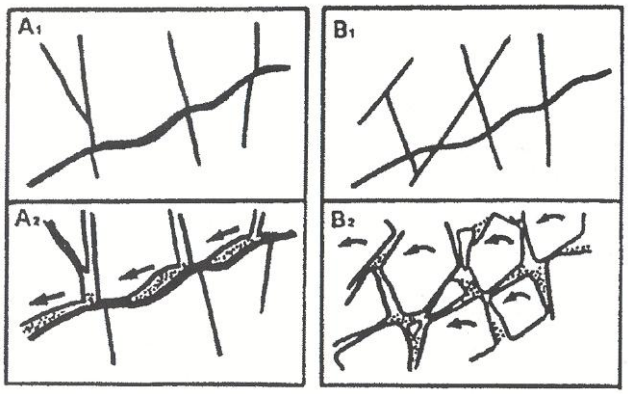

Fig 25. Advanced loosening of disturbed rock masses as was described for the rockslide of Centovalli (marked on Appendix A) (A) and the rockslide of Randa (B) *(Truffer, 1995)*.

2.6.4.10 Kinematics

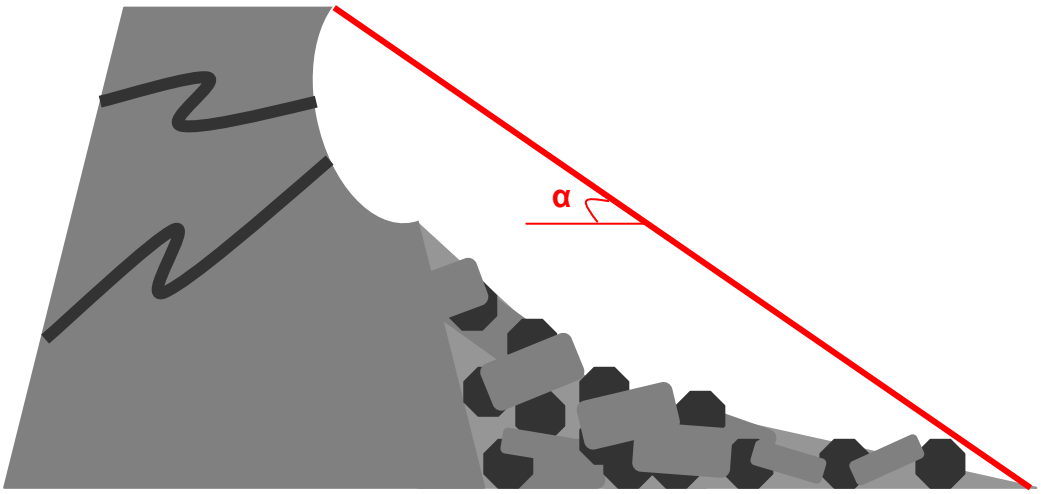

Fig 26. Simplified image depicting the falling gradient α *(LVdB)*.

The deposit is, as was mentioned earlier, characterised by a rather unusual morphology. Also, the effect of the preceding air blasts was minor. The falling gradient α is determined as the inclination of the line from the top point of the niche to the furthest point along the perimeter (Fig 26). If we now compare the falling gradient and the cubature to analogous events (e.g., the rockslide of Goldau in 1806, marked on Appendix A, p.96, with a displaced volume of $40x10^6m^3$) (Erismann & Abele, 2001), the deposit should have advanced 1.8 – 4 km in the valley, which it clearly did not. This is most likely due to the twin-stroke behaviour (two-phased process) of the rockslide, where individual falling rock masses never exceeded 10^6m^3 and thus were never able to sufficiently accelerate and cover higher distances.

2.6.4.11 Possible causes

The inertia of the masses does not allow us to search the cause in the last 10 to 20 years. The process likely must have started developing hundreds to thousands of years ago, though its features were not noticed earlier, or were judged as not-dangerous at the time by the local inhabitants.

First of all it has to be stressed once again that the region suffered intense brittle and ductile deformation, which has resulted in a dense network of disturbances and instabilities.

As was mentioned in section 2.6.4.6, the valley floor was free of ice at least 10 000 years ago. In addition, the global retreat of glaciers during the last 150 years - which is considered a sign that climatic warming started at the end of the Little Ice Age (ca. 1850) - has to be underlined (Kuhn, 1981; Jones & Henry, 2003; Oerlemans, 2005). For the Grossgufer area, this implies continues changes in force and pressure over the last millennia, which certainly had a negative influence on stability. Also, it is stated by Haeberli (1995) and Raffl et al. (2006) that rapid glacier retreat is generally more pronounced in mountainous landscapes with steep slopes, which are clearly prevalent in the Matter Valley. Thus, the quick retreat of the Bis glacier might have been of influence.

Another possible cause might be found in migration of the permafrost boundary. Appendix I (p.117) shows a map of the current permafrost distribution. Permafrost is invisible, extremely variable and heterogeneous, difficult to measure and to model, and currently undergoes rapid changes (Gruber & Haeberli, 2009). Thus it becomes clear, that the system will have lost a lot of its stability when frost no longer kept the disturbed masses together in a first phase, and that the retreat of permafrost still has an influence today, as this provides melting water to infiltrate the zones of disturbance present in the rocks.

Theoretically, all factors that can possibly create an over pressure or enhance the circulation of water in the rock mass can be seen as immediate trigger mechanisms. Thus, even rather short intense cycles of frost and thaw can be of significant influence on stability. The already precair balance of the rock masses might be further disturbed by sudden melting of ice caught in disturbances, which results in over pressure of the water. This lessens the resistance of the rock mass, and causes displacement of the loosened material. In addition, the rock is exposed to internal weathering, and fine-grained eroded material will act as a lubricant when the instability reaches a critical point (Fig 25). As was mentioned in section 2.6.4.8, earthquakes as well might act as a trigger for processes as these.

2.6.4.5 The rockslide area today

During the second period of fieldwork, the frequency of smaller rockfall events was severely enhanced by the alternation of frost and thaw. Therefore it was impossible to go in the field on a sunny day following a snowy day. Also, the influence of rain is not to be underestimated in the areas with relatively finer grained debris. The scarp area concentrates rain water, which initiates the formation of small streams, that locally rearrange the deposit. While the rock face seemed to be undisturbed during the first period of fieldwork, it seemed to be much influenced by the season during the second period of fieldwork. After warm periods, melting water was concentrated in the niche, which led to water running down the rock face after a couple of days, also enhancing rock fall activity. Due to the morphology of the deposit, there was no immediate danger for the lower and central regions of the cone.

Currently, a team of researchers of the *Eidgenössische Technische Hochschule Zürich* (*ETHZ*) permanently monitors the area, which resulted in a number of publications (Eberhardt et al, 2004; Heincke et al, 2005; Heincke et al, 2006; Spillmann et al, 2007a; Spillmann et al, 2007b; Willenberg et al, 2008a; Willenberg et al, 2008b). They recently equipped the zone immediately above the rock scarp with a meteorological station, crack extensometers, piezometers, rock thermometers, fiber optic strain sensors, borehole inclinometers, and seismometers. Also, several ground-based differential InSAR surveys (Gischig et al., 2009; Gischig et al., unpublished) were performed from a base station at the valley flank opposite from the instability, and a time-lapse camera registers an image every 3 hours. In addition, a large-scale geodetic network has been surveyed once or twice per year, since 1995. The monitoring points of the *ETHZ*, along with several graphics are shown in Appendix I (p.117). Figure 27 is a graphic based on values retrieved from the crack extensometers, showing the influence of a minor earthquake that took place during the second period of fieldwork. On 15 May at 05:09:43.9 UTC, it was registered at the Zmutt station, with an intensity of 3.4 MSK, its epicentre near St. Niklaus. Most likely, this event had a loosening effect and partially induced a fairly large rockfall event the next day.

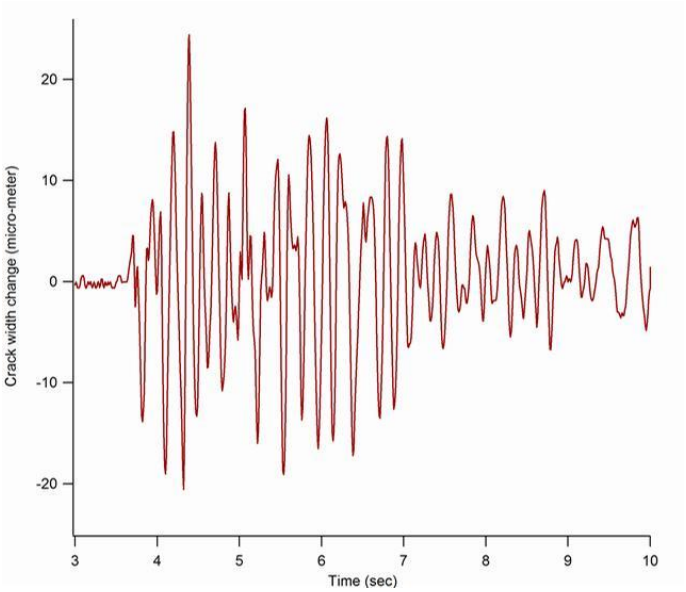

Fig 27. Variation in crack width (µm) during the earthquake on 15 May 2010 (*www.rockslide.ethz.ch, 2010*).

3 Literature Study

3.1 Dendrochronology

3.1.1 Introduction

Dendrochronology or tree-ring dating is a scientific method of dating based on the analysis of patterns of tree rings. Until relatively recently, radiocarbon dating of wooden objects was the only known scientific method of dating wooden objects. Generally being successful, it produced dates which have a range of plus or minus twenty years at best, and at worst could span two centuries or more (Pierson, 2007). The strength of dendrochronological methods lies in the possibility of accurately dating an event to the exact calendar year – even to the exact season - in recent history (Pierson, 2007); which is an area that is not covered by conventional dating techniques.

Fig 28. Felled larches *(LVdB)*.

Dendrochronology has numerous applications, most mass-movement studies however apply to the dating of geological hazards. Schweingruber (1983) states that a number of geomorphic processes can influence tree growth, and thus be recorded: volcanic events (ash rain, lava flows, climatic change), snow displacement (avalanches, snow creeping), mass movements (rock fall activity, erosion, debris flows, land slides), ice displacement (advancing glaciers), eolian processes (loess deposition, dune migration), and hydrologic changes (changing groundwater level, tidal influences); which underlines the potential of the method. For the assessment and management of hazards and risks (e.g., rockfall activity, snow avalanches, debris flows), understanding the processes and knowing their behaviour in space and time is crucial. However, systematic data acquisition on such processes is often lacking, and thus reconstruction becomes essential for the understanding of process dynamics. Pioneering work was done by Alestalo (1971) by his provision of results on the influence of slope movements on tree-ring formation. Other studies focussed on the reconstruction of spatio-temporal patterns of debris-flow activity (Bollschweiler et al., 2007; Bollschweiler et al., 2008; Stefanini & Ribolini, 2003; May & Gresswell, 2004), reconstruction of rockfall activity (Perret et al., 2006; Stoffel et al., 2006; Schneuwly et al., 2008), and analysis of rockfall activity in protection forests (Stoffel et al., 2005). In a similar way, past snow avalanches (Butler et al., 1992; Rayback, 1998; Hebertson & Jenkins, 2003) or landslides (Fantucci & Sorriso-Valvo, 1999; Stefanini, 2004) have been assessed with tree rings.

Only a minor number of successional studies are written, focussing on recently formed volcanic surfaces (Pierson, 2006), glacial forefields (McCarthy et al., 1991; Garbarino et al., 2010), and moraines (McCarthy et al., 1993).

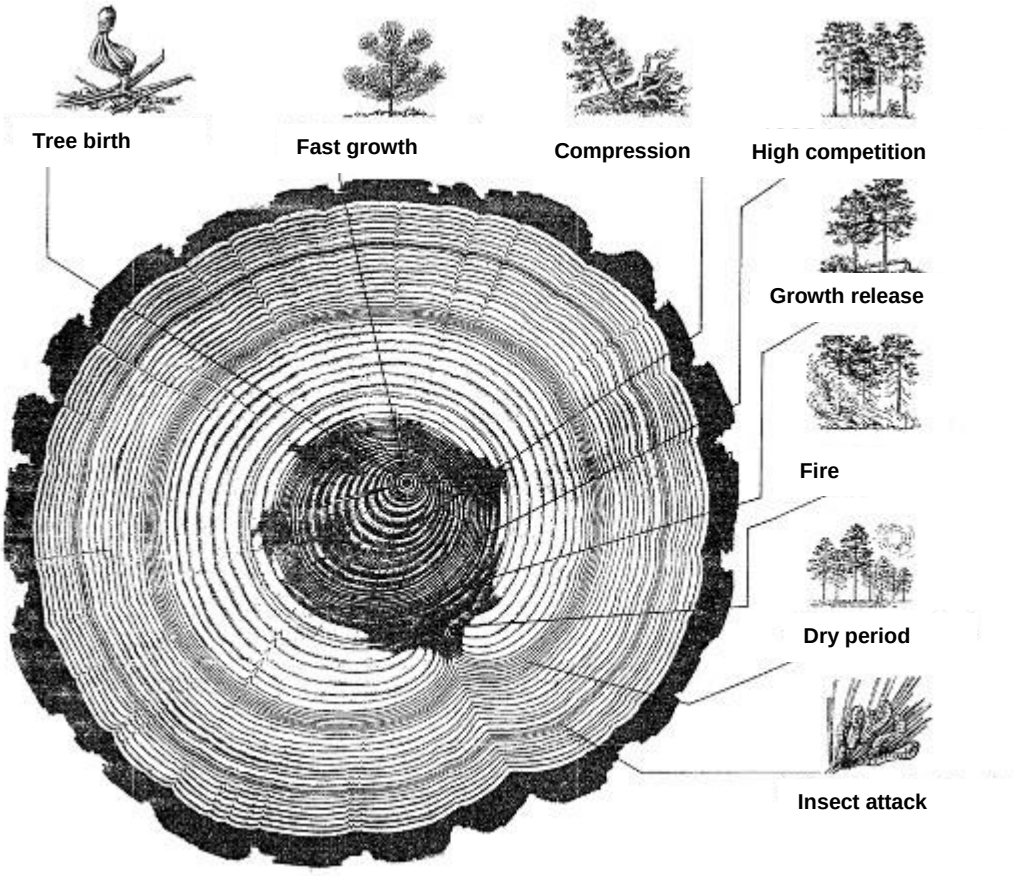

Fig 29. Cross section of a conifer *(Schweingruber,1983)*.

3.1.2 Dendrochronological principles

The ability of a woody plant to build growth rings depends on its systematic affiliation. Ferny and monocotyledonous plants, as well as cycads don not show growth rings (Schweingruber, 1983). The first appearance of tree rings is allocated to the *Cordaites*, the ancestors of the conifers, which thrived during the Late Devonian, about 395 – 345 Ma ago, in Europe and North America (Schweingruber, 1983).

For a better understanding of the methods used in dendrochronology, some knowledge on wood anatomy is required. Growth rings (Fig 28 & 29) are the result of new growth in the vascular cambium, a layer between the wood (xylem) and the bark (phloem). This layer is a lateral meristem, and is therefore synonymous with secondary growth. The rings result from a change in growth speed during the seasons of the year (Huber, 1961). Thus one ring usually marks the passage of one year in the life of the tree. The inner portion of a growth ring is formed early in the growing season, when growth is comparatively rapid and hence the wood is less dense (and therefore paler in species that show enough contrast). This part is known as earlywood. These new cells are large, but as the summer progresses, their size decreases until, in fall, growth stops and cells die, with no new growth until next spring (Fig 30). These smaller cells form the denser outer portion of the ring and are called latewood (comparatively darker in species that show enough contrast). Tree-ring width is partially genetically determined (Schweingruber, 1983). A poplar for example, will produce broader rings than a bilberry

shrub, under equal climatic conditions. The formation of the ring boundary is also partially genetically determined: boundaries are easier to recognise in the wood of the ring-porous ash tree, compared to the diffuse-porous apple tree (Schweingruber, 1983).

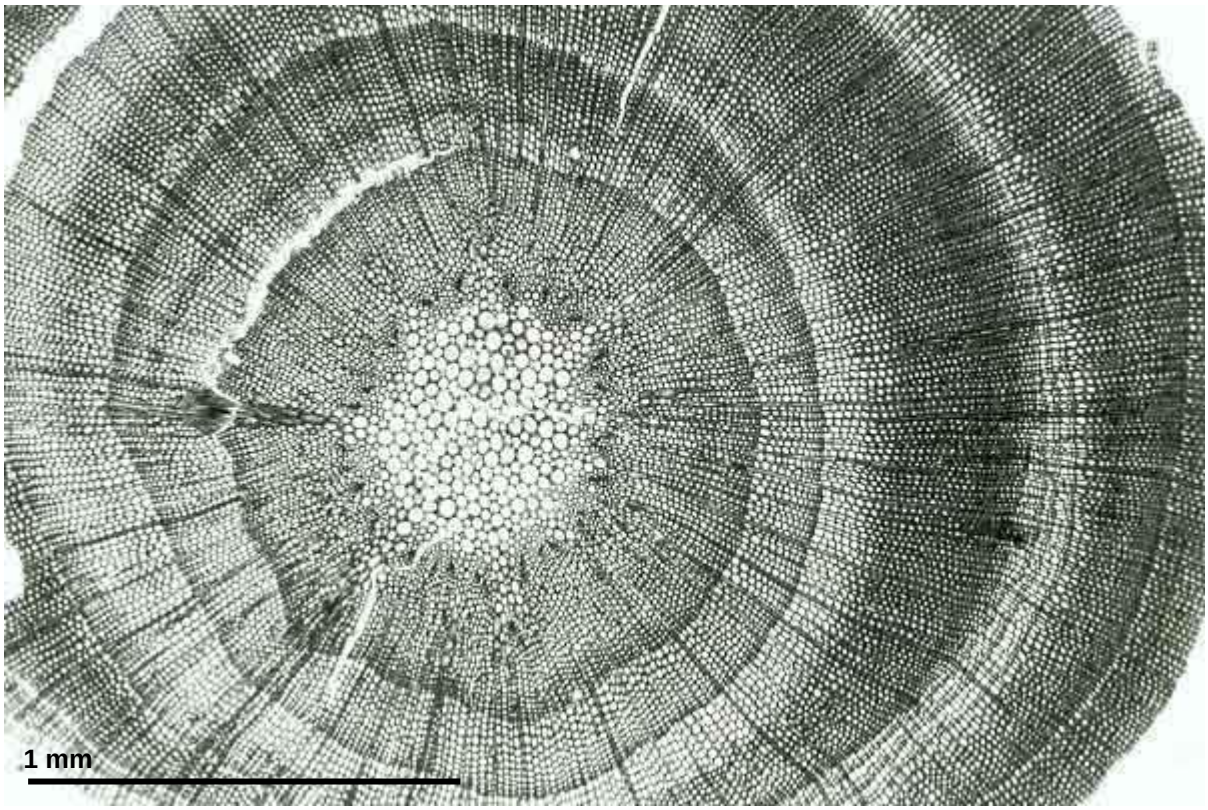

Fig 30. Branch of a larch under the microscope *(www.woodanatomy.ch, 2004)*.

Many trees in temperate zones make one growth ring each year, with the newest adjacent to the bark (Schweingruber, 1983). For the entire period of a tree's life, a year-by-year record or tree-ring pattern is formed that reflects the climatic conditions in which the tree grew (Fig 29). Adequate moisture and a long growing season result in a broad ring, whereas a drought year may result in a very narrow one. Trees from the same region will tend to develop the same patterns of ring widths for a given period (Schweingruber, 1983). Alternating poor and favourable conditions, such as midsummer droughts, can result in intra-seasonal wood-density fluctuations (varying cell wall thickness) (Schweingruber, 1983). Missing rings, indicating a year without secondary growth, can also occur (Schweingruber, 1983). Factors that can influence growth are slope gradient, sun, wind, soil properties, temperature and snow accumulation. The more the growth rate of a tree has been limited by such environmental factors, the more variation in ring to ring growth will be present. This variation is referred to as sensitivity, and the lack of variability is called complacency. Trees showing complacent rings may grow in constant climatic conditions such as high water table, good soil, or protected locations, or simply do not respond very well to possible influences.

3.1.3 Primary succession

Primary succession (Campbell, 2003) is one of two types of biological and ecological succession of plant life, occurring in an environment in which new substrate, devoid of vegetation and usually lacking soil, is deposited. Secondary succession, in contrast, occurs on substrate that previously supported vegetation before an ecological disturbance such as a forest fire, tsunami or flood destroying plant life (Campbell, 2003).

Massive natural phenomena such as glacier retreat, landslides and lava flows, that cause eradiction of all forms of life, give way to the establishment of primary successional surfaces. This process can be denounced as ecesis (from the Greek oikesis, a dwelling in), or the establishment of plant species in a new environment, and can take generations to complete. The term “ecesis” was first used by Clements (1904) to describe a variety of stages and processes that occur as plants colonize a site. In practice, the term leads back to the minimum (or average) interval that should be added to the earliest ring date from the oldest tree on a surface (McCarthy & Luckman, 1993).

In primary succession pioneer species like lichen, algae and fungus, as well as other abiotic factors like wind and water start to normalise the habitat. This creates conditions nearer optimum for vascular plant growth. Pedogenesis or the formation of soil is the most important process. Some important soil changes include large accumulations of organic matter and nitrogen, due to biological fixations of atmospheric carbon dioxide (CO_2) and dinitrogen (N_2) (Walker, 1993).

Pioneer plants can be relatively soon dominated and replaced by plants better adapted to less-austere conditions. These can be vascular plants like grasses, and some shrubs that are able to live in thin soils that are often mineral based. Succession may continue as there is no further disturbance, or paradoxically, only as the result of system perturbance (Clements, 1916).

According to Garbarino (2010), environmental characteristics that typify the deposit, such as topographical factors and distance from seed sources have an important influence on primary successional pathways, and at the same time, the biotic interactions of colonizing plants, including processes such as facilitation and inhibition, may be important mechanisms of successional change. For example, numerous studies have demonstrated the importance of nitrogen-fixing plants for facilitating the establishment of other plant species (Crocker & Major, 1955; Walker & Chapin, 1987; Vitousek & Walker, 1989; Walker, 1993; Chapin et al. 1994; Bellingham et al., 2001). Other studies (Blundon et al., 1993; Chapin et al., 1994; Schlag & Erschbamer, 2000; Mong and Vetaas, 2006) have shown that site modification through facilitation is not an important mechanism of establishment, and that plants can colonise for example bare moraine till. Finally, the life history attributes of colonising plants, especially seed dispersal ability, may contribute to determining vegetation composition during primary succession (Walker & Chapin, 1987; Chapin et al., 1994; Fastie, 1995; Jones & Henry, 2003; del Moral & Ellis, 2004). The early dynamics of primary succession are strongly influenced by abiotic factors, the importance of site conditions relative to biotic conditions may decrease with time. It is widely accepted that physical environmental factors are more important than biotic factors during the early stages of succession in determining the distribution and abundance of plants (Reader & Buck, 1986). Biological processes become more important later in succession, when development of the vegetation begins to transform the microenvironment (Matthews, 1992; Vetaas, 1994; Totland et al.,

2004). Consequently, “safe sites” such as large rocks and depressions tend to lose their importance for ecesis as succession advances (Jones & del Moral, 2005a; Raffl et al., 2006).

Pierson (2006) states that to estimate the year of landform creation, it is required that two time corrections are added to the obtained tree ages: (1) the time interval between stabilisation of the new landform surface and the germination of the sampled trees, which is known as the germination lag time or GLT, and (2) the interval between seedling germination and growth to sampling height, if the trees are not cored at ground level. The sum of these two time intervals is the colonisation time gap (CTG). In some cases, timing of such geomorphic changes can be critical to emergency planning. Also according to Pierson (2006), some uncertainties remain to resolve: (1) the oldest tree cannot be selected a priori, because the oldest tree is not necessarily the largest; (2) it may not be possible to ascertain that the oldest tree sampled belongs to the first cohort of colonisers; and (3) the CTG somehow must be reliably estimated.

3.1.4 Species found in Randa

Tree species found on the rockslide deposit are larch (*Larix decidua*), birch (*Betula pendula*), green alder (*Alnus viridis*), Norway spruce (*Picea abies*), European red elder (*Sambucus racemosa*), purple willow (*Salix purpurea*), goat / pussy willow (*Salix caprea*), trembling aspen (*Populus tremula*) and sycamore maple (*Acer pseudoplatanus*). Their features will in short be described below.
Other commonly seen plants are juniper (*Juniperus communis*), fireweed (unidentified *Epilobium* species), strawberry (unidentified *Fragaria* species), raspberry (unidentified *Rubus* species), rusty-leaved Alpenrose (*Rhododendron ferrugineum*), houseleek (unidentified *Sempervivum* species) grasses (unidentified *Gramineae*, unidentified *Cyperaceae,* unidentified *Juncaceae*), liverworts (unidentified *Marchantiophyta*), hornworts (unidentified *Anthocerotophyta*) and mosses (unidentified *Bryophyta*). Many other species can be found, but it is beyond our goal to identify and describe all of them in this study.

3.1.4.1 Larix decidua

Larches are conifers that can grow 15 – 50 m tall, with a stem diameter of up to 1.5 m (Godet, 1987). They are also deciduous trees, losing their leaves every year, and native to much of the cooler temperate northern hemisphere. Their shoots are dimorphic, with growth divided into long shoots, bearing several buds, and typically 10 – 50 cm long. The short shoots are only 1 – 2 mm long with just a single bud. The leaves are needle-like, 1.5 – 3 cm long, and slender (under 1 mm wide). They are borne singly, spirally arranged on the long shoots, and in dense clusters of 30-40 needles on the short shoots. The needles turn yellow and fall in late autumn, leaving the trees leafless through the winter. Larch cones (Fig 31) are erect, small, 1 – 9 cm long, green (pollen cones, male) or purple (seed cones, female), ripening brown 5 – 8 months after pollination (Kremer, 1998). The cones are erect, have an ovoid to conic shape, are 2 – 6 cm long, with 30 – 70 erect or slightly incurved seed scales (Kremer, 1998). They open to release the seeds when mature, 4 – 6 months after pollination (Kremer, 1998). The old cones commonly remain on the tree for many years, turning dull grey-black. The seeds

are 3 to 4.5 mm long and have a wing 5 – 6 mm broad, they ripen from September or October of the first year and are released before next spring (Godet, 1987). After their release they stay dormant for 4 – 5 weeks and germinable for 4 – 5 years (Kremer, 1998). Larches can become 600 – 800 years old. The young bark is yellowish and smooth, but changes with age into an up to 10 cm thick, chapped bark, that is grey brown on the outside, turning reddish violet towards the wood (Fig 28). The wood itself is light brown, with a tough and highly resinous core, which darkens with age and under the influence of sunlight (e.g., the numerous blackened chalets in the Alps). The density of air-dried wood is 600 – 750 kg/m^3 (Godet, 1987).

Fig 31. Young female and male cones (top), stages of ripening in female cones (middle), and old cone (bottom) on larches *(LVdB)*.

Also according to Godet (1987), larches only grow on deep, well-drained soils, avoiding waterlogged ground; they prefer well-aerated, nutrient-rich, loamy to clayey soils. Less favourable, though equally well colonised are avalanche couloirs, rocky slopes and landslide deposits of the subalpine zone. They are light-loving and prefer warm summers and dry air. They are however very cold tolerant as well, able to survive winter temperatures down to at least -50°C, and thus seem to be extremely well suited for the climate of the Visper Valleys. They are among the treeline trees in the Alps, reaching 2400 m a.s.l., though are most abundant from 1000 – 2000 m a.s.l. (Godet, 1987). They are regarded as pioneer species, tending to be the first trees to colonise bare moraine till or other fresh deposits. The needle litter of larches considerably improves the soil quality and even the path for more demanding species such as Norway spruce (*Picea abies*) and Swiss

stone pine (*Pinus cembra*).

3.1.4.2 Betula pendula

Birches are generally small to medium-size trees or shrubs, mostly of temperate climates. They can grow up to 20 – 30 m high, and can reach a stem diameter of 40 – 60 cm (Godet, 1987). The crown is slender and sharp in young individuals, and becomes rounded or irregularly shaped with age. Primary growth (the growth in length) starts to decrease with 20 and stops with 50 – 60 years (Godet, 1987). Birches can become over 100 years old. The buds form early and are full grown by midsummer, all are lateral, no terminal bud is formed as the branch is prolonged by the upper lateral bud. The leaves are alternate, doubly serrate, feather-veined, petiolate, and stipulate (Fig 32) (Kremer, 1998). They often appear in pairs, but these pairs are really borne on spur-like two-leaved lateral branchlets. The fruit is a small samara, although the wings may be obscure in some species (Kremer, 1998). They differ from alders (*Alnus*, other genus in the family) in that the female catkins are not woody and disintegrate at maturity, falling apart to release the seeds, unlike the woody cone-like female alder catkins. The lower stem is usually scaled and cracked, and its colour dark brown to black, with few white spots (Fig 32). Higher up on the stem and on the branches, the bark is smooth and shiny, of a silvery white to yellowish colour. The bark that is fairly impermeable to water, consists of two layers. An outer, snow-white layer, marked with long horizontal lenticels, that often separate into thin papery plates, which easily peel off, and an inner more resistant layer (Godet, 1987). The soft and shiny wood is yellowish white and turns reddish toward the pith. It has a satiny texture and is close-grained. According to Godet (1987), the density of air-dried wood is 600 – 700 kg/m^3.

Fig 32. Birch leaves (left) and stem (right, approximately 27 x 7 cm) *(LVdB)*.

Birches often form even-aged stands on light, well-drained, particularly acidic soils. They are regarded as pioneer species, rapidly colonising open ground, especially in secondary successional sequences following a disturbance or fire. Birches are early tree species to establish in primary successions.

3.1.4.3 Picea abies

The Norway spruce is a large, evergreen coniferous tree, native to Europe. Free-growing they can become up to 30 – 40 m tall, in a forest stand they reach up to 60 m (Godet, 1987). The shoots are orange-brown and glabrous. The leaves are needle-like, 12 – 24 mm long, quadrangular in cross-section (not flattened as those of larches), and dark green on all four sides with inconspicuous stomatal lines (Taylor, 1993). Needles become 4 to 7 years old. Seed cones are 10 – 16 cm tall, their scales are diamond-shaped, and at the widest near their middle, with a leathery structure and margins that are at the apex erose to toothed (Taylor, 1993). Trunk diameters can reach 1 – 1.5 m. Spruces tend to have a pyramid-like crown and a shallow and broad root system (Godet, 1987). They can become up to 600 years old. The young bark is smooth or slightly scaled, has a reddish brown colour, that turns greyish brown with age (Taylor, 1993). The wood is white to pale yellow, highly resinous and soft. The year rings show a clear contrast between early and late wood and therefore are easy to count. The density of the air-dried wood is approximately 450 kg/m^3 (Godet, 1987). Spruces tolerate acidic soils well, but do not do well on dry or deficient soils.

Fig 33. Young twigs (left) and cones (right) of Norway spruce *(Godet, 1987)*.

3.1.4.4 Acer pseudoplatanus

The sycamore maple is a deciduous tree that reaches to 25 – 30 m at maturity and can reach the age of 500 years under optimal conditions (Godet, 1987). They tend to grow very tall in woods, and are then branchless to high up the slender and straight stem. The bark of young trees has a distinctive brownish pale-grey colour, which is useful for identification. The buds are decussate, large and pale green and form palmate leafs (Godet, 1987). The leaves can become up to 15 – 30 cm long and are 10 – 16 cm broad. They are opposite, 10 – 25 cm long and broad with a 5 – 15 cm petiole, palmately veined with five lobes with toothed edges, and dark green in colour (Godet, 1987). The 5 – 10 mm diameter seeds are paired in samaras, each seed with a 20 – 40 mm long wing to catch the wind and rotate when they fall; this helps them to spread further from the parent tree (Godet, 1987). On young trees, the bark is smooth and grey but becomes rougher with age and breaks up in scales, exposing the pale-brown-to-pinkish inner bark. According to Godet (1987), the density of air-dried wood is approximately 650 – 750 kg/m^3.

Sycamore maples prefer meadow-sites of the mountainous and subalpine zone, with fresh to humid soils and preferably moist air (Godet, 1987). They often occur on borders of forest, along with rowans and spruces.

Fig 34. Leaves in autumn (left) and summer (right) of the sycamore maple *(Kremer,1998)*.

3.1.4.5 Alnus viridis

Green alder has a wide range across the cooler parts of the Northern hemisphere. These large shrubs (the only shrub-forming alder species in Europe) or small trees can reach a height of 3 – 12 m, and have a grey bark that stays rather smooth even in old age, when it is coloured black (Godet, 1987). Individuals can reach an age of up to 110 years. Leaves are shiny green, ovoid, 3 – 8 cm long and 2 – 6 cm broad (Godet, 1987). The buds are 1.2 – 1.5 cm long, shiny, of a violet colour and pointed (Kremer, 1998). The flowers are catkins, appearing late in spring after the leaves have emerged (unlike other alders which flower before leafing out). The male catkins are pendulous, 4 – 8 cm long; the female catkins are pointing upward, reddish-green, 1 cm long and 0.7 cm broad when mature in

late autumn (Kremer, 1998). They appear in clusters of 3 – 10 on a branched stem. The infructescence is green in summer, turns then pale reddish brown and is covered with 15 – 20 tiny fruitscales (Godet, 1987). The seed heads stay on the tree till next spring and are nearly black by then. The seeds are small, 1 – 2 mm long, light brown, with a narrow encircling wing. Individuals have a shallow root system, and are marked not only by vigorous production of stump suckers, but also by root suckers. The shrubs are light-demanding and fast-growing, and are also well-satisfied with poorer soils. Green alder is often seen as a highly characteristic colonist of avalanche chutes in mountains, where potentially competing larger trees are killed by regular avalanche damage. Alders survive avalanches by their ability to re-grow from roots and broken stumps (Godet, 1987). Green alder, unlike some other alders, does require moist soil, and is a colonist of screes and shallow stony slopes. It also commonly grows on subarctic river gravels, occupying areas similarly disrupted by ice floes during spring river ice breakup, in this habitat it commonly occurs mixed with shrubby willows. Alder is sometimes used for afforestation on infertile soils, which it enriches by means of its nitrogen-fixing nodules, while not growing large enough to compete with the intended timber crop. Some alder species are capable of adding 24.95 kg of nitrogen per acre per year to the soil (Ewing, 1996). Therefore they are also well-satisfied with immature soils, such as landslide deposits, since they can bind aerial nitrogen due to their symbiosis with the ray fungus Frankia (Godet, 1987). Green alders also proliferate by root sprouting and layering. They prefer humid slopes, forest borders and riparian sites. Green alders are pioneer species, that can help securing instable slopes. It is often the only tree species found on north-slopes endangered by avalanches. The density of air-dried wood is

Fig 35. Leaves (left) and fruit (right) of the green alder *(Godet,1987)*.

approximately 400 – 700kg/m^3 (Godet, 1987).

3.1.4.6 Salix purpurea

The purple willow is native to most of Europe and western Asia. Willows species are short-lived, oldest individuals reach an age of 70 years (Kremer, 1998). The deciduous shrubs grow 1 – 3 m tall (only few exceptions reach a height of 5 m), with purple-brown to yellow-brown shoots, that turn pale grey on old stems. The leaves are 2 – 8 cm long and 0.3 – 1 cm wide (Kremer, 1998). Above they are dark green, glaucuous green below (Fig 36). Unusually for a willow, they are often arranged in opposite pairs rather than alternate. The flowers are small catkins, 1.5 – 4.5 cm long, often purple or red in colour, hence the name of the species (Kremer, 1998).

Fig 36. Leaves (with galls) and purple twigs (left) of a purple willow (right, approximate height is 3 m) *(LVdB)*.

3.1.4.7 Salix caprea

The Goat or Pussy willow is native to Europe and western and central Asia. This deciduous shrub or small tree can grow 6 – 12 m tall, rarely reaches 20 m (Kremer, 1998). Individuals can become up to 60 years old. The leaves are 3 – 12 cm long and 2 – 8 cm wide, which is broader than in most willow species. The flowers are soft silky, silvery 3 – 7 cm long catkins, produced in early spring before the new leaves appear (Kremer, 1998). Male (maturing yellow) and female (maturing pale green) catkins are on different plants (dioecious). The fruit is a small (5 – 10 mm long) capsule, containing numerous minute seeds embedded in fine cottony hairs (Kremer, 1998). The seeds require bare soil to germinate; their fine hairs aide dispersal. Two varieties are known, *sphacelata* is the one native to the high altitudes in the mountains of central and northern Europe (Alps, Carpathians, Scotland and Scandinavia). This variety has leaves that are densely silky-haired on both sides, 3 – 7 cm long, with early deciduous stipules (Fig 37). Goat willow occurs both in wet environments such as riverbanks and lake shores, and in drier sites, wherever bare soil becomes available due to ground disturbance. As a pioneer species it is often found on fallow land, dumpings and clear fellings, preferring loamy and rocky immature soils (Godet, 1998). The species is typical for pre-forest associations of elders and

willows and introduces along with birches the first phase of natural forest establishment. The bark of the young trunks is greyish with diamond-shaped lenticels. Older individuals show a pattern of diamond-shaped warts on their grey to black-brownish bark. Young branches are grey-green and hairy. Their colour changes towards red-black and they progressively lose the little hairs. The density

Fig 37. Young furry leaves (left) and older leaves (right) of a goat willow (*Kremer, 1998)*.

of air-dried wood is approximately 400 – 600 kg/m^3 (Godet, 1987).

3.1.4.8 Sambucus racemosa

The European red elder is native to Europe, temperate Asia, and north and central North America (Kremer, 1998). The often treelike shrubs prefer riparian environments, woodlands and other, generally moist areas, and are short-living trees (Kremer, 1998). Individuals grow 2 – 6 m tall and their stems have a soft pithy centre. Leaves are composed of 5 – 7 leaflike leaflets, each of which is up to 16 cm long, lance-shaped to narrowly oval, and irregularly serrated along the edges (Kremer, 1998). Leaflets have a strong (according to some, rather disagreeable) odour when crushed. The flowers are white to creamy, very fragant, and each flower has small recurved petals and a star-shaped axis of 5 white stamens tipped in yellow anthers (Kremer, 1998). The fruit is a bright red drupe containing 3 – 5 seeds, very popular with birds, who distribute the seeds (Fig 38) (Kremer, 1998). Red elders prefer shady spots in forests and forest borders; they are however also commonly seen in forest clearings. In Central Europe it is commonly found at higher altitudes. The shrubs are quite resistant when it comes to cold and wind, they can however be damaged by drought and lime abundance. Preferred are sites rich in nitrate and poor in salt (Kremer, 1998).

Fig 38. European red elder (left, approximate height 1.5 m), detail of berries and leaves (right) *(LVdB)*.

3.1.4.9 Populus tremula

The trembling aspen is a poplar species native to cool temperate regions of Europe and Asia. It also occurs at one site in northwest Africa. In the south of its range, it occurs at high altitudes in mountainous regions. Its age rarely exceeds 100 years (Godet, 1987). These trees grow 10 – 25 m tall, trunk diameters reach up to 1 m (Godet, 1987). The bark is of a distinct pale greenish-grey and very smooth on young trees. Dark grey diamond-shaped lenticels can be seen, these become dark grey and fissured on older trees (Godet, 1987). The leaves of the adult trees are nearly round, slightly wider than long, 2 – 8 cm in diameter and with a coarsely toothed margin and a laterally flattened petiole (4 – 8 cm long) (Fig 39) (Kremer, 1998). The species owes its scientific name to the trembling caused even by the slightest breeze, due to the flattened petiole. The leaves on seedlings or on the fast-growing stems of root sprouts are very different, heart-shaped to nearly triangular and of a reddish-brown colour; their petiole is also less flattened (Fig 39) (Godet, 1998). The trees are dioecious, with male and female catkins on different trees. The wind-pollinated catkins are produced in early spring before the new leaves appear. The male catkins are patterned green and brown, 5 – 10 cm long when shedding pollen, the female catkins are green, 2 – 4 cm long at pollination, maturing in early summer to bear 10 – 20 capsules each containing numerous tiny seeds embedded in downy fluff (Godet, 1998). The fluff assists wind dispersal of the seeds when the capsules split open at maturity.

The species is very hardy and tolerates long, cold winters and short summers. Aspen is resistant to browsing pressure by fallow deer due to its unpleasant taste. These trees are often associated with

goat willows, birches, oaks and brooms, and can be found in wood (borders), rocky terrain and hedges. It's a pioneer species, often seen on fallow land and clear fellings (Godet, 1987). Aspen is not a very demanding species, however, well aerated, humid, alkalirich sandy to loamy or loess soils, rich in humus and nutrients are preferred (Godet, 1998). Lime deficiency has no influence whatsoever. As a light-loving species, it is seldomly found in shady spots. The density of air-dried wood is

Fig 39. Young (left) and mature (right) leaves of trembling aspen *(LVdB)*.

approximately 420 kg/m^3 (Godet, 1998).

3.1.4.10 Other plants

Juniper (*Juniperus sp.*) is a light-loving shrub commonly found on sunny pastures, rocky terrain and open forests (Finkenzeller, 2003). The shrub prefers dry, calcareous, alkalirich soils (Finkenzeller, 2003). Juniper can hardly compete with other woody plants and therefore usually gets dominated on dry, sandy or rocky sites. Epilobium (*Epilobium sp.*) is often abundant in wet calcareous to slightly acidic soils in open fields, pastures, and particularly burned-over lands (Fig 41). Its name derives from the species abundance as coloniser on burnt sites after forest fires. It's tendency to quickly colonise open areas with little competition, such as sites of forest fires and forest clearings makes it a clear example of a pioneer species (Finkenzeller, 2003). Plants grow and flower as long as there is open space and plenty of light, as trees and bushes grow larger, the plants die out, but the seeds remain viable in the soil seed bank for many years, when a new fire or other disturbance occurs that opens up the ground to light again, the seeds germinate. Some areas with heavy seed counts in the soil, after burning, can be covered with pure dense stands of this species and when in flower the landscape is turned into fields of colour.

Fig 40. An Alpenrose on the rockslide deposit (top) and a flowering specimen on an alpine meadow (bottom) *(LVdB)*.

Fragaria species grow along trails and roadsides, embankments, hillsides, stone and gravel laid paths and roads, meadows, young woodlands, sparse forest, woodland edges and clearings (Finkenzeller, 2003). It is a plant tolerant of a variety of moisture levels (except very wet or dry conditions). It can survive mild fires and / or establish itself after fires (Finkenzeller, 2003). Well-drained soils, rich in humus and nutrients are preferred.

Rubus species are pioneers on clearings and are an indication for nitrogen-rich soils (Finkenzeller, 2003). They prefer shady sites such as forest fellings or borders, with moist air and cool summers (Finkenzeller, 2003). Raspberries need well-drained soils, since they have very sensible rootsystems.

Alpine roses (Fig 40) prefer moist, mostly acidic conifer forests or open bushy areas. They tend to avoid calcareous soils (Finkenzeller, 2003). It grows from 500 to 2800 m altitude. Along with the Juniperus sibirica it is an important pioneer species (Finkenzeller, 2003).

Fig 41. Two Epilobium varieties *(LVdB)*.

Further on in this report all species will be named by their common names as they are mentioned above.

3.2 Previous work

In 1995 the Randa rockslide deposit was studied for the first time by Jeanette Gasser, a student at the *ETHZ*, under the supervision of Dr. B. O. Krüsi and Dr. M. Schütz. Her work will in short be described, and will also be related to in the discussion section. Between her and my own work, no further studies were conducted on the rockslide deposit.

3.2.1 Natural succession on the Randa rockslide deposit (Gasser, 1995)

(Original: *Vegetationsentwicklung auf dem Bergsturzkegel von Randa*)

The aim of this project was to characterise and determine early pioneer vegetation four years after the rockslide event. This thesis was the first vegetational study on a rockslide deposit ever. The importance of this project was mainly to be found in the analogy of the Randa rockslide deposit with artificial deposits as a result of tunnel construction and other broaching projects, as they are numerous in the Valais, and with future rockslide deposits. In addition, the author stresses that the study was meant as an introduction on the complete successional study, and therefore her results are to be completed within years or tens of years by further research. Gasser states her objectives by asking herself the following questions. Which species grow where and what is the vegetation density? Where do we find specific pioneers, under what circumstances do they survive, and how long can they stay before they are dominated by other species (in other words, what is the succession speed)? What is the origin of the plants, e.g., do they immigrate from nearby flanks, are the seeds wind- or animal-transported? How will the succession continue; will the deposit know its own evolution; or will the evolution be comparable to that of other regional deposits? Bellow, the working methods and results that are of any relevance for my own thesis are stated. It is important to stress that Gasser conducted a full vegetational, and not a dendrochronological study.

3.2.1.1 Procedure

The original idea was to survey the complete cone. Due to rockfall activity this was however considered as too dangerous, and therefore only the lower third of the deposit was studied, minus a small hazardous region near the north-western rock face. Gasser determined five substratum types for her research, that were distinguished as follows.

1. Large blocks. 50% of the material has a diameter > 20 cm (diameters above 10 m are found).
2. Smaller blocks. 50% of the material has a diameter from 2-20 cm, no significant influence of water.
3. Water-influenced debris. 50% of the material has a diameter from 2-10 cm, micro-topography due to water influence.
4. Fine-grained debris. 50% of the material has a diameter from 0.2-2 cm.
5. Silt. 50% of the material has a diameter ≤ 0.2 cm.

Gasser proceeded by describing square-meter plots for each substratum, completed by a full-species list per substratum. The according maps can be found in the appendix. She also surveyed four comparison plots that were not part of the deposit, and one plot on the artificially afforested part of the deposit. These five plots were described in order to (1) study differences and analogies with the

species on the rockslide deposit, (2) risk an educated guess concerning the further evolution of vegetation establishment, (3) find out whether artificial afforestation had been efficient.

3.2.1.2 Relevant results

In 1995 mosses were clearly the best represented plants, in all substratum types. Appendix K (p.121) shows a list of species found on the different substratum types. This shows that several species of woody plants were already present four years after the event. The percentages of woody plants compared to the complete number of plants (no mosses included) for the different substratum types is as follows: 2% for the large blocks, 30% for the smaller blocks, 38% for the water-influenced zones, 6% for the fine-grained debris, and 6% for the silt. Which plants are considered as woody plants can also be seen in Appendix K (p.121).

Gasser (1995) stresses the differences in vegetation density amongst the various substratum types. Four years after the event, the large blocks and water-influenced debris show the lowest number of individuals and species. Silty zones also have a lower number of individuals, compared to the zones with large and smaller blocks. It is clear that numerous variables influence the vegetation density, and even if all of them were known, it would be hard to impossible to say which of them are dominant. This becomes extremely clear within the micro-topography of the large blocks, where highly exposed surfaces are found only meters away from shady, moist areas.

A lot of species are found both on the deposit and on the comparison plots. Other species are found only in the comparison plots, which is not highly surprising, since not all plants do equally well on different surfaces, and much depends on seed dispersal. The number of species thriving on the deposit, and lacking on the comparison plots, however, is remarkable. Although Gasser did not find any woody plants among these, it is important to mention this fact, since it underlines the possibility of seed import over long distances.

In cases as these, that have never been studied before, trying to predict the future development is walking on a slippery slope. Gasser (1995) states that in general the vegetational cover will increase, and that possibly the number of woody plant species might decrease. It could however also increase. No further reasons are mentioned. The number of species per square meter is expected to increase. The total number of species will not significantly increase, the composition however will change. Gasser describes the afforestation as inefficient, based on the low variety of species, which massively lags behind the variety seen on the other deposit surfaces. She doubts whether this can ever be compensated for, since pioneer plants tend to be in high need of light, which they will not receive due to the dense cover of few species. The only way the variety of species, and therefore the quality would improve, were the fact that these seedlings might appear to be highly unadapted and become dominated by others.

Gasser (1995) compared her study to other pioneer vegetation studies on glacier forelands. This comparison shows that the succession in Randa clearly develops at higher speed. The rockslide deposit shows already after four years, species that thrive but after tens of years on glacial foreland. This is due to the better climatologic circumstances and the larger number of species in the valley, compared to glacial forelands.

4 Methods and material

4.1 Fieldwork and sample preparation

Fig 42. Fog and rain often hindered visibility *(LVdB)*.

The fieldwork was performed from 21 August 2009 to 21 September 2009 and from 27 March 2010 to 31 May 2010. As the growth season at this altitude starts after May and ends in early October no time correction (with respect to a new cycle of secondary and primary growth) had to be made. The first days of both periods were used for site inspection and to get acquainted with the terrain. An introduction to the different (sampling) methods in the field was held during the first week. Apart from two days used for surveying and mapping the fieldwork was done individually. The fieldwork during the second survey was considerably delayed by weather conditions (Fig 42), as well as by rock blastings at the lower boundary of the cone, which locally enhanced rockfall danger. Rain, fog, frost and snow often made the ascent too dangerous, causing debris flows, and enhancing rockfall activity. The following is a description of the used dendrochronological methods, as well as a detailed description of the procedure used in the field. Under Appendix M (p.129) a schematic representation of the fieldwork is shown.

4.1.1 Standard dendrochronological methods

There are two possible ways to conduct age determination by counting the rings of a tree. The first one is destructive and implies that the tree is felled, in order to count the rings in a horizontal transect. The second way is by using an increment borer, to produce a core either at breast height or at ground level. This method brings along the risk that the central ring (or pith at ground level) is missed and that therefore not all rings can be counted (it is however possible to extrapolate the number of rings, based on the curvature of the rings). For this reason, it is advisable to extract more than one core, as well as in order to record possible variability in tree-ring width due to the growing position. Coring at or near ground level is, in practice, not always possible, and therefore was not used for this study.

Growth rings are to be microscopically counted along three axes in order to prevent miscounting. The first ring is considered to be the first

Fig 43. Top: contrast-rich larch wood / Bottom: contrast-poor birch wood *(LVdB)*.

true ring outside the pith at the centre of the tree, and the final ring counted is adjacent to the active bark. When the contrast between the adjacent rings is too low (Fig 43), it can be enhanced by using a contrast agent such as chalk. For trees that show rings with great contrast between early- and latewood no contrast agent is necessary. The contrast can however diminish with time. In this case it can be enhanced again by repolishing the section or - which may be useful in the field - by making a fresh cut with a sharp knife and rubbing chalk against it (which has the same contrast enhancing function as the dust that comes free during the polishing). For tree species that do not show enough contrast to distinguish rings with the naked eye (such as birches), a photograph of the cross-section can be made and the contrast can be digitally enhanced (making a photocopy will have the same effect).

It is also possible to determine tree age of some species without felling, by counting the bud-scale scars on the stem (Fig 44). When the buds open, the bud scales fall away, leaving behind bud-scale scars on the surface of the twig. These are visible for a few years until they are covered over by bark. From the bud-scale scars it is possible to trace back the age and the growth in length of the shoots for a few years (Schweingruber, 1983).

Fig 44. Two encircled bud-scale scars on a larch twig *(LVdB)*.

4.1.2 Field and sampling procedures

A distinct area of the rockslide was divided into plots, hereby taking into account surface area, substratum type (Fig 45) and tree density, so as to give a representative image of the vegetation on the cone. The substratum was divided into three grain size categories:

1. large blocks (at least 50% of the blocks has a diameter > 1 m),
2. medium and smaller blocks (at least 50% of the blocks has a diameter from 1 – 0.3 m),
3. fine-grained debris and silt (at least 50% of the blocks / grains has a diameter < 0.3 m).

Thus 171 plots were marked, of different size and shape (see Appendix L, p.127). Every single plot was marked with a number from 1 to 171, and a measuring point. Marking of the measuring points was done with bright spray paint. Boundaries and vertices were marked with bright spray paint or marker band. Marks were sprayed in order to be seen from afar, so that measuring could be done individually afterwards. The plotted area is situated approximately between 1380 and 1500 m a.s.l. Plotting higher up the slopes, or along the northern and southern borders of the cone could not be done due to rockfall danger. Other areas were left out because human interference changed the structure of the original deposit or because the forest was only semi-natural (seeding, artificial afforestation etc). For 93 plots the exact number of trees was determined, the character of the substratum in terms of grain size was described and whenever relevant, comments on the non-tree

Fig 45. From left to right: (1) fine-grained debris and silt, (2) medium and smaller blocks, (3) large blocks *(LVdB)*.

vegetation were made. The remaining 78 plots were each individually compared to one of the exact surveyed plots, and as so, reliable estimates of tree density were made.

The division of plants in tree and non-tree vegetation was partially arbitrary and was merely established as such for personal convenience. Being well aware of the fact that for example both juniper and elder are woody plants of possibly equal size, the first was categorised as tree and the second as non-tree vegetation. Juniper was considered non-tree vegetation since there were only few representatives on the deposit, which in addition never reached a height above 30 cm, and most likely will soon be suppressed and dominated by other, better-suited species. As such, it is justifiable to classify them here, amongst individuals of a herbaceous nature. Thus, an accurate description and identification of all present non-tree species is of no relevance for this research, and therefore only grasses, fireweeds, strawberry, raspberry, juniper, and alpine rose have been taken into account. Their occurrence was divided into following classes:

1. grass,
2. raspberry or fireweeds or alpine rose or juniper,
3. raspberry and fireweeds,
4. raspberry, fireweeds and juniper,
5. raspberry, fireweeds, grass, juniper and alpine rose.

The division in these classes represents both species variability (ordered as such, classes show a higher number of species from class 2 to 5), and abundance (in practice, a higher number of species implies a higher number of individuals).

Fig 46. Damage due to rock impact on a larch *(LVdB)*.

For all the trees, possible damage due to rock impact (Fig 46), browsing (Fig 49) and fraying (Fig 48) were recorded. Possible dieback of the top was registered as well (Fig 47). For some plots it was not possible to reach all or even any of the trees within. In this case, estimations of height were made from a distance. Other denoted species-specific information is described below, as is the specific field procedure per species. Also, tree abbreviations are mentioned, that are used further on in several tables in the result section.

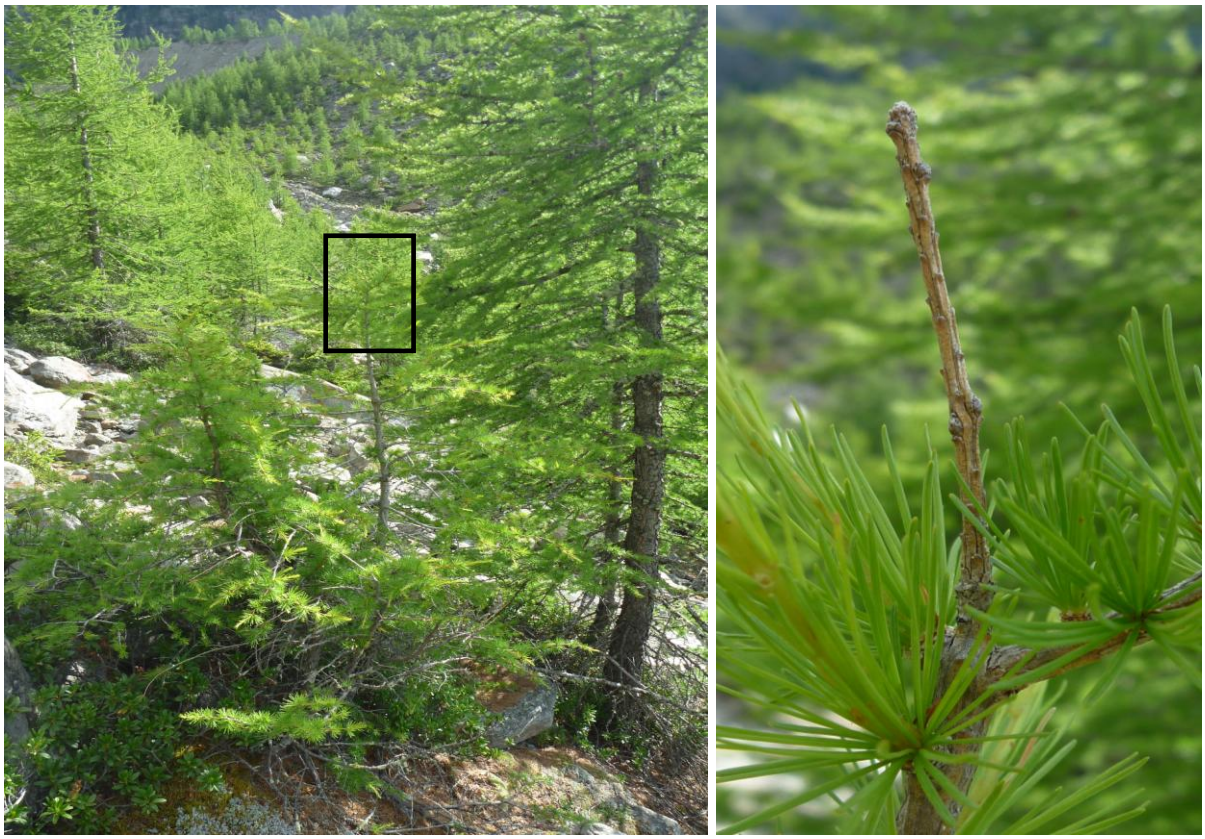

Fig 47. Dieback of the top of a larch (*LVdB*).

Larch (LADE)

For all larches, we measured their height and determined their age by counting the bud-scale scars. Approximately three larches per plot were felled, unless felling a higher number due to uncertainties seemed favourable. Growth rings of the felled trees were counted, so as to verify the bud-scale scar dating method.

Rings of larches generally show enough contrast, even to be counted in the field. This was done for some of the samples, others were taken to the lab, in order to gain time in the field or because a more precise analysis was required. For all felled larches the diameter (without bark) was measured, so as to obtain the average width of the growth rings for each tree.

For plots with a large quantity of (often very small) trees, that were mostly situated in areas with a relatively finely grained substratum, several height groups were established, into which the trees were placed by estimation. Instead of determining the age of every larch by counting its bud-scale scars, 10% of the trees of the respective height group were felled and growth rings were counted, in order to obtain a mean age for the trees of the group.

Fig 48. Damage due to fraying on a larch *(LVdB)*.

In some cases the tree of interest could not be felled at ground level, due to undisplaceable surrounding rocks. Whenever this occurred, the years obtained by counting the bud-scale scars between the ground and felling level were added to the age obtained by counting the rings.

On the northern side of the cone several trees were too large to be felled with the handsaw and were therefore felled with a chainsaw (Fig 50). This was necessary because, due to covering over of the stem with older bark, bud-scale scar age determination was rendered impossible. It is common knowledge that the largest trees are not necessarily the oldest, but considering the aim of our research, it seemed unwise not to sample this group. Increment borers could have also been used, but this would have been more time consuming and less efficient, considering that most of these trees were surrounded by implacable rocks, generally more than one sample core is required, and boring at ground level was not always possible.

Birch (BEPE)

For the birches the height of each individual was measured, unless (as in the case of the larches) for the plots with a relatively large quantity of trees. Here as well, height categories were established, for which the number of trees was estimated.

As to get an idea of the age of the birches, 39 trees of different height in random plots were felled. For all trees age determination was done in the lab, due to the need of enhancing the contrast between early- and latewood.

Norway spruce (PIAB)

For the spruces height was measured and approximately 10% of the trees were felled per plot in order to determine their age at the lab, since, in all of the cases, the rings were to narrow to be counted in the field, despite the very good contrast between early- and latewood.

Fig 49. Damage due to browsing on a larch *(LVdB)*.

Other trees

Trees of other species were registered as such, were counted, and their height was measured. Trees too small to determine their species were placed in a category 'undefined seedlings' (in figures and tables further on abbreviated as UNSE). Whenever relevant (e.g., for trees with no distinct leading stem), the surface area covered by the branches was estimated. Encountered species were green alder (ALVI), sycamore maple (ACPS), European red elder (SARA), purple willow (SAPU), goat willow (SACA), and trembling aspen (POTR).

All obtained samples were marked numerically (plot number) and alphabetically per species (tree letter). The samples were marked several times, either with lumber chalk or a plain pencil on the upper horizontal section or the bark (as to not polish the mark away), or by carving if the tree was producing too much resin (which makes writing unclear). Since most of the samples were not examined until a couple of weeks after felling, they were stored outside and well-aired whenever possible, in order to prevent moulding, which also makes writing unclear. All samples were polished with sanding belts of three different grain sizes (80, 150 and 320).

Fig 50. Nineteen years after the rockslide event, larches of a respectable diameter grow on the deposit *(LVdB)*.

4.1.3 Topographical survey

Distance measuring was done with a Nikon Laser 550AS device, compass and clinometer. Of every plot the sprayed measuring point and / or several vertices were precisely localised by measuring the distance to a point on the other valley flank that was marked on the topographical map used in the field (*Landeskarte der Schweiz* (Swisstopo, 2003), scale 1 : 25 000, Blatt 1328 Randa). Plot boundaries and at least one diagonal were measured so as to calculate the plot area. The compass

was used but for checking general directions, since measurements failed to attain the required precision.

4.2 Data processing

The data resulting from the field survey were gathered in two Excel-databases: (1) a database containing the data obtained at plot level (grain size, non-tree vegetation, number of trees per species, total number of trees, area), and (2) a database containing the data obtained at tree level (species, height, bud-scale scar age, growth-ring age, diameter, damage). The former was afterwards further extended by data retrieved from ArcGIS (Version 9.3) (ESRI, 2009). Statistical analysis and modelling of these data was done with R (Version 2.11.1) (R Development Core Team, 2010).

4.2.1 Geographical data processing with ArcGIS

In a first phase, the topographical data were used to map the surveyed area. Additional data were retrieved from ArcGIS as to complete the Excel-database containing the data obtained at plot level. All values were calculated for plot centroids: aspect (°), slope (°), altitude (m a.s.l.), distance to the Vispa river (m), and distance to the nearest wood border (m). Aspect azimuths range from 22° to 157°. For convenience, the exact values were transformed into classes:

1. 22° ≤ northeast-facing slopes (ne) < 67°,
2. 67° ≤ east-facing slopes (e) < 112°,
3. 112° ≤ southeast-facing slopes (se) < 157°.

These breaks of 45° were automatically set by ArcGIS. Further on in the result section, these three aspect classes will be used in stead of the exact aspect values. Distances to the Vispa river and the nearest wood border are of possible importance for seed dispersal: vegetation tends to thrive in a riparian environment, and nearby forests mainly consist of larches and spruces, thus both can be seen as possible sources of seeds.

In a second phase, several maps representing the (1) grain size distribution, (2) tree-density distribution for various species, (3) temporal distribution of seedling-abundance for larches, and (4) temporal larch density distribution were extracted. Variable colour classes were mostly derived by use of the Jenks (Natural Breaks) Optimisation method, so as to enhance visual perception. This is a data classification method, designed to determine the best arrangement of values into different classes, by minimising each class's average deviation from the class mean, while maximising each class's deviation from the means of other classes (Jenks, 1967). Thus, the method seeks to reduce the variance within classes and to maximise the variance between classes. The method however does not very well depict evolution of a variable with time, since the chosen classes will differ along with the distribution of the population. In this case equal breaks were set manually.
For this step, the results were classified in following age categories, established for larches, based on their exact bud-scale scar age (estimations were made for the 78 plots with no exact data):

1. 19 > age ≥ 15 (germinated in spring 1991 / 1992 / 1993 / 1994 / 1995),
2. 15 > age ≥ 12 (germinated in spring 1996 / 1997 / 1998),
3. 12 > age ≥ 9 (germinated in spring 1999 / 2000 / 2001),
4. 9 > age ≥ 6 (germinated in spring 2002 / 2003 / 2004),
5. 6 > age ≥ 3 (germinated in spring 2005 / 2006 / 2007),
6. 3 > age ≥ 0 (germinated in spring 2008 / 2009 / 2010).

Thus, the temporal development of larch abundance and density can be visualised for intervals of about three years. The first interval is set larger, since no seedlings are expected in the year of and the year after the rockslide.

4.2.2 Statistical data processing

The first phase of data processing consisted of descriptive statistics. Trends and variance were observed for tree height (ergo tree growth) and tree density. Distribution of tree age was studied to determine ecesis time. A second phase consisted of inferential statistics. Thus, tests, correlations, and models (explaining tree growth and tree density) were used to analyse the formerly observed trends and variances in growth and density. Also, the reliability of bud-scale scar age determination was tested by comparing it to growth-ring age determination. Used methods are described below.

4.2.2.1 Descriptive statistics

Bar charts

A bar chart is a chart with rectangular bars of which the length is proportional to the value they represent (Pinnekamp & Siegmann, 2001). The variant used in this study is a stacked bar chart, where several partial values are stacked, creating a full bar that represents the total of the partial values. This is useful when visualising percentages, as is done for tree abundance per grain size category.

Box plots

Box plots are the most convenient way to plot variables represented by non-overlapping categorical values to variables represented by a range of numerical values (Zuur et al., 2009). Thus, box plots are used to plot tree density to grain size and aspect.

A box plot is a way of graphically depicting groups of numerical data (per category) through their five-number summaries: both extreme values, the median, and two quartiles (quantile values that divide a sorted data set into four equal parts, so that each part represents one fourth of the sampled population) (Fig 51). The use of the box is uniform: bottom and top represent respectively the lower and upper quartiles, and the band near the middle is the median. In addition, the width of the box is set proportional to the number of observations per category. The whisker length however, is not uniform. According to Tukey (1977), the length of the whiskers is at maximum one and a half times the inter-quartile distance (1.5 x IQR). This however does not necessarily mean that each whisker ends at exactly this value. Whiskers end at the most extreme value within this range. Thus, whisker length is

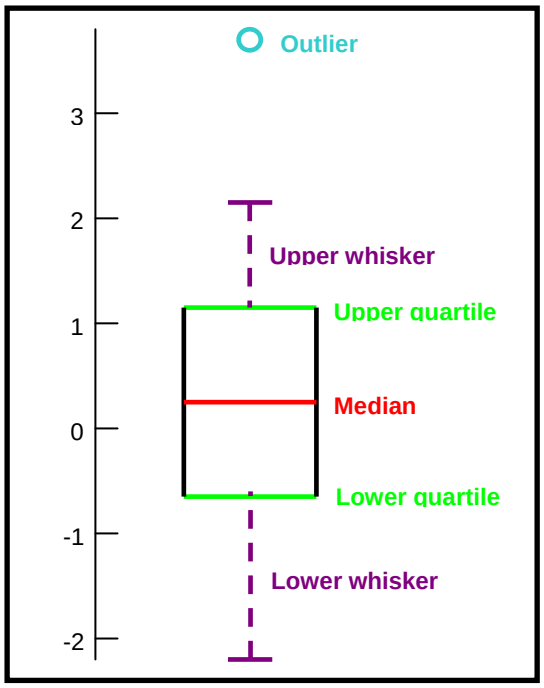

Fig 51. A Boxplot (*LVdB)*.

affected by the values in the database and by the inter-quartile distance, and therefore both whiskers are not necessarily of equal length. When there are no values outside of the 1.5 x IQR boundaries, as they are set by default in R, and used for the plots in this study, the whisker length depicts the maximum and minimum values (Zuur et al., 2009). If this however is not the case, the extreme values are plotted individually in the diagram. These values can be seen as (possible) outliers. Grubbs (1969) defines an outlier as "an outlying observation, or outlier, is one that appears to deviate markedly from other members of the sample in which it occurs".

Histograms

The total area of a histogram is equal to the number of data. The categories of a histogram are usually specified as consecutive, non-overlapping intervals of a variable (Zuur et al., 2009). The intervals must be adjacent, and are chosen to be of the same size. Histograms are used to show the height distribution for the sampled populations of larches, birches and spruces.

4.2.2.2 Inferential statistics

Kruskal-Wallis test

To find out whether the differences in tree density for different substratum groups are significant, a Kruskal-Wallis test can be used. The Kruskal-Wallis one-way analysis of variance by ranks is a non-parametric method for testing equality of population medians among groups (Kruskal & Wallis, 1952). Since the method is non-parametric, the test does not assume a normal population, unlike the analogous one-way analysis of variance (ANOVA). However, the test does assume an identically-shaped and scaled distribution for each group, except for any difference in medians. To find out between which groups differences exist, a post-hoc multi comparison test after Kruskal-Wallis is required (Zuur et al., 2009).

Spearman's rank correlation coefficient

Spearman's rank correlation coefficient (ρ), is a non-parametric measure of the statistical association between two variables (Zuur et al., 2009). It assesses how well their relationship can be described. If there are no repeated data values, a perfect Spearman correlation of + or – 1 occurs, when each of the variables is a perfect monotone function of the other.

Regression models

Modelling techniques are used to test the relationship between a response variable (based on a number of presumably independent observations) and a group of predictor variables. For this study we tried to explain variance in larch growth as a function of following predictor variables: altitude, slope, aspect, and possible tree damage. Variance in tree density can be a function of altitude, slope, aspect, non-tree vegetation, distance to the nearest wood-border, and distance to the Vispa river. The null hypothesis suggests that there is no relationship between the response and predictor variables (Zuur et al., 2009). This hypothesis is rejected if the p-value (which is the probability of obtaining a test statistic at least as extreme as the one that was actually observed, assuming that the null hypothesis is true) is smaller than or equal to the significance or α-level. If a test of significance gives a p-value lower than the significance-level, the null hypothesis is rejected. Such results are referred to as statistically significant (Zuur et al., 2009). The symbolic significance levels, arranged from higher to lower significance, set by R and used in the result section are the following:

1. 0 < *** < 0.001,
2. 0.001 < ** < 0.01,
3. 0.01 < * < 0.05,
4. 0.05 < . < 0.1,
5. 0.1 < < 1.

For this study two types of models were used and are in short described below.

Log-linear regression

Log-linear models study the relationship between a log-transformed response variable and one or more predictor variables. The model is usually defined as:

$$\text{Log}(y) = \beta_0 + \beta_1 x_1 + \beta_2 x_2 + \ldots + \beta_n x_n \quad (1)$$

where β_0 is called the intercept, and β_n is the regression coefficient of x_n. The intercept is the value of log(y) when the value of all independent variables is zero. The model is estimated using the least squares method (Zar, 1999) Each of the regression coefficients then describes the effect size of the predictor variable. A positive regression coefficient means that the predictor variable increases the value of the response variable, while a negative regression coefficient means that the predictor variable decreases the value of the response variable. A large regression coefficient means that the predictor variable strongly influences the value of the response variable, while a near-zero regression coefficient means that that predictor variable has little influence on the value of the response variable. Log(y) is a vector and depicts the log-transformed variable tree height, and x is a matrix, gathering the predictor variables. β is thus a vector with the regression coefficients. Due to the logtransformation of the response variable, it is asserted that the predicted height values are greater than zero. The effect of the predictor variables on the logarithmically transformed response variable is linear (Fahrmeir et al., 2007).

For the log-linear models, the adjusted R^2 is also presented, as this is a measure for the variance explained by the model; this term adjusts for the number of explanatory terms in a model. Unlike R^2, the adjusted R^2 increases only if a new term improves a model more than would be expected by chance (Zuur et al., 2009).

Poisson regression

The predictor variables considered of influence to model tree density are: altitude, slope, aspect, distance to the nearest wood border, distance to the Vispa river and substratum type. For variables that have categories as input values such as aspect and substratum type, R sets one of the categories (in this case eastern aspect and large blocks respectively) as reference category for comparison with the other categories. As we are modelling count data (observations that are non-negative integer values that arise from counting or from derived variables such as tree density), use of a Poisson regression model is appropriate (Zuur et al, 2009). Poisson regression assumes that the response variable y has a Poisson distribution, and that the logarithm of its expected value can be modelled by a linear combination of unknown parameters. The Poisson distribution function is given by

$$f(y;\mu) = \frac{\mu^y \times e^{-\mu}}{y!} \quad (2)$$

which gives the probability for count y given the expected value μ. The expected value μ is estimated using the following regression model:

$$y = \exp(\beta_0 + \beta_1 x_1 + \beta_2 x_2 + \ldots + \beta_n x_n) \quad (3)$$

which can be converted into eq. 1, however it is fitted using maximum likelihood estimation (Zuur et al., 2009). One of the assumptions of the Poisson distribution is that its mean is equal to its variance. However, for the studied data it was found that the observed variance is greater than the mean. This is known as overdispersion, and has to be corrected for. Thus, a quasi Poisson model is used, where an overdispersion factor is calculated (Zuur et al., 2009).

5 Results

5.1 Grain size

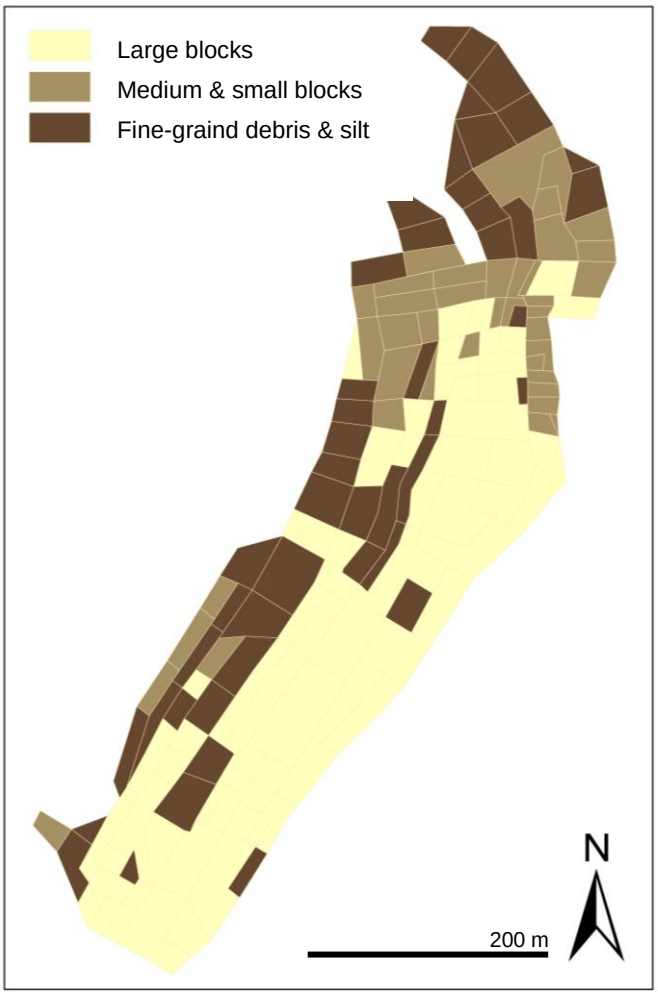

Fig 52. Map representing grainsize distribution: large blocks (0), medium and small blocks (1), fine-grained debris and silt (2).

The surveyed area covers 123 259 m^2 or 12.3 ha, which is 18% of the area covered by the deposit cone. Different grain sizes and their distribution are shown in fig 52. For a total of 171 plots, 84 plots were mapped as having a substratum of large blocks (at least 50% of the blocks has a diameter > 1 m), 40 as having a substratum of medium and small blocks (at least 50% of the blocks has a diameter from 1 – 0.3 m), and 47 as having a substratum of fine-grained debris and silt (at least 50% of the blocks / grains has a diameter < 0.3 m). Towards the northern rim of the surveyed area we find mostly fine-grained debris and silt. In the southeast, where the deposit borders on the Vispa river, large blocks dominate. Between these two rather uniform areas, a transition zone of medium and small blocks can be seen. In the west we find fine-grained debris again, which continues beyond the borders of the surveyed area. As the map shows, some plots with fine-grained debris and silt seem to have intruded the area of large blocks. Observations during fieldwork show that these plots are rather un-exposed, thus most likely allowing accumulation of dust and fine-grained material shortly after the event of 1991. Combined with the influence of weathering and erosion, this can explain their presence.

The pattern in the map largely corresponds with the pattern an observer could describe when looking at the cone from a distance (only the “intruding” plots are hard to distinguish from afar) (see Appendix N, p.130). The northern and southern borders of the deposit are funnel-shaped and not very exposed, thus fine-grained debris and silt could accumulate here. At closer look, one can observe a distinct micro-topography of gullies and small channels within these regions. The largest blocks have a more central position at the outer (eastern) rim of the deposit, and are covered by finer material in the west. They originally also occurred beyond the boundaries of the surveyed area, but they were broached to clear the bed of the Vispa river. One could summarise that, along a north-south axis, the transition from the outer to the inner regions of the deposit, respectively from fine-grained debris and silt to large

blocks, goes over medium and small blocks. This transition can also be seen on the map, for the northern rim of the surveyed area. Along an east-west axis, we see a less gradual transition from large blocks to fine-grained debris and silt.

5.2 Accuracy of the bud-scale scar age determination method

The ages of 1769 larches were determined by means of the bud-scale scar method, 243 of these individuals were also felled, and their growth rings were counted. As can be seen in table 1 both methods resulted in the same age for 116 samples, which is 47.7% of the total number of samples. Another 73 samples showed a difference of only one year, accounting for another 30.1% of the samples. For two individuals a rather high difference of five years was registered.

Table 1. Summary of bud-scale scar age determination (compared to the tree-ring method).

Difference (years)	*Number of samples (n)*	*Additive % of samples*	*Number of overestimated samples (n)*	*Number of underestimated samples (n)*
0	116	47.7 %		
1	73	77.8 %	48	25
2	36	92.6 %	26	10
3	11	97.1 %	11	0
4	5	99.2 %	5	0
5	2	100 %	2	0
subtotal	127		92	35
subtotal %			72.44 %	27.56 %
Total	243	243		

Table 1 also shows that a tendency toward overestimating the age of a larch by counting its bud-scale scars exists: 72% of the samples have an overestimated age, 28% are underestimated. A mean difference of 0.855967 years (≈ 1 year) from the actual age was calculated using the values of all samples. When considering the mean deviance as a percentage of the actual age, it would range from approximately 5% for an old tree of 17 years old, to approximately 43% for a young tree of 2 years old. This can lead us to conclude that the age of old trees can be obtained with a very high accuracy, quite contrary to the accuracy obtained for smaller trees.

The relevance of a mean deviance value generalised over all ages however is doubtful. One easily senses that the likeliness of obtaining a correct bud-scale scar age is related to the age and growth rate of the respective tree. Thus, table 2 shows mean deviances calculated for each actual age value:

Table 2. Mean deviance on the bud-scale scar age, calculated per age class.

Age (years)	*Number of samples (n)*	*Mean deviance (years)*
5	5	0.00
6	6	0.50
7	11	0.73
8	9	0.67
9	9	0.67
10	21	0.48
11	30	0.77
12	36	0.75

13	27	0.85
14	38	0.97
15	33	1.64
16	18	2.33
17	1	0.00

Again, caution is required, since the number of trees felled per age class can hardly be called representative. As expected though, there is a tendency towards higher deviances for older trees: the more bud-scale scars are present, the more can be missed while counting. Only one 17 year old tree was felled, but it is likely that if more were felled, the deviance between both methods would be around two years as well. Comparing all deviance results, we can still conclude that the counting bud-scale scars is a fairly accurate way of determining tree age, provided that the counting is done patiently, and with an experienced eye. A Spearman rho of 0.85 affirms this.

5.3 Primary succession

5.3.1 Spatial and temporal regeneration patterns for larches

As mentioned before, the ages of 1769 larches were determined in the field by means of the bud-scale scar method. The oldest trees on the deposit, of which the age was determined according to this method, were 17 years old (1993). Eight such individuals were found. An additional 18 individuals were found, which were 16 years old (1994). The age distribution of the studied population can be seen in Fig 53A. Estimations based on bud-scale scar data (as is explained in section 4.1.2) resulted in a number of 555 trees with an age above 14 years.

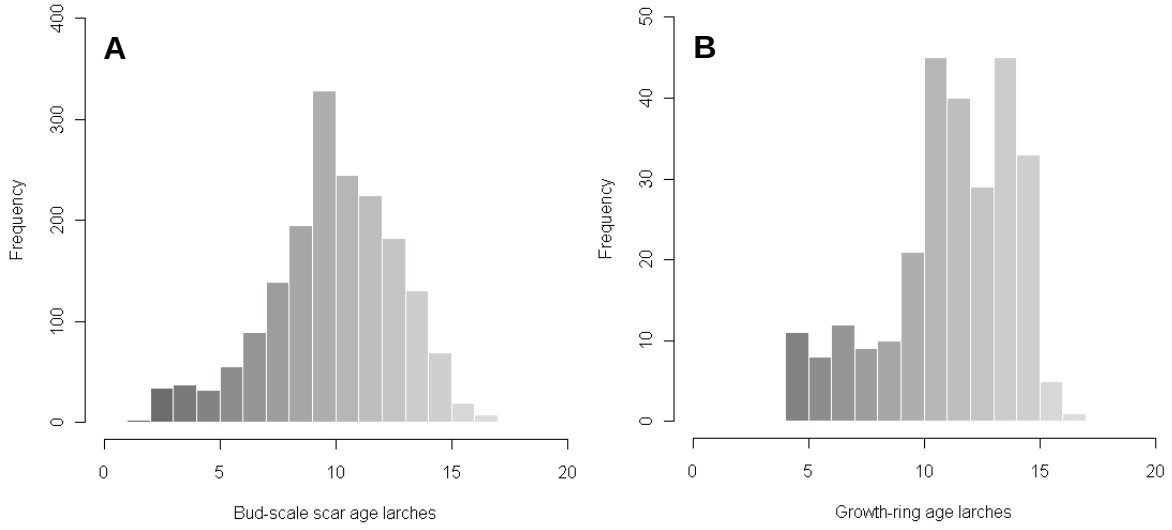

Fig 53. Histograms show the age distribution for larches: (A) bud-scale scar method, (B) growth-ring method.

In addition, growth rings were counted for 269 individuals (for 26 of these individuals, no corresponding bud-scale scar age was determined due to woodening of the bark). The oldest tree of which the age was determined according to this method was also 17 years old. The plot where this

individual was found is marked with a black arrow in Fig 54. An additional five individuals of 16 years were found. Their age distribution can be seen in Fig 53B.
The earlier determined mean deviance for the bud-scale scar method comprises approximately one year when all samples are taken into account. As stated before, no reliable deviance could be retrieved for 17 year old larches alone, although it is likely to be above two years. Therefore we could not conclude from the bud-scale scar data alone that the oldest tree is *a priori* 17 years old. However, the result is affirmed for this one individual by the growth-ring method, and thus we can conclude that two years after the event, some larch seeds had reached the deposit and managed to germinate. Though highly unlikely, we can not fully exclude the possibility of larch germination already one year after the 1991 event.

The maps of fig 54 show the relative distribution of larch seedlings as a percentage of today's total population per plot, at various points in time (as determined in section 4.1.2). The classes are established by the Jenks natural-breaks method and thus each map is at best studied individually. Fig 54A shows that from 1991 to 1995 the surveyed area remains largely un-colonised. The most extreme exceptions can be seen in the east, where in some plots already 50% of the current larch population is thriving. This is also the region where the oldest sample was taken, showing that primary succession most likely must have started here. Other, less explicit exceptions (5 to 10% of the current population) are also present, and they seem to concern plots with substrata of medium and small blocks, and fine-grained debris and silt, as comparison with the grain size map (p.61) shows. Fig 54B, expressing the situation from 1996 to 1998 suggests a fairly explosive phase of colonisation: in the most perceptive plots, 89% of the full population germinated at that time. What does become very clear, is the preserved lack of larches in plots of the large-blocks substratum, whereas plots of other substrata slowly become populated. Highest colonisation rates are still recorded in the northern and eastern regions of the surveyed area. From 1999 to 2001 (Fig 54C), the regions with the highest percentages seem to shift towards the south, and now also the large-blocks substratum is colonised. Less clear is the pattern from 2002 to 2004, in Fig 54D. Some plots are colonised by their full larch-population at this time, others receive no new seedlings whatsoever. Colonisation values diminish again from 2005 to 2007 (Fig 54E); a maximum of 40% of the current population establishes in some plots. We do however distinguish a revival for plots situated in the north, a phase that continues until today. During the last three years (Fig 54F) clearly no new seedlings managed to survive on most of the deposit: especially in the southern and large-block substratum regions colonisation stagnates.

Fig 54 thus shows that there is a distinct difference in the way colonisation progresses, which is likely to be related to the substratum type. And indeed, when verifying ecesis values derived from the growth-ring age for different substratum types, this becomes clear. The oldest larch growing on a substratum of large blocks is 16 years (1994; 3 years ecesis time), compared to 17 years (1993; 2 years ecesis time) on the medium and small blocks, compared to 15 years (1995; 4 years ecesis time) on the fine-grained debris and silt.

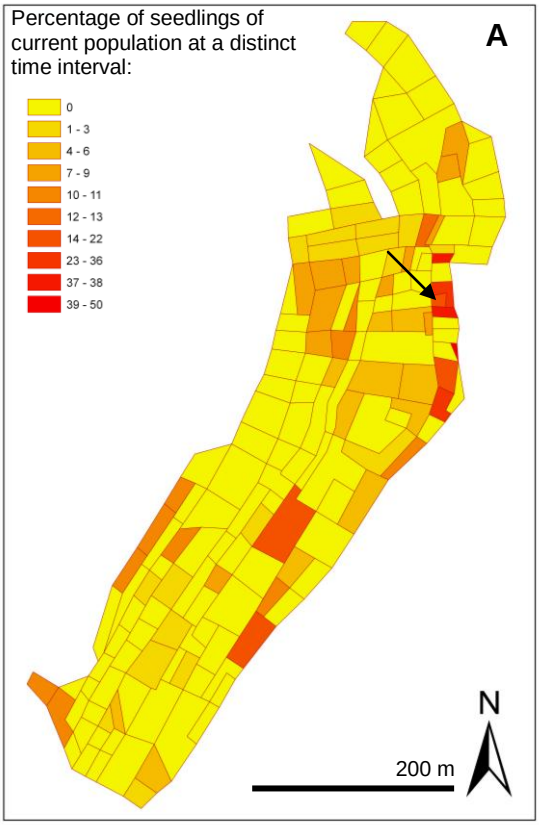
Percentage of seedlings of current population at a distinct time interval:
A
0
1 - 3
4 - 6
7 - 9
10 - 11
12 - 13
14 - 22
23 - 36
37 - 38
39 - 50
N
200 m

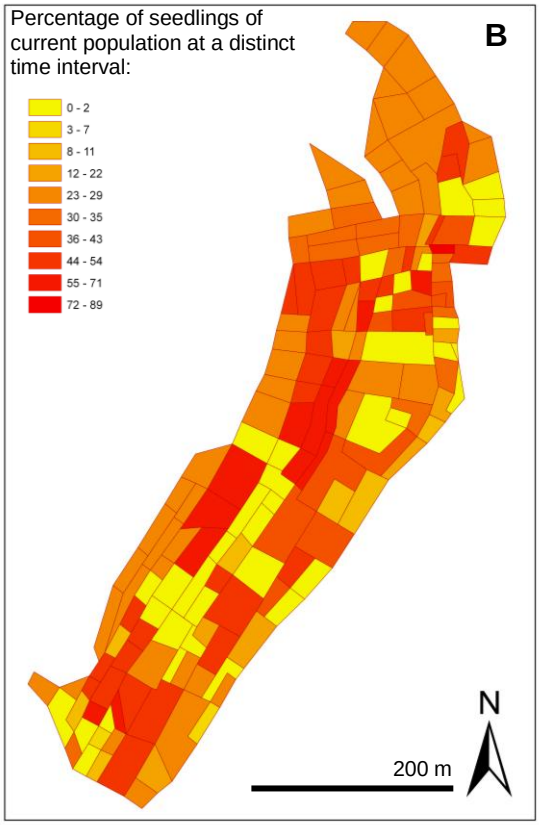
Percentage of seedlings of current population at a distinct time interval:
B
0 - 2
3 - 7
8 - 11
12 - 22
23 - 29
30 - 35
36 - 43
44 - 54
55 - 71
72 - 89
N
200 m

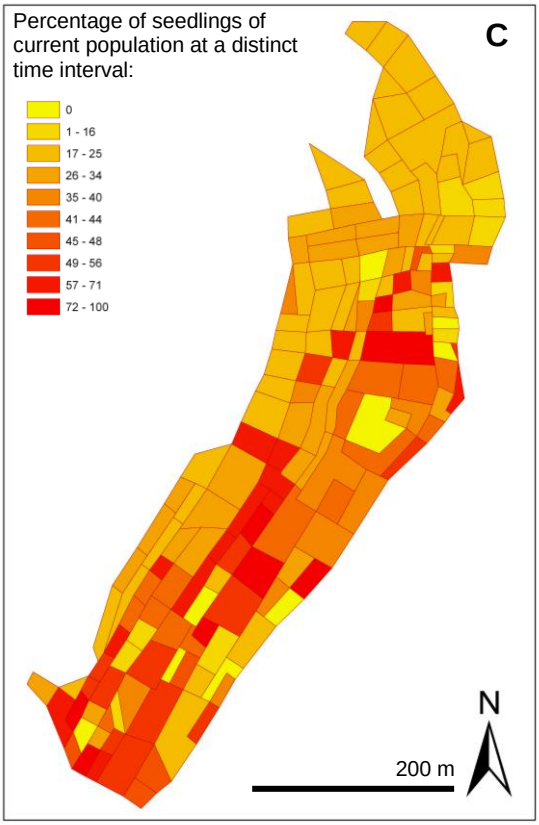
Percentage of seedlings of current population at a distinct time interval:
C
0
1 - 16
17 - 25
26 - 34
35 - 40
41 - 44
45 - 48
49 - 56
57 - 71
72 - 100
N
200 m

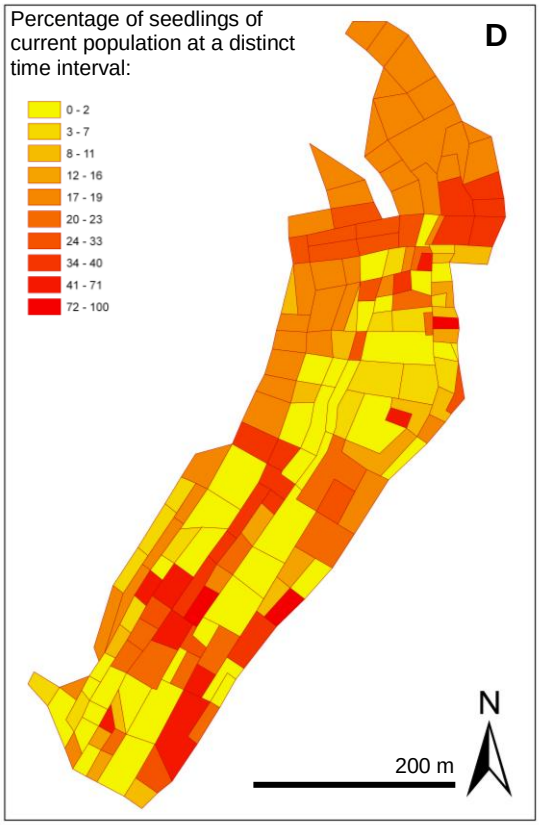
Percentage of seedlings of current population at a distinct time interval:
D
0 - 2
3 - 7
8 - 11
12 - 16
17 - 19
20 - 23
24 - 33
34 - 40
41 - 71
72 - 100
N
200 m

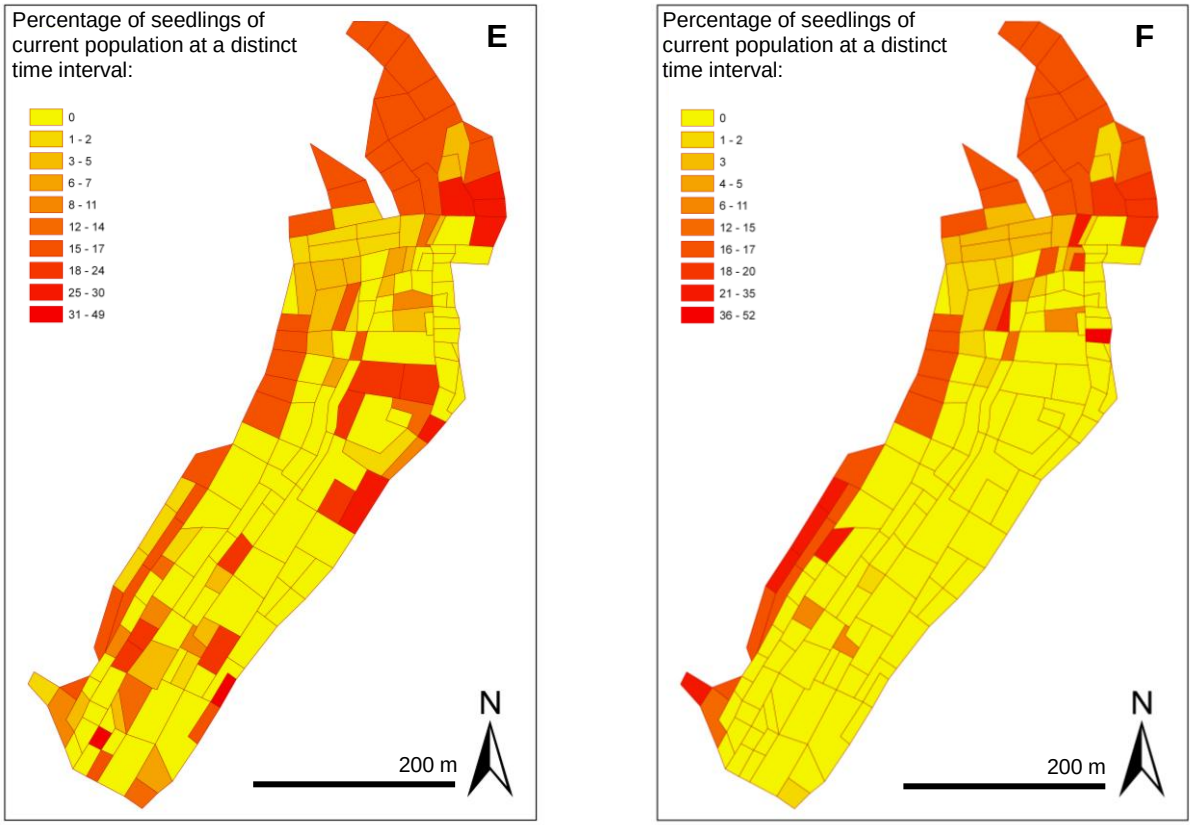

Fig 54. The maps in the figure show the number of new larch seedlings (over a given time interval) compared to the current larch population per plot (expressed as a percentage): (A) 1991 – 1995, (B) 1996 – 1998, (C) 1999 – 2001, (D) 2002 – 2004, (E) 2005 – 2007, and (F) 2008 – 2010. The black arrow in map A points to the plot containing the oldest tree (17 years), according to the growth-ring method. Classes are set by the Jenks natural-break method.

5.3.2 Temporal regeneration patterns for birches

A total of 39 birches was felled, in random plots, spread over the whole surveyed area. Their age distribution can be seen in Fig 55A. The oldest birch found, was 14 years old (1996), followed by two individuals of 13 years (1997), and five individuals of 12 years (1998). Due to the very limited amount of felled birches it is exceedingly unlikely that the oldest individual was felled. Therefore no reliable conclusions, other than that birches were prevalent on the deposit at the latest 5 years after the event, can be drawn. Since birches are well-known for their pioneering behaviour, it is however likely that they colonised the fresh deposit alongside of or even before the larches.

5.3.3 Temporal regeneration patterns for spruces

A total of 45 spruces was felled. Their age distribution can be seen in Fig 55B. One individual had a growth-ring determined age of 17 years old (1993). Nine individuals of 15 years old (1995) were registered. This is rather astonishing, since spruces are not known for being pioneer species, and rather populate an environment during a secondary phase of succession. We can however conclude that, as for the larches, the first seedlings were present already 2 years after the event.

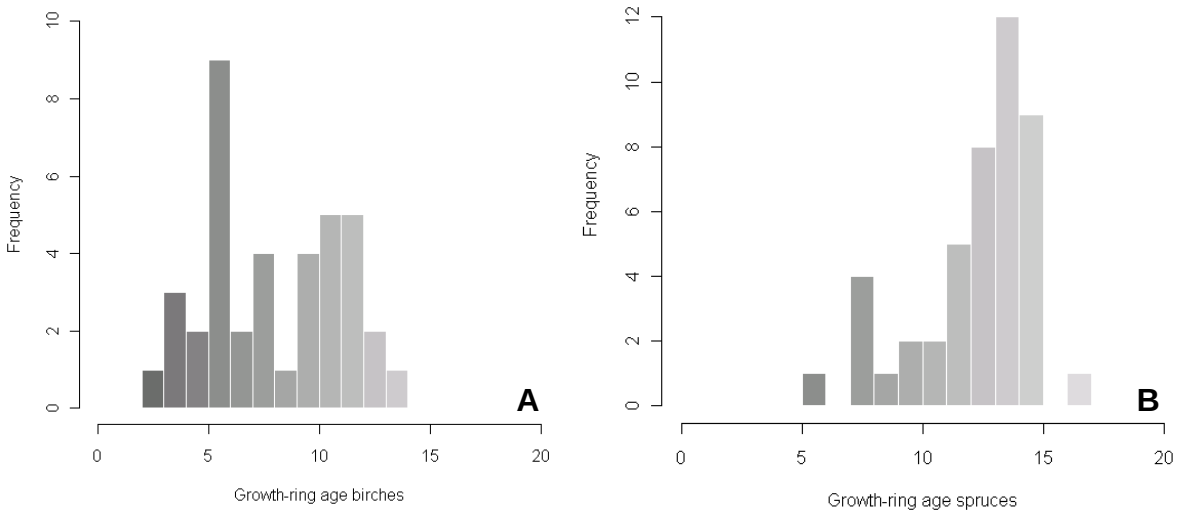

Fig 55. Histograms of age distribution (of felled samples) for (A) birches and (B) spruces.

5.4 Tree abundance and density

5.4.1 Overall abundance and density

Numbers registered for the total surveyed area are listed in Table 3. Used abbreviations are derived from the Latin species names, as mentioned in section 3.1.4. Birches are with 46% dominant over the whole area, followed immediately by larches with an abundance of 45%. The number of spruces lags far behind them, as do the numbers of other species, that are for this and the following sections, conveniently grouped in a REST-categorie. A total density of 4062 individuals per hectare is registered.

The maps in Fig 56 represent tree density of all species, larches, birches, and spruces. When interpreting the images, one has to be aware that classes are defined by the Jenks natural-break method for improving the visual perception within each image, which however does not allow comparison amongst individual maps. All maps show a tendency of higher density towards the northern and western rims of the surveyed area, which seems to be in accordance with the grain size distribution (see map on p.61). Slight anomalies can however be noticed for birches and spruces. For spruces, the distribution is less gradual, we can distinguish plots with a very high density and plots with a very low density, intermediate plots are not very abundant.

Table 3. Absolute and relative abundances of species, and species densities over the surveyed area.

Number of trees

Species	*Absolute*	*Relative*	*Per ha*
LADE	22526	44.996 %	1828
BEPE	22980	45.903 %	1864
PIAB	3028	6.048 %	246
ALVI	373	0.745 %	30
SACA	522	1.043 %	
POTR	338	0.675 %	
SARA	43	0.086 %	
SAPU	66	0.132 %	
ACPS	2	0.004 %	
UNSE	184	0.368 %	
REST	1528	3.052 %	124
TOTAL	50062	100.000 %	4062

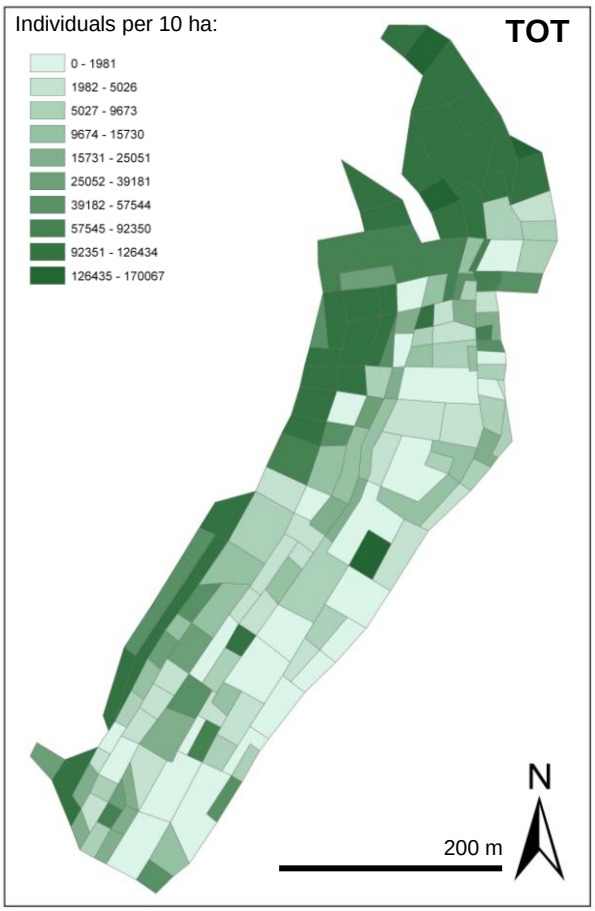
Individuals per 10 ha:
TOT
0 - 1981
1982 - 5026
5027 - 9673
9674 - 15730
15731 - 25051
25052 - 39181
39182 - 57544
57545 - 92350
92351 - 126434
126435 - 170067
N
200 m

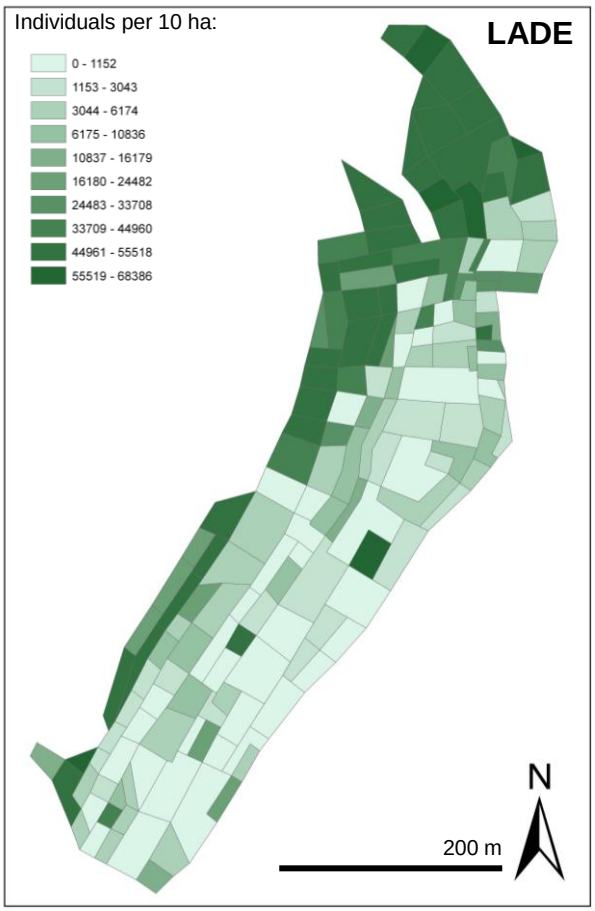
Individuals per 10 ha:
LADE
0 - 1152
1153 - 3043
3044 - 6174
6175 - 10836
10837 - 16179
16180 - 24482
24483 - 33708
33709 - 44960
44961 - 55518
55519 - 68386
N
200 m

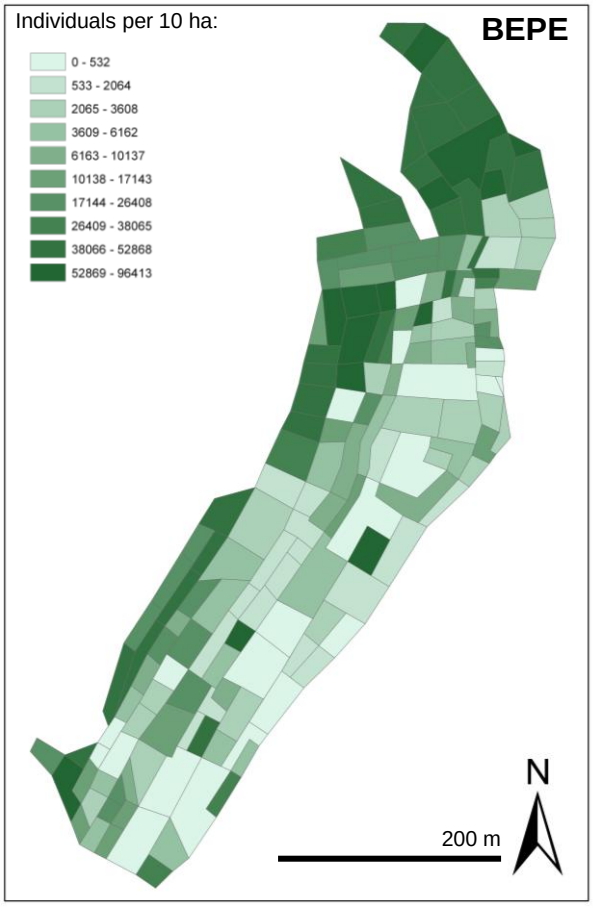
Individuals per 10 ha:
BEPE
0 - 532
533 - 2064
2065 - 3608
3609 - 6162
6163 - 10137
10138 - 17143
17144 - 26408
26409 - 38065
38066 - 52868
52869 - 96413
N
200 m


Individuals per 10 ha:
PIAB
0 - 136
137 - 519
520 - 946
947 - 1653
1654 - 2924
2925 - 4410
4411 - 5556
5557 - 7634
7635 - 10394
10395 - 12132
N
200 m

Fig 56 (page 69). Tree densities (individuals per 10 hectare) for all species (TOT), larches (LADE), birches (BEPE), and spruces (PIAB). Classes are defined by the Jenks natural-break method.

5.4.2 Density and abundance per substratum type

In the following section tables with the absolute and relative numbers of trees per species, and the number of trees per hectare are shown. Pie charts and box plots are added to stress the observed differences between substratum types.

5.4.2.1 Large blocks

Table 4. Absolute and relative abundance of species, and tree densities for a substratum of large blocks.

Number of trees

Species	*Absolute*	*Relative*	*Density (number per ha)*
LADE	2021	41.82 %	321
BEPE	2544	52.64 %	404
PIAB	135	2.79 %	21
ALVI	37	0.77 %	
SACA	9	0.19 %	
POTR	20	0.41 %	
SARA	38	0.79 %	
SAPU	3	0.06 %	
ACPS	2	0.04 %	
UNSE	24	0.50 %	
REST	133	2.75 %	21
TOTAL	4833	100.00 %	767

Plots characterised by this substratum cover a total area of 62 992 m^2 (6.3 ha), which is 51% of the surveyed area, and 9.3% of the area covered by the deposit cone. For plots with a substratum consisting of large blocks, the difference in abundance (more than 10%) and density between larches and birches is more explicit than for the overall deposit (as described under section 5.4.1). Spruces and other species (REST-category) are represented by approximately equal numbers. A density of 767 individuals per hectare is registered.

5.4.2.2 Medium & small blocks

Table 5. Absolute and relative abundance of species, and tree densities for a substratum of large blocks.

Number of trees

Species	*Absolute*	*Relative*	*Density (number per ha)*
LADE	6979	46.75 %	3070
BEPE	7096	47.53 %	3149
PIAB	608	4.07 %	270
ALVI	117	0.78 %	
SACA	127	0.85 %	
POTR	1	0.01 %	
SARA	0	0.00 %	
SAPU	1	0.01 %	
ACPS	0	0.00 %	
GEMU	0	0.00 %	
UNSE	246	1.65 %	109
TOTAL	14929	100.00 %	6624

The area covered by plots characterised by a substratum consisting of medium and small blocks is 22 535 m^2 (2.3 ha), which is 18.3% of the surveyed area, and 3.3% of the area covered by the deposit cone. Birches and larches are the leading species, the difference between their abundances being less than 1%. The abundance of spruces lags far behind them, this is however still about 2.5% higher than the abundance of the "rest"-species. A density of 6624 individuals per hectare is registered.

5.4.2.3 Fine-grained debris & silt

Table 6. Absolute and relative abundance of species, and tree densities for a substratum of large blocks.

Number of trees

Species	*Absolute*	*Relative*	*Density (number per ha)*
LADE	13524	44.64 %	3584
BEPE	13340	44.03 %	3535
PIAB	2285	7.54 %	606
ALVI	219	0.72 %	
SACA	386	1.27 %	
POTR	317	1.05 %	
SARA	5	0.02 %	
SAPU	62	0.20 %	
ACPS	0	0.00 %	
UNSE	160	0.53 %	
REST	1149	3.79 %	305
TOTAL	30298	100.00 %	8030

Plots with a substratum of fine-grained debris and silt cover an area of 37 732 m^2 (3.8 ha), which is 30.6% of the surveyed area, and 5.6% of the area covered by the deposit cone. Comprising less than 0.5%, the difference in abundance between larches and birches can be neglected. The abundance of spruces however lags far behind, as in turn does the abundance of other species (REST). A density of 8030 individuals per hectare is registered.

5.4.3 Trends in tree density

Birches and larches are clearly the dominant species over the whole deposit, and within the different substratum types. The differences between their respective abundances seems to diminish with grain size: from approximately 10% for the large blocks to approximately 0.5% for fine-grained debris and silt. Their abundances are massively ahead over that of the spruces. In turn, spruces are much more abundant than the single, un-grouped other species (REST). Variation of tree density with grain size becomes clear when looking at the box plot of Fig 57. Densities clearly increase with decreasing grain size. The same trend as for tree abundance is observed: differences in density between larches and birches diminishes with decreasing grain size. These patterns could also be clearly noticed in the field. Another field observation was that density seemed to increase towards the north of the deposit. A quick look at Appendix O (p.132) learns that most of these plots have a north-easterly aspect. It also is clear that tree density as a sum of all species increases with decreasing grain size. A closer look will be taken at these and other relationships when modelling tree density.

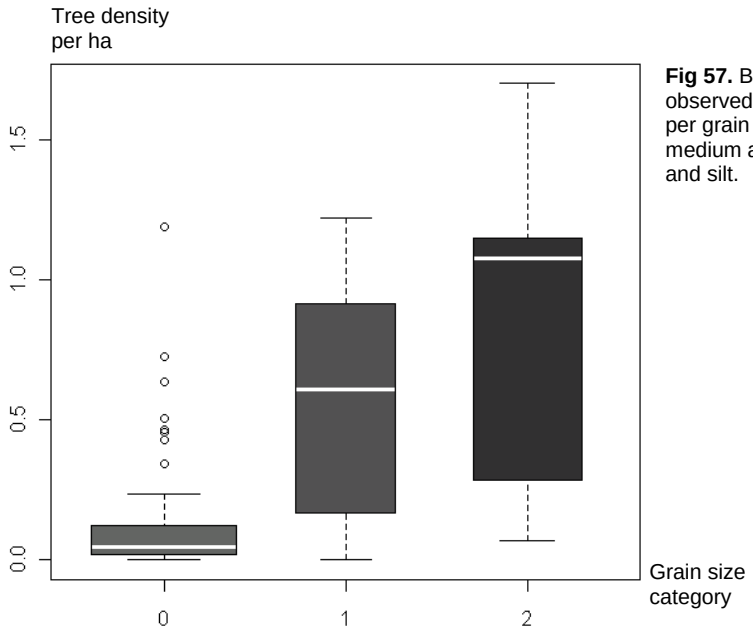

Fig 57. Box plot A shows the differences observed in tree density (individuals per hectare) per grain size category: (0) large blocks, (1) medium and small blocks, (2) fine-grained debris and silt.

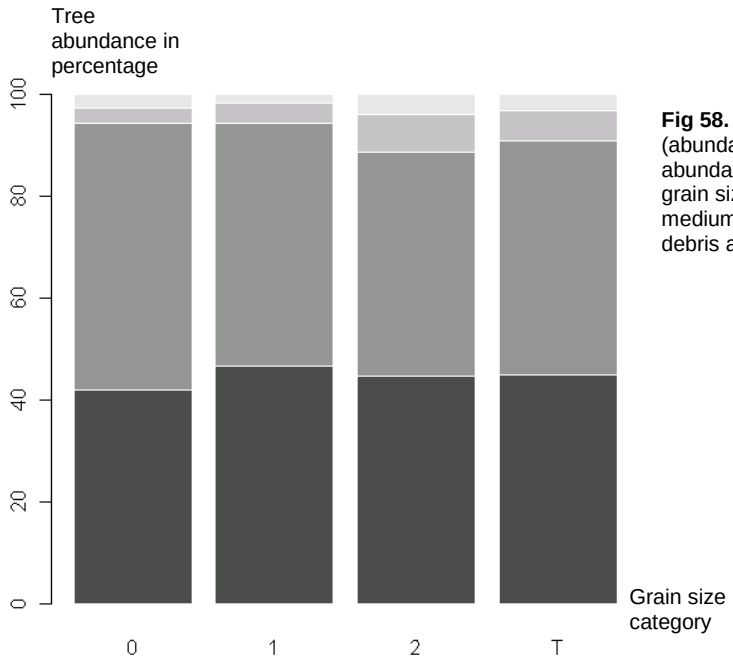

Fig 58. Relative tree abundance (abundance per species / total abundance; as a percentage) for each grain size category: (0) large blocks, (1) medium and small blocks, (2) fine-grained debris and silt.

5.4.4 Modelling tree density

For all models, initially, the distance from the plot centroid to the Vispa river was incorporated. However, this parameter seemed to mask the influence of others and is positively autocorrelated with altitude, and negatively autocorrelated with slope. Thus this parameter was eliminated. In the following densities of larches, birches, spruces, and all species are modelled (quasi Poisson regression model, see equations (1) and (2) on p.60).

5.4.4.1 Larches

Table 7. Summary of the larch density model. Results obtained on 171 observations.

Coefficients

	Estimate	*Std. Error*	*t value*	*Pr(>|t|)*	*α-level*
(Intercept)	-7.820	6.617	-1.182	0.239	
Altitude	0.011	0.005	2.137	0.034	*
Slope	-0.020	0.022	-0.931	0.353	
Northeast	0.727	0.173	4.192	4.52E-05	***
Southeast	-0.089	0.216	-0.410	0.683	
Distance to wood border	-0.002	0.002	-1.154	0.250	
Medium & small blocks	1.359	0.250	5.442	1.90E-07	***
Fine-grained debris & silt	1.674	0.220	7.619	1.98E-12	***

The table above shows that the variance in density amongst larches can be explained mainly by aspect, and grain size. We can derive that larch density is higher on northeast-facing slopes relative to east-facing slopes. A possible cause for this might be the reduced danger of dehydration on northeast-facing slopes. The most important factor is however substratum: density is higher within the medium & small blocks, and highest on fine-grained debris and silt, relative to the large blocks. This seems logical, since trees can not grow on bare rock, and the colonisable environments are thus rare within the large-block substratum. Larch density also seems to depend on altitude, though in a minor way. Densities increasing at higher altitudes are however not the relationship one would expect. Thus, caution is bid: it is easily sensed that larch density will not continue to increase with altitude beyond the boundaries of the surveyed deposit, therefore this relationship should not be generalised. Slope and the distance to the nearest wood border have no significant influence on the density of larches. For the surveyed area, the variation in slope is minor. However, when looking at the cone, it becomes clear that tree density significantly diminishes in regions with a steeper slope, at higher altitude. The correlation (however not significant) between density and distance to the nearest wood border is as expected: densities increase closer to wood borders.

5.4.4.2 Birches

Table 8. Summary of the birch density model. Results obtained on 171 observations.

Coefficients

	Estimate	*Std. Error*	*t value*	*Pr(>|t|)*	*α-level*
(Intercept)	1.641	6.634	0.247	0.805	
Altitude	0.003	0.005	0.680	0.498	
Slope	-0.016	0.022	-0.702	0.484	
Northeast	0.588	0.190	3.098	0.002	**
Southeast	0.088	0.222	0.395	0.693	

Distance to wood border	1.398	0.253	5.535	1.22E-07	***
Medium & small blocks	1.588	0.215	7.398	6.92E-12	***
Fine-grained debris & silt	0.000	0.002	0.230	0.819	

Variance in density amongst birches can mainly be explained by distance to the nearest wood border, and substratum. The model shows that most variance in density is explained by the substratum type: birch density is significantly higher on plots with medium and small blocks (relative to large blocks). This has the same cause as mentioned for the larches: the space that can be effectively colonised increases with decreasing grain size. There seems to be a rather significant correlation with the distance to the nearest wood border as well: the density increases with increasing distance. At first sight this does not seem a very logical relationship. The nearest forests however, have mainly conifers in their population, birches are hardly encountered. Aspect has a minor influence: the density is higher on northeast-facing slopes. Altitude and slope have no significant influence for the surveyed area.

5.4.4.3 Spruces

Table 9. Summary of the spruce density model. Results obtained on 171 observations.

Coefficients

	Estimate	*Std. Error*	*t value*	*Pr(>|t|)*	*α-level*
(Intercept)	-20.791	8.274	-2.513	0.013	*
Altitude	0.019	0.006	2.994	0.003	**
Slope	-0.031	0.026	-1.213	0.227	
Northeast	0.701	0.218	3.210	0.002	**
Southeast	-0.130	0.249	-0.523	0.602	
Distance to wood border	-0.005	0.002	-2.091	0.038	*
Medium & small blocks	1.450	0.375	3.867	0.000	***
Fine-grained debris & silt	2.514	0.334	7.522	3.43E-12	***

Variance amongst spruce density seems to be well-accounted for by a higher number of variables, compared to larches and birches. The table shows that variance is mainly accounted for by substratum type. Spruces seem to thrive in fine-grained debris and silt, and still do better in the medium and small blocks substratum than they do in the large blocks substratum. Again, we can explain this by the surface area which can effectively be colonised: this increases with decreasing grain size. Less influential parameters are altitude and aspect. More spruces seem to grow at higher altitude. This relationship probably is related to grain size: hardly any spruces were found in the large-block substratum, compared to other types. For the surveyed area, this substratum occurs mainly at lower altitudes. Again, one has to be aware that this relationship can not be extrapolated beyond the boundaries of the surveyed area. Distance to the nearest wood border is of least influence, but still significant. Spruce density increases with decreasing distance to the wood border. As for other species, density is higher on northeast-facing slopes. Slope itself has no significant influence on spruce densities.

5.4.4.5 All species

Table 10. Summary of the tree density model. Results obtained on 171 observations.

Coefficients

	Estimate	*Std. Error*	*t value*	*Pr(>|t|)*	*α-level*
(Intercept)	-2.348	6.361	-0.369	0.712	
Altitude	0.007	0.005	1.469	0.144	
Slope	-0.018	0.021	-0.846	0.399	
Northeast	0.666	0.175	3.807	0.000	***
Southeast	0.002	0.209	0.010	0.992	
Distance to wood border	-0.001	0.002	-0.462	0.645	
Medium & small blocks	1.367	0.243	5.613	8.36E-08	***
Fine-grained debris & silt	1.680	0.210	8.003	2.16E-13	***

The total tree density seems to be related to aspect and substratum type, the variables that also account for the variance observed for each species. Density is - as for al individual species - higher on northeast facing slopes. It is higher as well within the medium and small blocks, and fine-grained debris & silt substrata. Altitude, slope and distance to the nearest wood border have no significant influence on the overall tree density, whereas altitude was of significance for larches and spruces, and distance to the nearest wood border for birches and spruces.

The relationship between tree density and various parameters was also checked by conducting Spearman rank correlation and Kruskal-Wallis tests. Obtained rho values are: 0.54 for distance to the nearest wood border (implying that density increases with increasing distance), -0.17 for distance to the Vispa river (density decreases with increasing distance), -0.01 for altitude (density decreases with increasing altitude), and -0.32 for slope (density decreases with increasing slope). This implies that tree density has the strongest relationship with distance to the nearest wood border, and the weakest with altitude; relationships that are not affirmed by the model. Conducted Kruskal-Wallis tests affirm that the differences in density are significant between all substratum types, but only with a significance value of 0.01 between the fine-grained debris and silt, and the medium and small blocks. Significance values for the other substrata are 0.005.

5.4.5 Evolution of tree density with time

Fig 59 shows the evolution of tree density (as a total of all species) with time. Categories are set with equal breaks and thus the maps can be compared to each other. From the figure it becomes clear that tree density has always been higher in the north and west of the surveyed area and that the contrast has enhanced over time. Again, the previously mentioned correlation between tree density and grain size becomes clear.

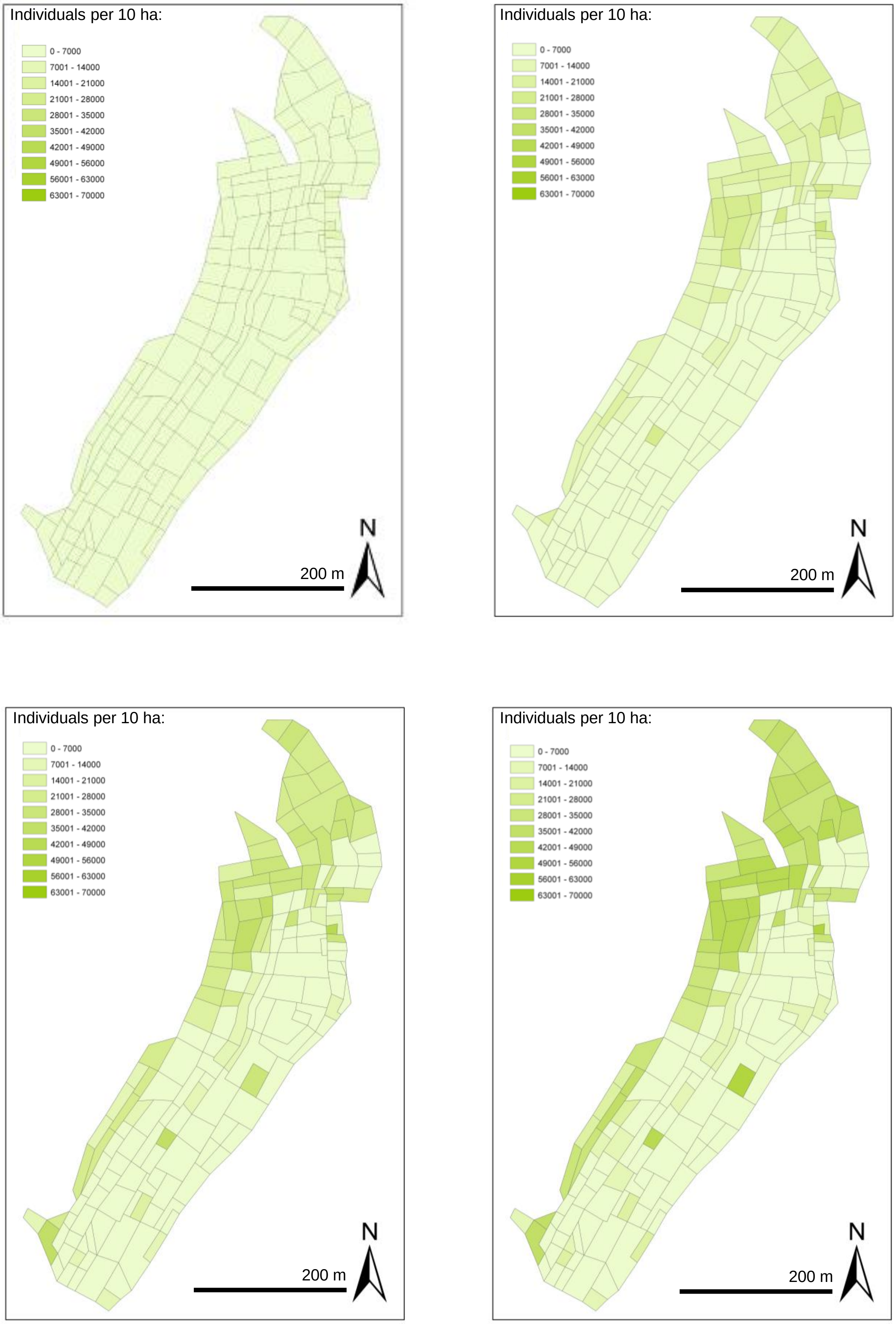
Individuals per 10 ha:
0 - 7000
7001 - 14000
14001 - 21000
21001 - 28000
28001 - 35000
35001 - 42000
42001 - 49000
49001 - 56000
56001 - 63000
63001 - 70000
N
200 m

Fig 59. Evolution of tree density per plot over distinct time intervals: (A) 1991 – 1995, (B) 1996 – 1998, (C) 1999 – 2001, (D) 2002 – 2004, (E) 2005 – 2007, and (F) 2008 – 2010. Classes are manually set with equal breaks of 7000 trees per 10 ha.

5.5 Tree growth

Tree growth is regarded per species. The following models try to explain variance in growth rates (log-lineair regression model, see equation (1) page 59). A Kruskal-Wallis test conducted on height of all species versus grain size, shows that the difference between all grain size groups is significant (α-level = 0.001).

5.5.1 Larches

Table 11. Summary of the larch growth model. Results obtained on 1769 observations.

Coefficients					
	Estimate	*Std. Error*	*t value*	*Pr(>|t|)*	*α-level*
(Intercept)	-12.874	1.810	-7.113	1.64E-12	***
Bud-scale scar age	0.243	0.006	38.534	< 2.00E-16	***
Browsing	-0.248	0.125	-1.983	0.047	*
Dieback of the top	-0.073	0.154	-0.475	0.635	
Rock impact	0.043	0.315	0.136	0.892	
Medium & small blocks	0.212	0.069	3.052	0.002	**
Fine-grained debris & silt	-0.147	0.060	-2.443	0.015	*
Grass	-0.337	0.084	-4.027	5.89E-05	***
Raspberry / Fireweeds / alpine rose / Juniper	-0.063	0.053	-1.193	0.233	
Raspberry & Fireweeds	0.301	0.137	2.195	0.028	*
Raspberry, Fireweeds & Juniper	-0.079	0.092	-0.853	0.394	
Raspberry, Fireweeds, Juniper, gras & alpine rose	0.407	0.081	4.999	6.33E-07	***
Altitude	0.007	0.001	5.769	9.39E-09	***
Northeast	0.815	0.152	5.371	8.87E-08	***
Southeast	0.321	0.057	5.635	2.04E-08	***
Slope	0.011	0.006	1.760	0.079	.
Tree density	-0.247	0.056	-4.403	1.13E-05	***

This model explains 51% of the variability in larch height (adjusted R^2 value of 0.5122 and p-value of $2.2x10^{-16}$). The height of a larch is mainly determined by its (bud-scale scar) age, by the surrounding non-tree vegetation, by the altitude at which it grows, by aspect, and by the density of the surrounding tree population. The age of the individual is by far the most controlling factor: the older the tree, the taller it can be. Larches at higher altitude seem to become taller. Again, it needs to be stressed that this is true only for the surveyed area and not for the whole deposit. Larches growing on northeast- and southeast-facing slopes thrive, compared to those growing on east-facing slopes. Whenever tree density is high, individuals remain smaller. This can be explained by competition between trees. A highly variable non-tree vegetation seems to be stimulating tree growth. A vegetation as such might be an indication of good soil quality, which would explain increasing tree growth. On the other hand, a non-tree vegetation of only grass seems to decrease growth. This relationship as such does not make very much sense, however, the explanation might again be sought in the soil quality. Grasses are not very demanding, perhaps colonise certain areas that are hardly good enough to be colonised by other species, and thus indicate a rather poor soil quality. Other, less affecting factors are the substratum, damage due to browsing and the slope. The fact that the tallest trees grow on a substratum of medium

and small blocks already became clear during the fieldwork. Competition seems to dominate on the plots with high tree density, of which the majority happens to have a substratum of fine-grained debris and silt, thus limiting tree growth. Plots with large blocks on the other hand, have only a small colonisable surface, where trees seem to struggle to survive. The larches that colonised the medium and small blocks substratum however, exceedingly reach heights above four meters and corresponding circumferences (this is where repeatedly no bud-scale scar age could be determined and a chainsaw was used for felling). The significance of browsing damage is not very high, the relationship is however logical: browsed trees have growing difficulties. No influence comes from other damage. The least significant factor is slope.

5.5.2 Birches

Table 12. Summary of the birch growth model. Results obtained on 39 observations.

Coefficients

	Estimate	*Std. Error*	*t value*	*Pr(>|t|)*	*α-level*
(Intercept)	-1.7E+01	5.93E+00	-2.937	0.007	**
Growth-ring age	9.18E-02	2.93E-02	3.132	0.004	**
Grass	-3.01E-01	3.09E-01	-0.977	0.338	
Raspberry / Fireweeds / alpine rose / Juniper	-5.29E-02	2.51E-01	-0.210	0.835	
Raspberry & Fireweeds	-9.22E-02	4.13E-01	-0.223	0.825	
Raspberry, Fireweeds & Juniper	6.04E-01	4.45E-01	1.359	0.186	
Raspberry, Fireweeds, Juniper, gras & alpine rose	6.90E-01	3.10E-01	2.229	0.035	*
Medium & small blocks	7.06E-02	3.63E-01	0.195	0.847	
Fine-grained debris & silt	-3.57E-01	3.82E-01	-0.935	0.359	
Altitude	1.24E-02	4.25E-03	2.910	0.007	**
Northeast	5.10E-01	2.38E-01	2.142	0.042	*
Southeast	-3.63E-01	3.81E-01	-0.951	0.351	
Slope	-4.22E-04	3.36E-02	-0.013	0.990	
Tree density	-9.66E-01	3.73E-01	-2.589	0.016	*

This model explains 76% of the variability in birch height (Adjusted R^2 of 0.7555 and p-value of 6.473×10^{-7}). The height of birches depends mainly on their age (however, a higher number of samples would have been favourable to affirm this), and on the altitude. Birches growing at higher altitudes grow taller than those at lower altitudes. Again, this should not be extrapolated beyond the boundaries of the surveyed area. Other less clear influences come from non-tree vegetation, aspect and tree density. A rather species-rich non-tree vegetation seems to stimulate the growth of birches. As for the larches, this might be an indication of soil quality. Also, one sees that the larches on northeast-facing slopes are thriving, compared to those on east- and southeast-facing slopes.

5.5.3 Spruces

Table 13. Summary of the spruce growth model. Results obtained on 3028 observations.

Coefficients

	Estimate	*Std. Error*	*t value*	*Pr(>|t|)*	*α-level*
(Intercept)	-2.614	0.844	-3.097	0.002	**
Browsing	0.159	0.143	1.113	0.266	
Medium & small blocks	-0.079	0.060	-1.301	0.193	
Fine-grained debris & silt	-0.067	0.060	-1.111	0.267	
Grass	0.101	0.050	2.032	0.042	*
Raspberry / Fireweeds / alpine rose / Juniper	0.373	0.163	2.295	0.022	*
Raspberry & Fireweeds	0.379	0.305	1.243	0.214	
Raspberry, Fireweeds & Juniper	-0.101	0.161	-0.626	0.531	
Raspberry, Fireweeds, Juniper, gras & alpine rose	0.0258	0.133	0.194	0.846	
Altitude	0.001	0.001	1.620	0.105	
Northeast	0.091	0.039	2.293	0.022	*
Southeast	0.046	0.032	1.436	0.151	
Slope	-0.006	0.003	-1.685	0.092	.
Tree density	0.012	0.045	0.270	0.787	

The first model that was ran for spruces also contained their growth-ring determined age, and explained 4% of the variability in spruce height (adjusted R^2 of 0.0413 and p-value of 0.3524). In this case, growth-ring determined age was however the only significant variable. When removing it, we see an influence of non-tree vegetation, aspect, and slope. This model explains 0.2% of variability in spruce height (adjusted R^2 of 0.00255 and p-value of 0.07901). The presence of non-tree vegetation stimulates spruce growth. Most likely this is (as for the two former species) an indication for enhanced soil quality. As with the other species, a northeast-facing slope implies improved growth rates. Also, a logical relation is seen between growth and slope: trees do not grow (tall) on steep slopes. Whether or not it is sensible to remove the age from the model is point of discussion, since it is only logical that spruces can grow taller with increasing age. Both models however have a very low adjusted R^2 value, and thus none of them is very reliable.

6 Discussion

6.1 Previous work

The classes and distribution of substratum type used in this study (3 classes as specified under section 4.1.2, p.51), significantly differ from that used by Gasser (1995) (5 classes as specified under section 3.2.1.1, p.47, and mapped under Appendix K, p.121). Over the past 19 years, the deposit has undergone continuous changes. Erosion by wind and water has further moulded topography. Continued rock fall activity over nearly two decades might also have had an influence, although minor within the surveyed area. The deposit's topography, and the released volumes generally do not allow rock transport over a distance long enough to reach the surveyed area. Frost and thaw also have an important influence. The classification used by Gasser (1995) is therefore no longer sufficient. In addition, it became clear during fieldwork that establishing more than three classes would neither improve data quality, nor efficiency.

When we compare the maps of the area surveyed in this study, and that of the grain size zones of Gasser (1995), we can conclude that geographically, the large blocks crudely correlate with Gasser's class 1, the medium and small blocks with Gasser's class 2, and the fine-grained debris and silt with Gasser's class 4 (see section 3.2.1.1, p.47). As so, this research affirms that the lowest number of tree seedlings is found in the large-blocks substratum. Gasser (1995) also described a higher seedling number for the medium and small blocks. Results for the fine-grained debris and silt however differ significantly. Whereas this study suggests high seedling numbers, Gasser (1995) suggests low numbers. However, this may be partially due to the fact that the classes still differ. Possibly a mixing value of Gasser's classes 3, 4 and 6 should be taken into account (see section 3.2.1.1, p.47).

Gasser (1995) also stated that seed dispersal over large distances was likely, which might explain the lack of correlation between distance to the nearest wood border within the density models. She correctly predicted that the vegetational cover would increase, this research however did not confirm her assumed decrease in number of woody plant species.

Although not explicitly surveyed while not among the goals of this study, a word can be said on the artificially afforested zone northeast of the deposit. Gasser (1995) stated in her survey this happened in a highly inefficient manner, that would hardly prove to be successful unless competition became more important. Fifteen years later can clearly be observed that the afforested zone is thriving with larches, most likely with the highest density of the whole deposit. Grain size in this zone ranges from small and medium blocks to fine-grained debris and silt, from which we may conclude that the afforestation was rather efficient since analogous plots in general show a comparable tree density, but smaller tree heights for the given ages.

6.2 Method

6.2.1 Modelling of tree density and tree growth

The obtained models allow prediction of tree density and growth on analogous deposits. Predictions of tree density were made with a 95% confidence interval (expresses the possibility of obtaining a predicted value equal to the measured value). The predicted values were then - by hand and plotting - compared to the observed values, so as to check the validity of the model. The difference between both values was in general acceptable, however to obtain a fully reliable validation check for the models, another analogous deposit should be sampled, in order to have a second data set (differing from those on which the model is based) to compare to the predicted values. Apart from the fact that no such recent analogous deposit exists (which implies that an older deposit should be studied, with older trees that are considerably harder to sample, since the destructive method is not an option), this would imply an additional high amount of fieldwork and sampling. However, this can be avoided by splitting the existing data set: 75% of the data are thus used to base the model on, the other 25% are used to verify the model.

6.2.2 Patterns in tree density and tree growth

The maps retrieved from ArcGIS that show the current density distribution of various tree species (Fig 56, p.69), and the models that explain tree density, all show a tendency of higher values towards the west. Caution is wanted here and the reader has to be aware of the fact that this tendency only applies to the surveyed area and not to the whole deposit. Field observations clearly show that beyond the boundaries, tree density markedly diminishes towards the west. Possible causes are the steepening terrain, the increased distance from wood borders and the Vispa river, the grain size which implies maximal exposure of plant individuals (fine-grained debris and silt, with no larger blocks to provide any shade for seedlings), the increased influence of rock fall activity, and the increased influence of water. The same factors can influence tree growth, and here as well caution has to paid, not to extrapolate the explaining values beyond the boundaries of the surveyed area. Also, it has to be remembered that altitude is positively autocorrelated with proximity to the Vispa river and negatively autocorrelated with proximity to wood borders. Theoretically, variables should be independent of each other, in practice however this condition is very hard to fulfil.

6.2.3 Future rockslide age determination using dendrochronology

The obtained results allow dating of other analogous rockslide deposits in the Matter Valley and beyond (see Appendix D, p.99). For dating of such deposits some guidelines have to be kept in mind. When casting a look at the forests in the valley, it becomes clear that the abundance of birches will diminish with time (they become outcompeted) and that conifers will finally be dominant. Thus, only the results obtained for spruces and larches will be of relevance within aged forest stands (as all on rockslide deposits in the Visper Valleys are). This study has shown that tree growth and density for larches mainly seem influenced by aspect and substratum type, and as so, these parameters have to be kept in mind when sampling another rock slide deposit due to their dominant influence on the germination and survival of seedlings.

It is only natural that the rockslide deposits undergo further changes with time (e.g., geomorphological and pedogenic changes), and therefore it might not be evident to recognise substratum classes analogous to the ones defined within this study. However, the classification of substratum types in this study was kept simple and forward, and so it is considered feasible to largely distinct analogous types on other rockslides.

As for the aspect, we can not be sure that the same effects will dominate. First of all are most rockslide deposits in the valley are situated on eastern flanks (see Appendix D, p.99), which implies that these deposits will not have eastern-facing slopes like the Randa deposit. Also, aspect is a measure that gathers a number of climatic influences such as wind direction, amount of rain fall, and hours of sunshine. It can clearly be sensed that especially parameters such as wind direction can be highly variable in mountainous terrain, even over very short distances. Thus, one has to be careful when interpreting and including this parameter in future research.

6.2.4 Possibilities of future research

The collected samples contain an additional highly informative source of information: the width of the individual growth rings. This parameter is partially incorporated in the measurements of stem diameters of the samples, which is of course a function of growth ring width. Diameter values were however not used for the modelling since the correlation with tree age was found to be too strong. Individual ring width however is not correlated with tree age. A relationship with soil parameters, tree exposition, or tree stand is more likely, and thus these data could be used to improve the existing models. Collecting and processing these data, implies several additional weeks of work, and therefore was not conducted in the frame of this study. In the future however, this will be done.

It would be sensible to incorporate an additional class of water-influenced debris, as is described by Gasser (1995), in case the surveyed area would be further expanded in future. The influence of erosion by water was not significant for any of the described plots, however the influence did become significant just north and south of the described area. During the second period of fieldwork it became clear that after heavy rainfall repeatedly new gullies and small channels were formed, that collect high amounts of water which are capable of derooting trees up to 2 m high. It is clearly sensed that this has a considerable influence on tree density.

As stated under the previous heading, it might be of interest to sample and study a second historically described rockslide deposit as to verify the models explaining tree density and tree growth.

6.3 Ecesis determination in glacial forefields

Several studies have been conducted on the tree-ring dating of moraine surfaces. As for this study, the germination date of the oldest tree provides a minimum estimate for stabilisation of the surface; and a closer estimate is obtained by adding an ecesis value to the age of the oldest tree. Ecesis values determined in such studies estimate the time elapsed between deglaciation (or moraine formation and stabilisation) and germination of the first tree to survive and be sampled. Some exemplary obtained ecesis values are: 6 to 30 years on Coleman Glacier, Mt. Baker, USA (Heikkinen, 1984); 10 to 20 years in the Canadian Cordillera (McCarthy & Luckmann, 1993); 10 to 20 years on

Morteratsch Glacier, Switzerland (see Appendix A, p.96) (Bleuler, 1986; Burga, 1999); and 14 to 34 years on Ventina Glacier, Italian Alps (Garbarino et al, 2010). In all cases, exept the latter, various conifer species were sampled. In the study of Garbarino et al. (2010) however, only takes larches are taken into account. These results clearly show that fresh surfaces resulting from glacier retreat need 3 to 17 times more time than fresh rockslide surfaces to stabilise. Responsible for this rather large time difference can be a number of environmental factors: the number of "safe sites" (e.g., depressions, shaded sites created by large rocks) is clearly higher on the rockslide surface than on a moraine surface; the nearest wood borders are in general rather far away from a glacier front, thus seed dispersal is inhibited; considerably lower temperature ranges (ice-box effect) (Holtmeier, 2003) and cold wind harshen the glacier front environment and make it unfavourable for colonisation; glacier front terrain is a more favourable dwelling for several animal species (e.g., deer, chamois, and ibex), which would imply increasing tree damage due to fraying and browsing; and the mostly fine-grained material of a moraine surface is easily eroded by wind and water.

6.4 Importance of this study

Age determination of various other rockslide deposits might allow us to gain insight into the possible causes of these processes (as the are listed for the rockslide of Randa in section 2.6.4.11, p.30). Compared to other rockslides in the Saas and Matter Valleys, the Randa rockslide is of medium size. The rockslide events of Täschgufer, ABC-Gufer, and Moosgufer (events of a size equal to the Randa event; also situated in the Matter Valley; see also Appendix D, p.99) were dated with lichenometry. Their ages were set between 600 and 1500 years (Bloetzer et al., 1998). Additional dating by means of dendrochronology seems favourable.

The causes of rockslides seem to be of multiple nature. For one thing, their origin has to be sought in long term processes such as changes in pressure, internal rock balance, and forces due to the glacier retreat since the Last Ice Age (10 000 a). These factors continue to weaken already disturbed rock masses over longer time. However, it is most likely that one or more triggering factors give the final push for the event to happen. Systematic age determination of all of these processes might allow us to discover trends and patterns in the rockslide frequency in recent years in the Matter and Saaser Valleys. As Appendix D (p.99) clarifies, most deposits are found on the eastern valley flanks, due to its previously mentioned reduced stability (section 2.6.3, p.22). However, dating of these rockslide deposits becomes of relevance when one is interested in the frequency and nature of possible triggering factors. It is clear that it is of utmost importance to have the most accurate age determinations possible for this purpose. Thus, age determination can be coupled to existing data on earthquake magnitude or frequency, unusual climatic extremes (e.g., harsh winters, hot summers, extreme rain falls), or abrupt glacier retreat (section 2.6.4.11, p.30). As so, triggering mechanisms can be defined (and their number might be further extended), which will be of use to hazard and risk management.

7 Conclusion

The area surveyed for this research is characterised by three substratum types: (1) large blocks, (2) medium and small blocks, (3) fine-grained debris and silt. By means of counting bud-scale scars and growth rings on larches, as to determine their age, primary succession and colonisation rates have been studied. We managed to retrieve a reliable age determination for surface stabilisation, which seems to be largely controlled by substratum type. The oldest trees are found on a substratum of large blocks, these are 17 years (1993). Trees of 16 years (1994) are found on a substratum of medium and small blocks. The oldest tree found on a substratum of fine-grained debris and silt is only 15 years old (1994). Colonisation by larches started in the north-eastern regions of the deposit. The oldest birch found is 14 years old (1996), however, colonisation by birches probably started along with that of larches. The oldest spruce found is 17 years old (1993).

Also, the scientific value of age determination by means of counting bud-scale scars was studied by comparison with growth-ring age determination. The difference between both methods obtained on all samples comprises one year. We can conclude that the counting of bud-scale scars is a fairly accurate way of determining tree age, provided that the counting is done patiently, and with an experienced eye.

It was the aim of this research to study tree growth and density distribution of various tree species. Birches and larches are clearly the dominant species over the whole deposit, and within the different substratum types. The differences between their respective abundances seems to diminish with grain size. Their abundances are massively ahead over that of the spruces. In turn, spruces are much more abundant than the single other species. We can conclude that highest tree densities were registered on slopes with a northeast-facing aspect (which is possibly related to humidity) and on a substratum of fine-grained debris and silt. Tree growth seems to be mainly correlated with tree age for all species.

The results of this study are of a precision that allows dating of other analogous rockslide deposits, using the obtained ecesis values. They will permit researchers to find out more about the causes of these hazardous phenomena. It is generally assumed that these are to be sought on a large time scale (thousands of years), combined with a sudden triggering effect. The importance of this study mainly lies in learning more about the nature and frequency of these triggering processes, as is allowed by the accuracy of age values obtained with dendrochronology.

8 Samenvatting

In 1991 bedekte een *bergsturz* het gehucht Unnär Lerch, een deel van het Zwitserse bergdorp Randa, gelegen in het kanton Wallis. Hierbij vielen geen dodelijke slachtoffers, wel werden de enige dalweg, de bedding van de Vispa, het tandradspoor en een aantal stallen en vakantiehuisjes begraven onder de rotsmassa. Een deel van de lokale veestapel kwam om en op verschillende plaatsen in Randa accumuleerde tot 50 cm stof. Het atypische verloop van de *bergsturz*, gekenmerkt door een relatief langzaam afbrokkelen van de steenmassa in verschillende fasen, voorkwam ergere schade. De kantonale regering besliste om de na de vrijmaking van dalweg, treinspoor en rivierbedding, de afzetting onveranderd te laten en als wetenschappelijk studiegebied te bestemmen. In dit kader werd reeds één vegetatieve studie doorgevoerd in het gebied (Gasser, 1995).

De Zwitserse geologie laat zich van noord naar zuid grofweg opdelen in drie zones: (1) het Helveticum, (2) het Penninicum en (3) het Oostalpien. Het dorp Randa is gelegen in het Matterdal, dat deel uitmaakt van het Zwitserse Penninicum, een nappencomplex gekarakteriseerd door de hoogste graad van metamorfisme in de Alpen. Specifieker situeert zich de *bergsturz*-afzetting in de Siviez-Mischabelnappe, waar de basis opgebouwd is uit pre-Alpien gemetamorfoseerde sedimenten, graniet en lava's. Deze werden gemetamorfoseerd tot een gneissokkel, men spreekt in dit verband ook wel van Randagneis. De sedimentaire deklagen die werden afgezet op deze sokkelgesteenten worden nu teruggevonden als *Bündnerschiefer* (een schistsoort met hoog glimmergehalte), lokaal spreekt men van *Altkristallin*. De alpiene orogenese startte 65 Ma geleden in het zuiden en eindigde 25 Ma geleden in het noordelijke molassebekken. De tektoniek van de zuidelijke bergketens en dus de regio Randa, wordt sterk beïnvloedt door een fase van *roll back*. In het Matterdal manifesteert zich dit in de aanwezigheid van de Mischabelplooi, die lokaal de sedimentaire deklagen onder de sokkel brengt.
De voet van de bergflank waar de *bergsturz*-afzetting is gesitueerd, bestaat uit massieve en relatief ongestoorde Randagneis, waarboven sterk gestoord *Altkristallin* komt. Op 18 april 1991 verplaatste zich in een eerste fase 20 x 10^6 m^3 richting dal. Hierbij bestond het merendeel van het verplaatste volume uit Randagneis, een kleinere hoeveelheid *Altkristallin* brokkelde af. In een tweede fase, op 9 mei 1991, brokkelde nog 10 x 10^6 m^3 af. Hierbij ging het uitsluitend om het sterk gestoorde *Altkristallin*. Tussen beide fasen werd continu steenslagactiviteit waargenomen. Dit zeer ongewoon tweeledig verloop wordt ook wel beschreven als *twin-stroke behaviour* en is uniek voor het geval Randa.

Het Matter- of Nikolaidal is uitgesleten door glaciale erosie en wordt gekenmerkt door een relatief hoog aantal (al dan niet historisch gedocumenteerde) *bergsturz*-afzettingen. Exacte datering ontbreekt evenwel voor de meeste van deze afzettingen. Aangezien al deze processen plaatsvonden na het terugtrekken van de gletsjers uit de vallei, is een dateringstechniek met hoge resolutie en geschikt voor jonge ouderdommen gewenst. Aldus is dendrochronologie, gezien de aard van de afzettingen, de enige geschikte dateringsmethode.
Belangrijke geologische toepassingsgebieden van dendrochronologie in de Alpen zijn de studie van natuurgevaren en primaire successie. De meeste studies leggen zich toe op onderzoek van de distributie in ruimte en tijd van natuurgevaren zoals modderstromen, steenslag en steenlawines. De

frequentie van dergelijke processen schijnt toe te nemen in de laatste jaren en systematische data zijn doorgaans niet voorhanden. Reconstructie is aldus van belang voor risicomanagement. Studies gewijd aan primaire successie onderzoeken bijvoorbeeld de kolonisatie van glaciaal voorland en kunnen zo de veranderende uitbreiding van gletsjers in kaart brengen. In geen van beide gebieden werd tot nog toe onderzoek verricht naar *bergsturz*-afzettingen, wat deze masterproef een pioniersstatus verleent. Het doel van deze studie is een zo nauwkeurig mogelijke bepaling van de tijdsduur tussen het afzettingsproces en kolonisatie door pionierssoorten. Men spreekt in dit kader ook wel van *ecesis*. Bovendien wordt de distributie van de boomdichtheid en het verloop van de kolonisatie door lorken in ruimte en tijd onderzocht. Er wordt gezocht naar verklaringen voor de ruimtelijke variatie in boomgroei en boomdichtheid. Met deze gegevens kunnen in een volgend stadium ongedateerde *bergsturz*-afzettingen in de regio gedateerd worden. Tevens wordt de wetenschappelijke waarde van ouderdomsbepaling door het tellen van knoppenlittekens getoetst (door vergelijking met de jaarringenouderdom; secundaire groei) bij lorken (*Larix decidua*), aangezien ook hier geen vergelijkbare studies voorliggen. De knoplittekenmethode bestaat erin, de littekens te tellen die achterblijven na de jaarlijkse vorming van een nieuwe scheut aan een stamtop of twijguiteinde (primaire groei).

Het veldwerk bestond in het registreren, karakteriseren en exact lokaliseren van de aanwezige boomsoorten en het bepalen van het substraattype naar korrelgrootte. Dit werd uitgevoerd in augustus en september 2009 en van maart tot mei 2010. Het dient beklemtoond dat de ongure weersomstandigheden in 2010 aanzienlijke vertragingen in de hand gewerkt hebben en dat onder meer optimale condities een nog groter oppervlak van de puinkegel had kunnen onderzocht worden. De verzamelde gegevens zijn evenwel compleet en nauwkeurig, wat analyse en modellering toelaat zonder enig kwaliteitsverlies of nefaste invloed op de resultaten.
Het te onderzoeken gebied werd onderverdeeld in 171 plots, deze werden getypeerd door substraat, hoogteligging, expositie en helling, factoren die een invloed kunnen uitoefenen op de dichtheid en groei van de vegetatie. Verschillende substrata werden geklasseerd als (1) grote blokken (minstens 50% van het materiaal heeft een diameter > 1 m), (2) middelgrote en kleine blokken (minstens 50% van het materiaal heeft een diameter tussen 1 m en 30 cm) en (3) fijnkorrelig puin en silt (minstens 50% van het materiaal heeft een diameter kleiner dan 30 cm). Voor elk plotcentrum werd de afstand tot de dichtstbijzijnde woudgrens en de Vispa bepaald, om de mogelijke relatie met zaaddispersie te bekijken. Alle plots werden nauwkeurig ingemeten met een lasermeter en vervolgens in kaart gebracht met ArcGIS. Wat betreft de aanwezige boomsoorten ging de aandacht in hoofdzaak uit naar lorken, berken (*Betula pendula*) en sparren (*Picea abies*), die samen met lorken de meest abundante boomspecies vertegenwoordigen. Voor de andere boomsoorten werd van elk individu de hoogte en soort bepaald. Voor de lorken werd binnen het onderzochte gebied voor elke vertegenwoordiger de hoogte alsook de leeftijd bepaald, door tellen van jaarringen of knoplittekens. Van berken werd de hoogte bepaald, alsook de ouderdom van 39 specimen door middel van de jaarringenmethode. Dezelfde procedure werd toegepast bij de sparren, hier werden 45 specimen geveld. Voor elke boom werd mogelijke schade door steenslag, knagen en schuren door wild, sneeuwdruk of koprot

opgenomen. Indien relevant werden per plot aanvullende aantekeningen gemaakt betreffende mogelijks competitieve struiken en kruidige planten. Van de 171 plots werden 93 plots gedetailleerd opgenomen, de overige 78 werden elk individueel vergeleken met een gedetailleerd opgenomen plot en zo afgeschat.
De stamdoorsneden van de gevelde bomen werden opgeschuurd, waarna hun leeftijd en stamdiameter bepaald werden in het lab. De verkregen gegevens werden nadien geordend in twee databases in Excel (één met data opgenomen op boomniveau en één met data opgenomen op plotniveau), om geografische analyse met ArcGIS en statistische analyse met R mogelijk te maken.
De analyse met ArcGIS resulteerde in een aantal kaarten die de boomdichtheid per soort en als som van alle soorten voorstellen. Bovendien wordt voorgesteld waar de kolonisatie door lorken op de puinkegel startte en hoe de verdere distributie van nieuwe zaailingen verliep. Verder werd onderzocht hoe de dichtheid van lorken per plot evolueerde doorheen de jaren.
De statistische analyse met R leidde tot de grafische weergave van verbanden en relaties tussen verschillende opgenomen parameters (bv. tussen hoogteligging en boomdichtheid). Verschillende statistische tests werden doorgevoerd om de correlatie van de opgenomen variabelen te onderzoeken. Bovendien werd geprobeerd om de ruimtelijke variatie in boomgroei en boomdichtheid (voor de drie belangrijkste species en als totaal der species) te verklaren aan de hand van respectievelijk een loglineair- en een poisson-regressiemodel. Op deze manier worden vergelijkingen opgesteld aan de hand van een groep predictor-variabelen, die het gedrag van deze twee response-variabelen verklaren.

De resultaten van dit onderzoek wijzen uit dat de ouderdom van een jonge lork accuraat kan vastgesteld worden door een geoefend persoon. De gemiddeld optredende afwijking hierbij bedraagt één jaar. Kolonisatie van de afzetting door lorken vond plaats uiterlijk in 1993 en aldus kan geconcludeerd worden dat het afzettingsoppervlak zich lokaal stabiliseerde 2 jaar na afzetting. Deze datering werd verkregen met de knoplittekenmethode en bevestigd door de jaarringenmethode. Hoewel hoogst onwaarschijnlijk, is het niet uit te sluiten dat reeds één jaar na afzetting al lorken voorkwamen. De kolonisatie van de afzetting door lorken startte in het noordoosten. Ecesis blijkt een samenhang te vertonen met het substraattype. De jaarringenmethode wijst uit dat het oudste individu voorkomt op een substraat van middelgrote en kleine blokken (17 jaar; 1993), gevolgd door het substraat van grote blokken, waar het oudste individu 16 jaar is (1994). De langste ecesistijd wordt vastgesteld voor een substraat van fijnkorrelig puin en silt, hier is het oudste individu 15 jaar (1995).
De kans op kiemen van zaad en overleving van de zaailing schijnt in grote mate gestuurd te worden door de korrelgrootte van het substraat en de expositie. Hierbij worden de hoogste boomdichtheid geobserveerd op een substraat van fijnkorrelig puin en silt en op hellingen met een noordoostelijke expositie (mogelijks gerelateerd aan de vochtigheidsgraad). Algemeen levert dit een beeld op met sterke kolonisatie en hoge dichtheden in het noorden tot noordoosten, en duidelijk lagere dichtheden tussen de grote blokken in het zuiden van de afzetting. Deze resultaten bevestigen gedeeltelijk de resultaten bekomen bij de eerste doorgevoerde studie (Gasser, 1995). Belangrijk hierbij is evenwel dat

de afzetting in de afgelopen 15 jaar significante geomorfologische en bodemkundige veranderingen ondergaan heeft.
Het meest abundant zijn berken, op de voet gevolgd door lorken. Modellering van de variabiliteit in boomdichtheid wees uit dat deze parameter in hoofdzaak gerelateerd is aan: substraattype en expositie voor lorken, substraattype en nabijheid van de bosgrens voor berken en substraattype voor sparren. Modellering van de variabiliteit in boomgroei wijst uit dat deze parameter in hoofdzaak afhangt van ouderdom, hoogteligging, niet-boom vegetatie, expositie en boomdichtheid voor lorken; van ouderdom en hoogteligging voor berken en van niet-boom vegetatie en expositie voor sparren. Deze modellen laten toe voorspellingen te maken inzake boomgroei en boomdichtheid op analoge afzettingen. Vergelijking van de opgenomen waarden met voorspelde waarden (voor een confidentie-interval van 95%) levert bevredigende resultaten; men dient hierbij edoch in rekening te brengen dat vergelijking met een dataset die niet werd gebruikt voor het opstellen van het model preferabel is.

De bekomen resultaten laten toe andere *bergsturz*-afzettingen in het Matter- en Saaserdal te dateren. Van belang hierbij is zich te realiseren op welk substraattype de bomen groeien, en hoe de helling waarop ze groeien geëxposeerd is, aangezien deze parameters dominant zijn voor de verklaring van boomdichtheid en boomgroei. Vergelijking met studies die de datering van glaciaal voorland bestuderen; tonen aan dat de kolonisatie van *bergsturz*-afzettingen 3 tot 17 maal sneller is dan die van glaciaal voorland. Dit is te wijten aan verschillende omgevingsfactoren.
De oorzaken van *bergstürzen* werken enerzijds op lange termijn (terugtrekking van gletsjers sinds de laatste ijstijd en de daaraan gerelateerd druk- en spanningsval in het gesteente; verschuiven van de permafrostgrens); anderzijds is het waarschijnlijk dat actuele processen een triggerende werking hebben (extreme weersomstandigheden, aardbevingen, acute gletsjerterugtrekking). Door nauwkeurige datering van de *bergsturz*-afzettingen kan aldus uitsluitsel gegeven worden over de aard van deze factoren; waardoor het verloop van de processen op zich verduidelijkt wordt. Bovendien is dit een belangrijke stap naar voorspelling en risicomanagement toe.

In het kader van deze masterproef kwam een nauwe samenwerking tot stand met onderzoekers van de Universiteit Bern (Markus Stoffel en Michelle Bollschweiler) en van de *Eidgenössische Technische Hochschule* te Zürich (Christof Bigler).

9 Bibliography

General

[1] *(website)* DENDROLAB. Informations on the Dendrolab. *http://www.dendrolab.ch/.*

[2] *(website)* ETHZ. Informations on the ETHZ. *http://www.ethz.ch/.*

[3] *(website)* METEOSCHWEIZ (2004). Climate in Zermatt. *http://www.meteoschweiz.admin.ch/web/de/klima/klima_schweiz/klimadiagramme/zer.html.* Consulted on 02/06/2010.

[4] BUNDESAMT FUER LANDESTOPOGRAFIE (2004). *Atlas der Schweiz.* Wabern.

[5] BUNDESAMT FUER LANDESTOPOGRAFIE (2003). *1 : 25 000 Landeskarte der Schweiz Swisstopo, Blatt 1328 Randa.* Wabern.

[6] *(website)* BUNDESAMT FUER UMWELT (2010). Statistical maps. *http://www.bafu.admin.ch/*.

[7] *(website)* WIKIPEDIA (2005). Blank map of Switzerland. *http://en.wikipedia.org/wik/File: BlankMap_Switzerland.png.* Consulted on 05/06/2010.

Geology

[8] BLOETZER, W., EGLI, T., PETRASCHECK, A., SAUTER, J., STOFFEL, M. (1998). *Klimaänderungen und Naturgefahren in der Raumplanung*. Vdf Hochschulverlag AG an der ETH Zürich.

[9] BURRI, M. (1992). *Erkenne die Natur im Wallis, die Gesteine*. Editions Pillet Martigny.

[10] *(website)* Earthquake Statistics Group, ETHZ. *http://www.earthquake.ethz.ch/research/Swiss_Hazard/Maps_plots/Hazard_Maps/box_feeder/sw_h_10000_5. Consulted on 09/08/2010.*

[11] *(website)* Swiss permafrost Monitoring Network. *http://www.permos.ch/.*

[12] EBERHARDT, E., STEAD, D., COGGAN, J.S. (2004). *Numerical analysis of initiation and progressive failure in natural rock slopes – the 1991 Randa rockslide.* International Journal of Rock Mechanics & Mining Sciences, 69-87, 41.

[13] ERISMANN, T.H., ABELE, G. (2001). *Dynamics of Rockslides and Rockfalls.* Springer-Verlag.

[14] GASSER, J. (1995). *Vegetationsentwicklung auf dem Bergsturzkegel von Randa (VS)*. ETHZ (Eidg. Forschungsanstalt für Wald, Schnee und Landschaft (WSL)).

[15] GISCHIG, V., LOEW, S., KOS, A., MOORE, J.R., RAETZO, H., LEMY, F. (2009). *Identification of active release planes using ground-based differential InSAR at the Randa rock slope instability, Switzerland.* Natural Hazards and Earth System Sciences, 2027-2038, 9.

[16] GISCHIG, V., AMANN, F., MOORE, J.R., LOEW, S., EISENBEISS, H., STEMPFHUBER, W. (2010). *Composite rock slope kinematics at the Randa instability, Switzerland, based on remote sensing and numerical modeling.* Unpublished.

[17] GRUBER, S., HAEBERLI, W. (2009). *Mountain Permafrost.* Permafrost Soils, Springer Verlag.

[18] HEINCKE, B., GREEN, A.G., VAN DER KRUK, J., HORSTMEYER, H. (2005). *Acquisition and processing strategies for 3D georadar surveying a region characterized by rugged topography.* Geophysics, K53-K61, 70, 6.

[19] HEINCKE, B., MAURER, H., GREEN, A.G., WILLENBERG, H., SPILLMANN, T., BURLINI, L. (2006). *Case History, Characterizing an unstable mountain slope using shallow 2D and 3D seismic tomography.* Geophysics, B241-B256, 71, 6.

[20] LABHART, T.P. (1992). *Geologie der Schweiz* (6th edn). OTT Verlag Thun.

[21] MARAZZI, S. (2005). *Atlante orografico delle Alpi. SOIUSA.* Pavone Canavese (TO), Priuli & Verlucca editori.

[22] OERLEMANS, J.H. (2005). *Extracting a climate signal from 169 Glacier Records.* Science Magazine, 657-677, 308.

[23] PFIFFNER, O.A. (2009). *Geologie der Alpen.* Haupt UTB Verlag.

[24] *(website)* Progressive Rockslope Failure, ETHZ. *http://www.rockslide.ethz.ch/*

[25] SCHINDLER, C., CUENOD, Y., EISENLOHR, T., JORIS, C.-L. (1993). *Die Ereignisse vom 18. April und 9. Mai 1991 bei Randa (VS) – ein atypischer Bergsturz in Raten.* Eclogae Geologicae Helveticae, 643-665, 86.

[26] SPILLMANN, T., MAURER, H., WILLENBERG, H., EVANS, K.F., HEINCKE, B., GREEN, A.G. (2007). *Characterization of an unstable rock mass based on borehole logs and diverse borehole radar data.* Journal of Applied Geophysics, 16-38, 61.

[27] SPILLMANN, T., MAURER, H., GREEN, A.G., HEINCKE, B., WILLENBERG, H., HUSEN, S. (2007). *Microseismic investigation of an unstable mountain slope in the Swiss Alps.* Journal of Geophysical Research, 112.

[28] STAMPFLI, G.M., MOSAR, J., MARQUER, D., MARCHANT, R., BAUDIN, T., BOREL, G. (1998). *Subduction and obduction processes in the Swiss Alps.* Tectonophysics, 159-204, 296.

[29] TRUFFER, B. (1995). *Der Bergsturz von Randa 1991 - Eine Dokumentation*. Naturforschende Gesellschaft Oberwallis.

[30] WILLENBERG, H., LOEW, S., EBERHARDT, E., EVANS, K.F., SPILLMANN, T., HEINCKE, B., MAURER, H., GREEN, A.G. (2008a). *Internal structure and deformation of an unstable crystalline rock mass above Randa (Switzerland): Part I – Internal structure from integrated geological and geophysical investigations.* Engineering Geology, 1-14, 101.

[31] WILLENBERG, H., EVANS, K.F., EBERHARDT, E., SPILLMANN, T., LOEW, S. (2008b). *Internal structure and deformation of an unstable crystalline rock mass above Randa (Switzerland): Part II – Three-dimensional deformation patterns.* Engineering Geology, 15-32, 101.

Dendrochronology and primary succession

[32] ALESTALO, J. (1971). *Dendrochronological interpretation of geomorphic processes.* Fennia, 1-139, 105.

[33] BELLINGHAM, P.J., WALKER, L.R., WARDLE, D.A. (2001). *Differential facilitation by a nitrogen-fixing shrub during primary succession influences relative performance of canopy tree species.* Journal of Ecology, 861-875, 89.

[34] BLEULER, R.M. (1986). *Jahrringanalysen von Laerchen in Gletschervorfeldern.* Dissertation, University of Zuerich.

[35] BLUNDON, D.J., MACISAAC, D.A., DALE, M.R.T. (1993). *Nucleation during primary succession in the Canadian Rockies.* Canadian Journal of Botany, 1093-1096, 71.

[36] BOLLSCHWEILER, M., STOFFEL, M., EHMISCH, M., MONBARON, M. (2007). *Reconstructing spatio-temporal patterns of debris-flow activity using dendrogeomorphological methods.* Geomorphology, 337-351, 87.

[37] BOLLSCHWEILER, M., STOFFEL, M., SCHNEUWLY, D.M. (2008). *Dynamics in debris-flow activity on a forested cone – A case study using different dendroecological approaches.* Catena, 67-78, 72.

[38] BURGA, C.A. (1999). *Vegetation development on the Glacier Forefield Morteratsch (Switzerland).* Applied Vegetation Science, 17-24, 2.

[39] BUTLER, D.R., MALANSON, G.P., WALSH, S.J. (1992). *Snow-avalanche paths: conduits from the periglacial-alpine zone to the subalpine-depositional zone.* Periglacial Geomorphology. John Wiley and Sons, London.

[40] CHAPIN, F.S., WALKER, L.R., FASTIE, C.L., SHARMAN, L.C. (1994). *Mechanisms of primary succession following deglaciation at Glacier Bay, Alaska.* Ecological Monographs, 149-175, 64.

[41] CLEMENTS, F.E. (1916). *Plant succession: An analysis of the development of vegetation*. Carnegie Institution of Washington, Publication, 242.

[42] CROCKER, R.L., MAJOR, J. (1955). *Soil development in relation to vegetation and surface age at Glacier Bay Alaska.* Journal of Ecology, 427-448, 43.

[43] DEL MORAL, R., ELLIS, E.E. (2004). *Gradients in heterogeneity and structure on lahars, Mount St. Helens, Washington, USA.* Plant Ecology, 273-286, 175.

[44] EWING, S. (1996). The Great Alaska Natural Factbook. Alaska Northwest Books Portland.

[45] FANTUCCI, R., SORRISO-VALVO, M. (1999). *Dendrogeomorphological analysis of a slope near Lago, Calabria (Italy).* Geomorphology, 165-174, 30.

[46] FASTIE, C.L. (1995). *Causes and ecosystem consequences of multiple pathways of primary succession at Glacier Bay, Alaska.* Ecology, 1899-1916, 76.

[47] FINKENZELLER, X. (2003). Alpenblumen, Erkennen & bestimmen (2nd edn). Verlag Eugen Ulmer GmbH & Co.

[48] GARBARINO, M., LINGUA, E., NAGEL, T.A., GODONE, D., MOTTA, R. (2010). *Patterns of larch establishment following deglaciation of Ventina glacier, central Italian Alps.* Forest Ecology and Management, 583-590, 259.

[49] GODET, J.-D. (1987). *Bäume und Sträucher, Einheimische und eingeführte Baum- und Straucharten*. Arboris-Verlag.

[50] GUTSELL, S.L., JOHNSON, E.A. (2002). *Accurately ageing trees and examining their height-growth rates: implications for interpreting forest dynamics.* Journal of Ecology, 153-166, 90.

[51] HEBERTSON, E.G., JENKINS, M.J. (2003). *Historic climate factors associated with major avalanche years on the Wasatch Plateau, Utah.* Cold Regions Science and Technology, 315-332, 37.

[52] HOLTMEIER, F.-K. (2003). *Mountain Timberlines: Ecology, Patchiness, and Dynamics*. Kluwer Academic Publishers, Dordrecht.

[53] JONES, C.C., DEL MORAL, R. (2005a). *Effects of microsite conditions on seedling establishment on the foreland of Coleman Glacier, Washington.* Journal of Vegetation Science, 293-300, 16.

[54] JONES, G.A., HENRY, G.H.R. (2003). *Primary plant succession on recently deglaciated terrain in the Canadian High Arctic.* Journal of Biogeography, 277-296, 30.

[55] KREMER, B.P. (1998). *Die Bäume Mitteleuropas*. Kosmos.

[56] MATTHEWS, J.A. (1992). *The Ecology of Recently-Deglaciated Terrain. A Geoecological Approach to Glacier Forelands and Primary Succession.* Cambridge University Press, Cambridge.
[57] MCCARTHY, D.P., LUCKMAN, B.H. (1993). *Estimating Ecesis for Tree-Ring Dating of Moraines: A Comparative Study from the Canadian Cordillera.* Arctic and Alpine Research, 63-88, 25, 1.
[58] MCCARTHY, D.P., LUCKMAN, B.H., KELLY, P.E. (1991). *Sampling Height-Age Error Correction for Spruce Seedlings in Glacial Forefields, Canadian Cordillera.* Arctic and Alpine Research, 451-455, 23, 4.
[59] MONG, C.E., VETAAS, O.R. (2006). *Establishment of Pinus wallichiana on a Himalayan glacier foreland: stochastic distribution or safe sites?* Arctic, Antarctic, and Alpine Research, 584-592, 38.
[60] PERRET, S., STOFFEL, M., KIENHOLZ, H. (2006). *Spatial and temporal rockfall activity in a forest stand in the Swiss Prealps – A dendrogeomorphological case study.* Geomorphology, 219-231, 74.
[61] PIERSON, T.C. (2006). *Dating young geomorphic surfaces using age of colonizing Douglas fir in southwestern Washington and northwestern Oregon, USA.* Earth Surface Processes and Landforms, 811-831, 32.
[62] RAFFL, C., MALLAUN, M., MAYER, R., ERSCHBAMER, B. (2006). *Vegetation succession pattern and diversity changes in a glacier valley, Central Alps, Austria.* Arctic, Antarctic, and Alpine Research, 421-428, 38.
[63] RAYBACK, S.A. (1998). *A dendrogeomorphological analysis of snow avalanches in the Colorado Front Range, USA.* Physical Geography, 502-515, 19.
[64] READER, R.J., BUCK, J. (1986). *Topographic variation in the abundance of Hieracium floribundum: relative importance of differential seed dispersal, seedling establishment, plant survival and reproduction.* Journal of Ecology, 815-822, 74.
[65] SCHLAG, R.N., ERSCHBAMER, B. (2000). *Germination and establishment of seedlings on a glacier foreland in the Central Laps, Austria.* Arctic, Antarctic, and Alpine Research, 270-277, 32.
[66] SCHNEUWLY, D.M., STOFFEL, M. (2008). *Spatial analysis of rockfall activity, bounce heights and geomorphic changes over the last 50 years – A case study using dendrogeomorphology.* Geomorphology, 522-531, 102.
[67] SCHUBIGER-BOSSARD, C.M. (1988). *Die Vegetation des Rhonegletschervorfeldes, ihre Sukzession und naturräumliche Gliederung.* Diss. Bot. Inst. Basel.
[68] SCHWEINGRUBER (1983). *Der Jahrring. Standort, Methodik, Zeit und Klima in der Dendrochronologie.* Paul Haupt, Bern.
[69] STEFANINI, M.C. (2004). *Spatio-temporal analysis of a complex landslide in the Northern Apennines (Italy) by means of dendrochronology.* Geomorphology, 191-202, 63.
[70] STEFANINI, M.C., RIBOLINI, A. (2003). *Dendrogeomorphological investigations of debris-flow occurrence in the Maritime Alps (northwestern Italy).* Debris-flow Hazard Mitigation: Mechanisms, Prediction, and Assesment. Millpress Rotterdam.
[71] STOFFEL, M., PERRET, S. (2006). *Reconstructing past rockfall activity with tree rings: Some methodological considerations.* Dendrochronologica, 1-15, 24.

[72] STOFFEL, M., SCHNEUWLY, D., BOLLSCHWEILER, M., LIEVRE, I., DELALOYE, R., MYINT, M., MONBARON, M. (2005). *Analyzing rockfall activity (1600-2002) in a protection forest – a case study using dendrogeomorphology.* Geomorphology, 224-241, 68.

[73] TAYLOR, R.J. (1993). *Sections on Picea and Tsuga*. Flora of North America Editorial Committee: Flora of North America North of Mexico, 2. Oxford University Press.

[74] TOTLAND, O., GRYTNES, J., HEEGAARD, E. (2004). *Willow canopies and plant community structure along an Alpine environmental gradient.* Arctic, Antarctic, and Alpine Research, 428-435, 36.

[75] VETAAS, O.R. (1994). *Primary succession of plant assemblages on a glacier foreland – Bodalsbreen, Southern Norway.* Journal of Biogeography, 297-308, 3.

[76] VITOUSEK, P.M., WALKER, L.R. (1989). *Biological invasion by Myrica faya in Hawaii: plant demography, nitrogen fixation, ecosystem effects.* Ecological Monographs, 247-265, 59.

[77] WALKER, L.R. (1993). *Nitrogen fixers and species replacements in primary succession.* Primary Succession on Land. Blackwell, Oxford.

[78] WALKER, L.R., CHAPIN, F.S. (1987). *Interactions among processes controlling successional change.* Oikos, 131-135, 59.

Statistics

[79] FAHRMEIR, L., KNEIB, T., LANG, S. (2007). *Regression: Modelle, Methoden und Anwendungen.* Springer Verlag.

[80] GRUBBS, F.E. (1969). *Procedures for detecting outlying observations in samples.* Technometrics, 1-21, 11.

[81] JENKS, G.F. (1967). *The Data Model Concept in Statistical Mapping.* International Yearbook of Cartography, 186-190, 7.

[82] KRUSKAL, W., WALLIS, W.A. (1952). *Use of ranks in one-criterion variance analysis.* Journal of the American Statistical Association, 583-621, 260, 47.

[83] PINNEKAMP, H.J., SIEGMANN, F. (2001). *Deskriptive Statistik* (4th edn). Oldenbourg.

[84] SCHOCH, W., HELLER, I., SCHWEINGRUBER, F.H., KIENAST, F. (2004). *Wood anatomy of Central European species, online version: http://www.woodanatomy.ch/species.php?code=LADE/*

[85] TUKEY, J.W. (1977). *Exploratory Data Analysis*. Addison-Wesley Reading MA.

[86] ZAR, J.H. (1999). *Biostatistical analysis.* Prentice Hall Upper Saddle River N.J.

[87] ZUUR, A., IENO, E.N., WALKER, N., SAVEILIEV, A.A., SMITH, G.M. (2009). *Mixed effects models and extensions in ecology with R.* Springer New York.

Software

[88] ESRI (ENVIRONMENTAL SYSTEMS RESEARCH INSTITUTE) (2009). *ArcGIS (Version 9.3)* [Software].

[89] GOOGLE INC. (2009). *Google Earth (Version 5.2)* [Software]. Available from: http://earth.google.com/

[90] R DEVELOPMENT CORE TEAM (2010). R. *A language and environment for statistical computing (Version 2.11.1)* [Software]. R Foundation for Statistical Computing, Wien. Available from: http://www.r-project.org/

10 Appendixes

Appendix A. Map of Switzerland.

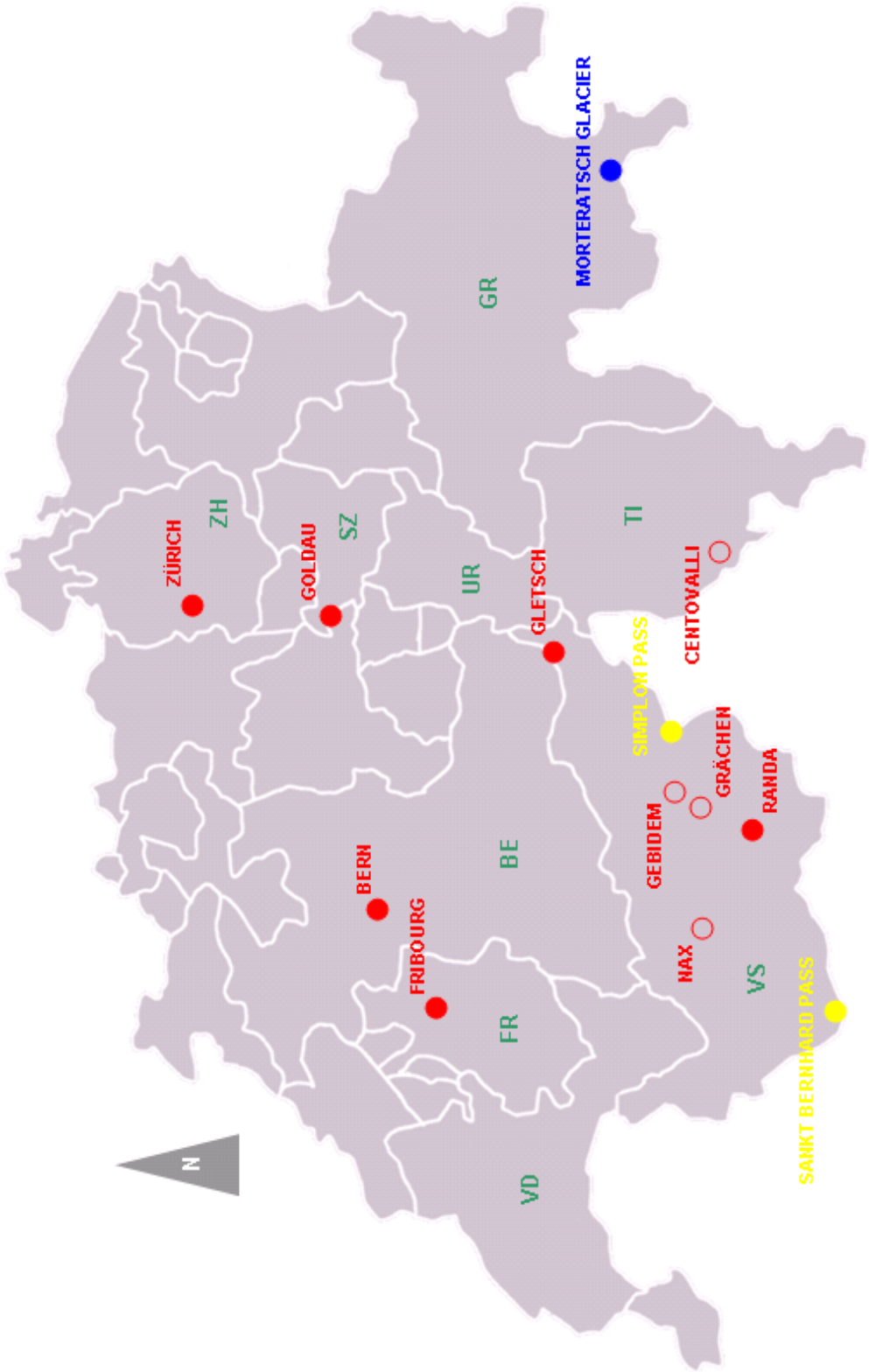

Fig A1. Map showing locations mentioned in this study. Official canton abbreviations (green) are: Vaud (VD), Fribourg (FR), Valais (VS), Berne (BE), ZH (Zurich), Tessin (TI), Schwyz (SZ), Uri (UR), Graubünden (GR) *(Modified from Wikipedia, 2005)*.

Appendix B. SOIUSA classification according to Marazzi (2005).

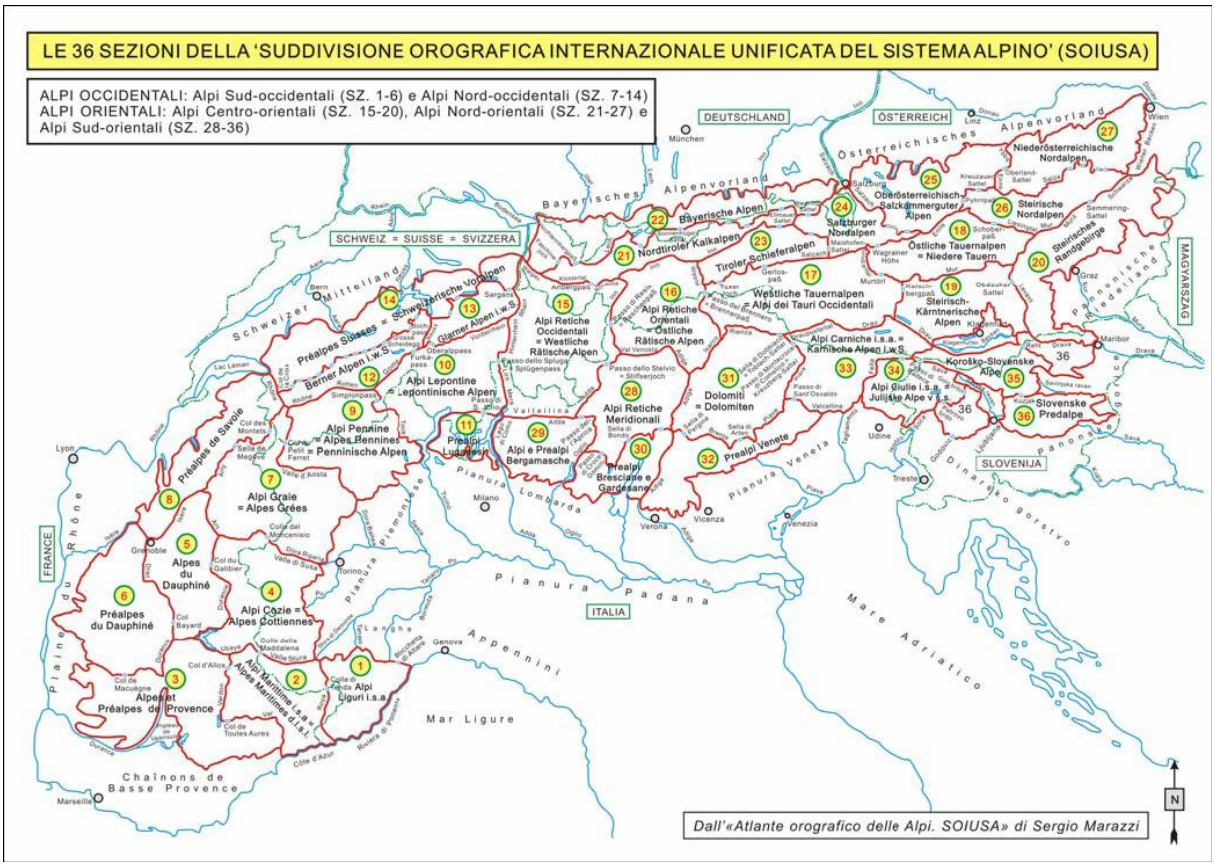

Fig B1. Map representing the SOIUSA classification. The Valais is situated in the Pennine (number 9), Lepontine (number 10), and Bernese Alps (number 12) *(Marazzi, 2005)*.

Appendix C. Satellite image of the Visper Valleys.

Fig C1. Satellite image showing the Rhone Valley in the north, where Visp is marked, and the Visper Valley branching of to the south. The Visper Valley splits in two near Stalden: the eastern Saaser Valley and the western Matter Valley. The white arrow points toward the rockslide deposit. The red arrow indicates north. The yellow line marks the border of Switzerland and Italy *(Google Earth, 2010)*.

Appendix D. Natural hazards in the Matter Valley.

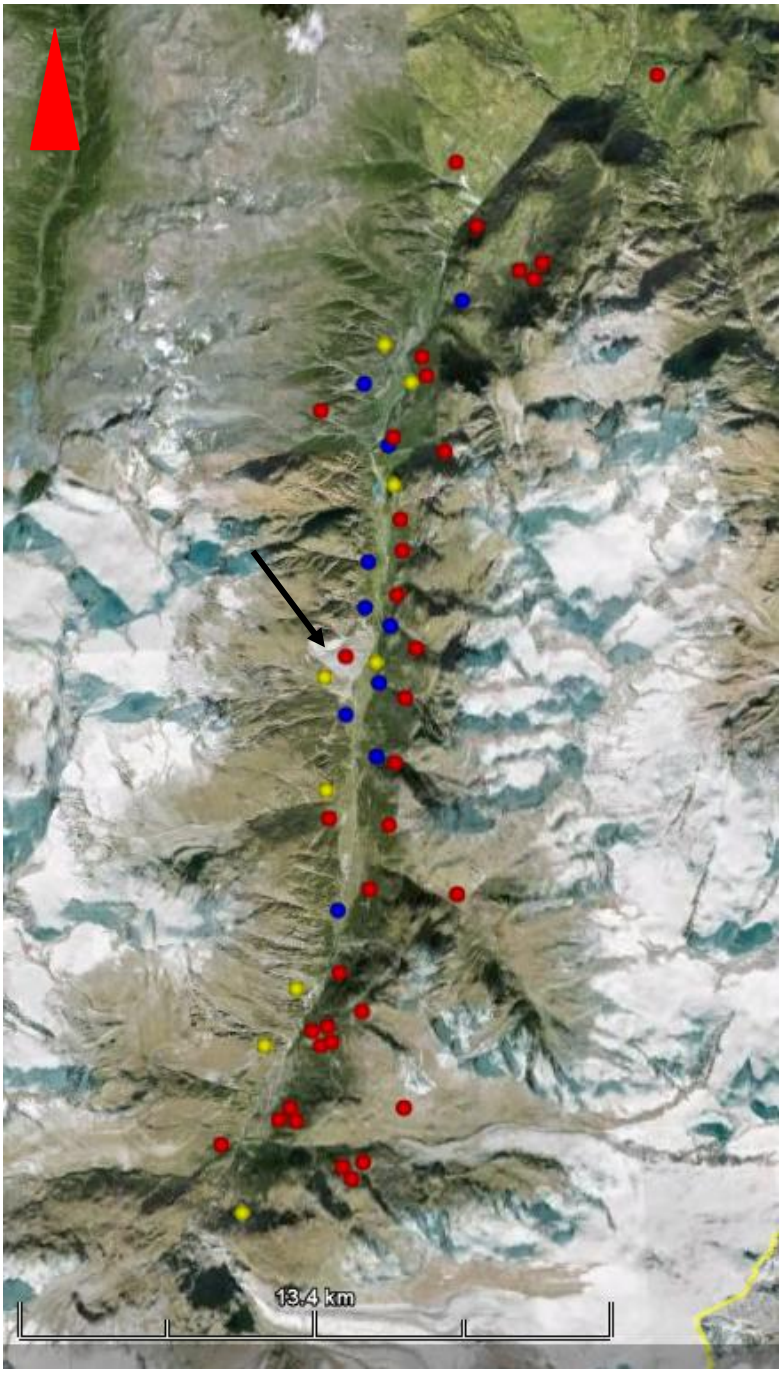

Fig D1. Satellite image showing the Matter Valley. Marked are numerous rockslide deposits (red dots), debris flow deposits (blue dots), and a limited selection of rock fall sites (yellow dots). The yellow line marks the border of Switzerland and Italy. The red arrow indicates north. The black arrow points towards the Randa rockslide deposit *(Google Earth, 2010)*.

Appendix E. Saggings.

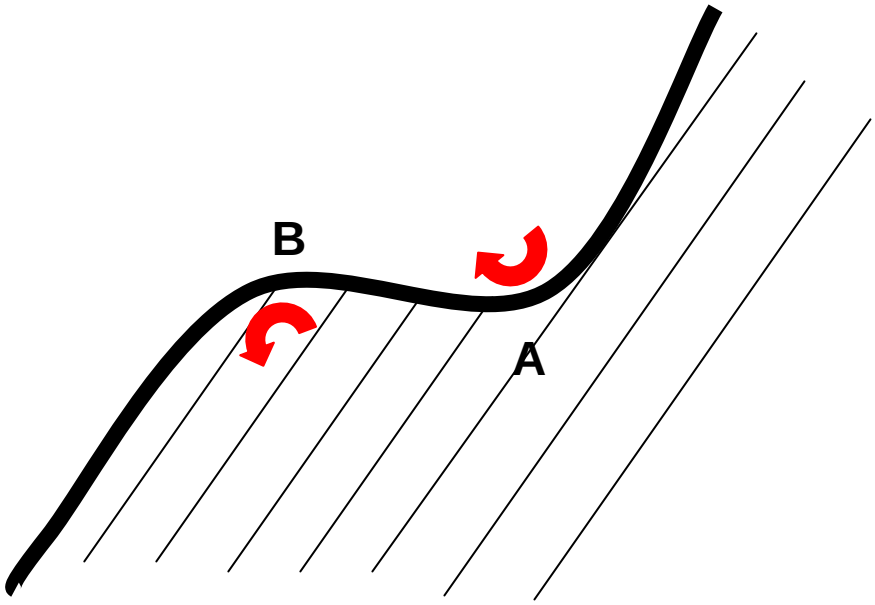

Fig E1. Simplified image of a sagging in cross section. The black line shows the surface of the slope, that is characterised by a depression (A) in the upper regions and an elevation in the lower regions (B). The rocks undergo partial rotations around two parallel axes (that are orientated perpendicular to the cross section) as is pointed out by the red arrows *(LVdB)*.

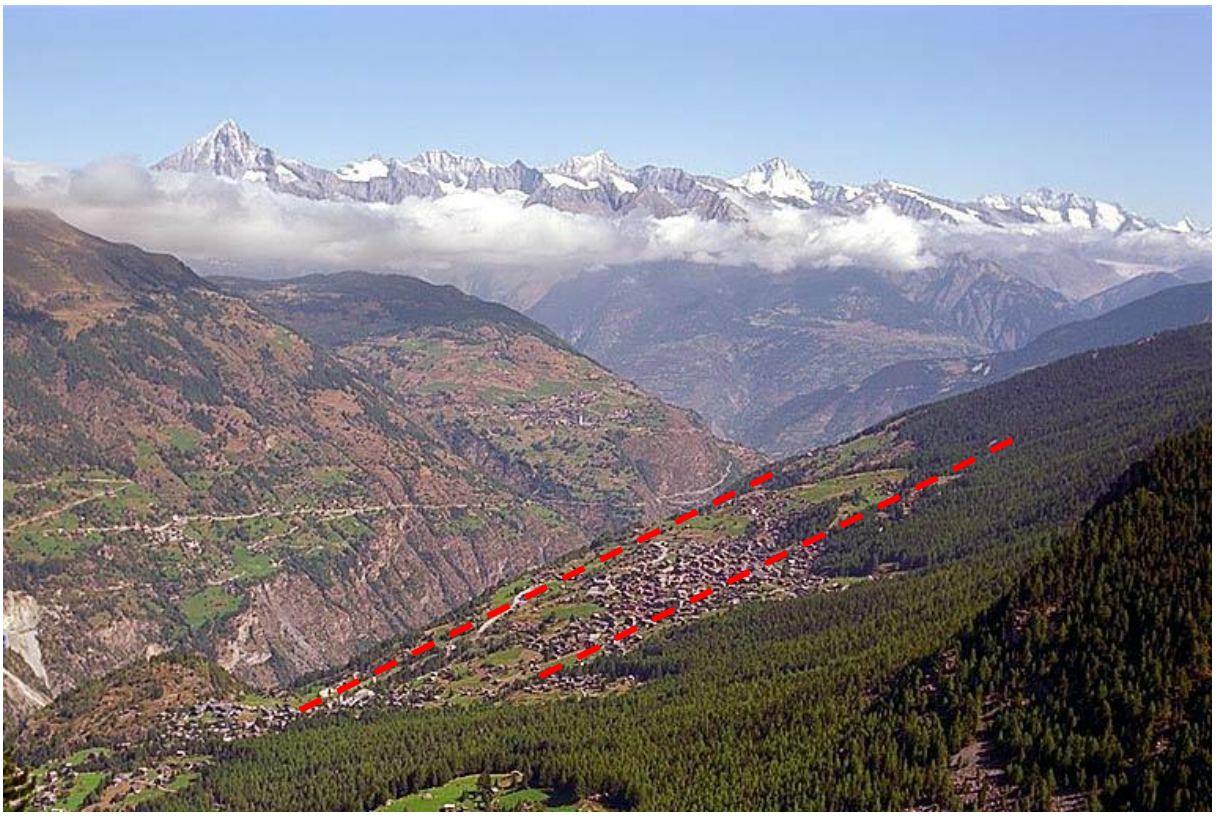

Fig E2. The mountain village of Grächen (Valais, see also Appendix A, p.96) lies in a zone of sagging. The two rotational axes (also marked in Fig E1) are stapled and marked in red *(LVdB)*.

Appendix F. Geological map of Switzerland after Labhart (1992).

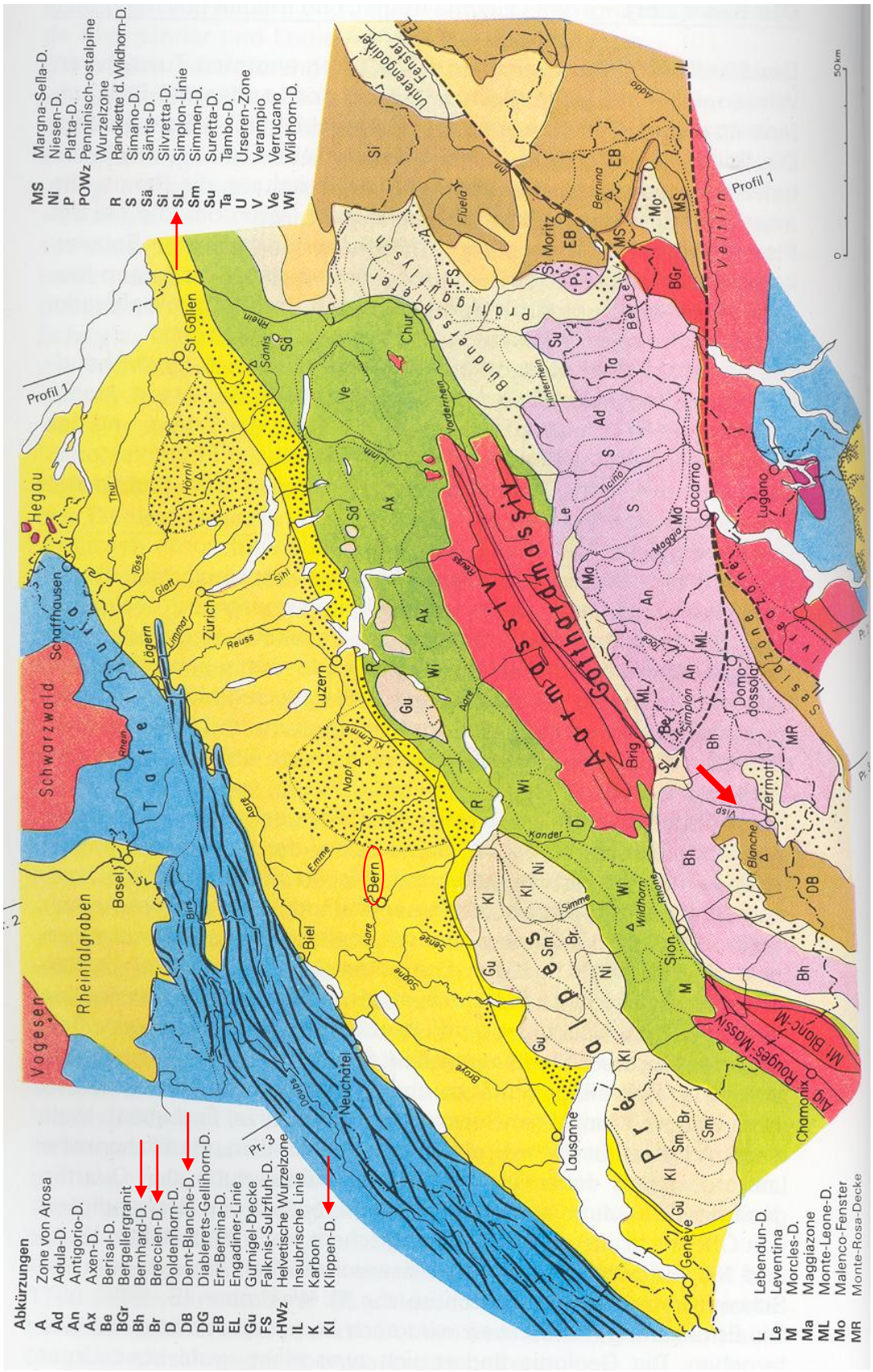

Fig F1. The geological map op Switzerland, the legend lists the different nappes and massifs. The black arrow indicates north. The narrow red arrows mark those mentioned in this study. Bern is circled in red, and Randa is marked with a fat red arrow *(Labhart, 1992)*.

Appendix G. Penninic Palaeogeography.

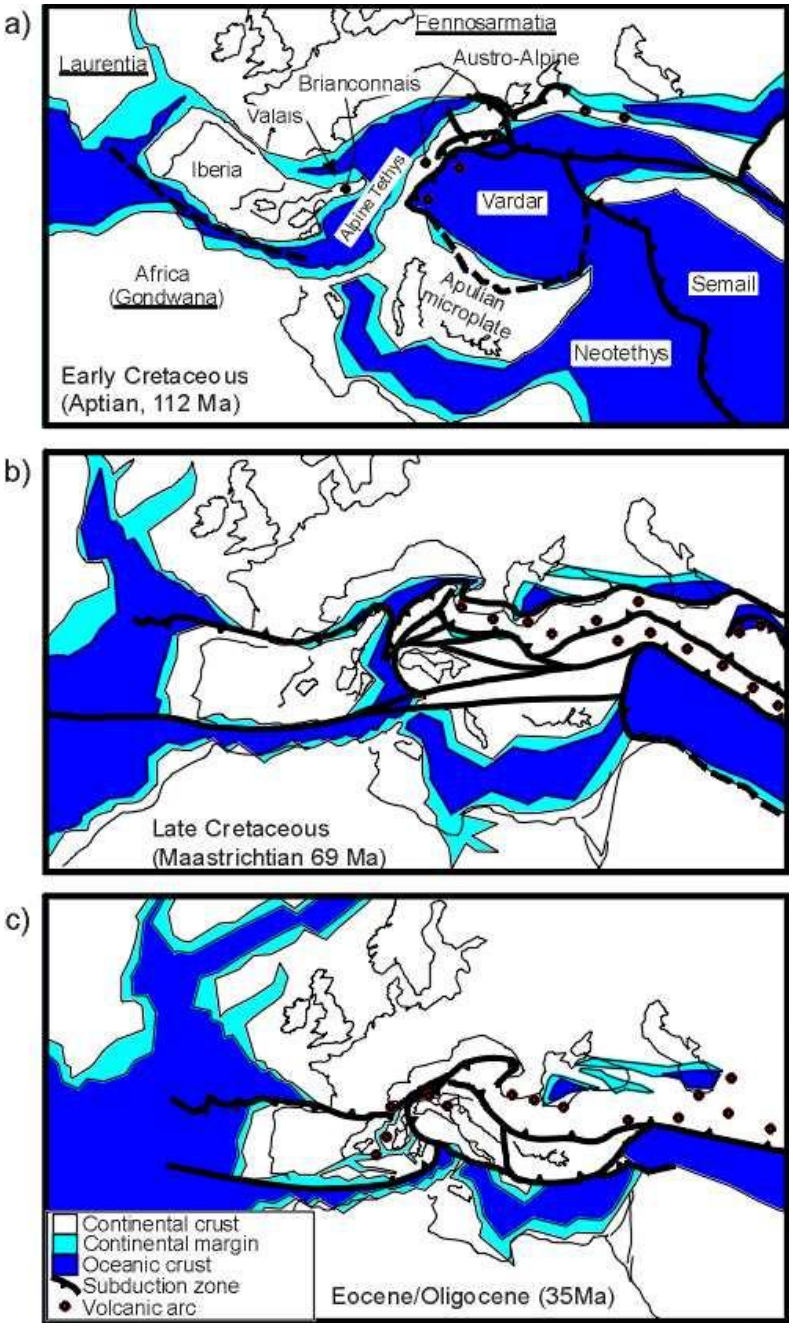

Fig G1. Plate-tectonic reconstructions at 112, 69 and 35 Ma for the Alpine realm showing interpreted locations of microplates, ocean basins, subduction zones and volcanic arcs (Stampfli et al., 1998).

Appendix H. 1991 Randa rockslide event in images. All pictures are published with the courtesy of Lina Summermatter.

Fig H1. Second event on 9.5.1991.

Fig H2. Second event on 9.5.1991.

Fig H3. Second event on 9.5.1991.

Fig H4. Second event on 9.5.1991.

Fig H5. Second event on 9.5.1991.

Fig H6. Second event on 9.5.1991.

Fig H7. Second event on 9.5.1991.

Fig H8. Second event on 9.5.1991.

Fig H9. Second event on 9.5.1991.

Fig H10. Second event on 9.5.1991.

Fig H11. Second event on 9.5.1991.

Fig H12. Second event on 9.5.1991.

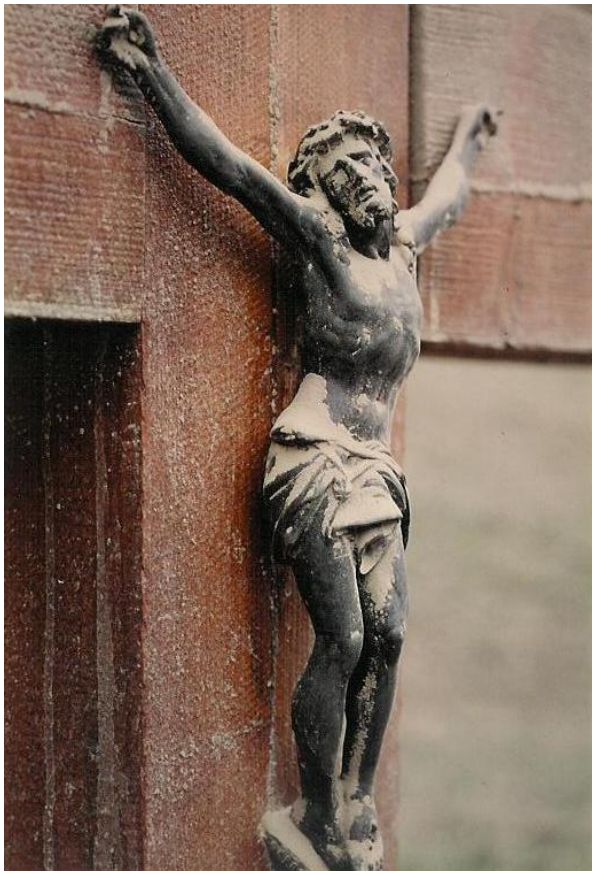

Fig H13. Cross covered in dust.

Fig H14. A farmer crossing his meadow where the cattle could no longer graze due to the thick dust layer.

Fig H15. A car covered in dust.

Fig H16. A door lock covered in dust.

Fig H17. Villagers cleaning the streets.

Fig H18. Sign pointing toward the hamlet of Lärch, that disappeared under the deposit.

Fig H19. Dust on the valley road.

Fig H20. Stables covered in dust.

Fig H21. Meadows covered in dust.

Fig H22. The deposit destroyed the railway track and dammed the Vispa river.

Fig H23. The fresh deposit after the second event.

Fig H24. The railway covered with debris and dust.

Fig H25. The second event destroyed the railway and some chalets.

Fig H26. The meadows bordering on the deposit. Up to 50 cm of dust were measured.

Fig H27. The rock face after the second event. Anew the springs are activated.

Fig H28. After the second event the Vispa river was dammed for weeks. A lake formed and the water level increased rapidly.

Fig H29. Some chalets completely disappeared under the surface of the Vispa lake.

Fig H30. Streets and railway trail are flooded. At the background we see the rockslide deposit.

Fig H31. The Swiss army organised the evacuation of the flooded village.

Appendix I. Permafrost map of Switzerland.

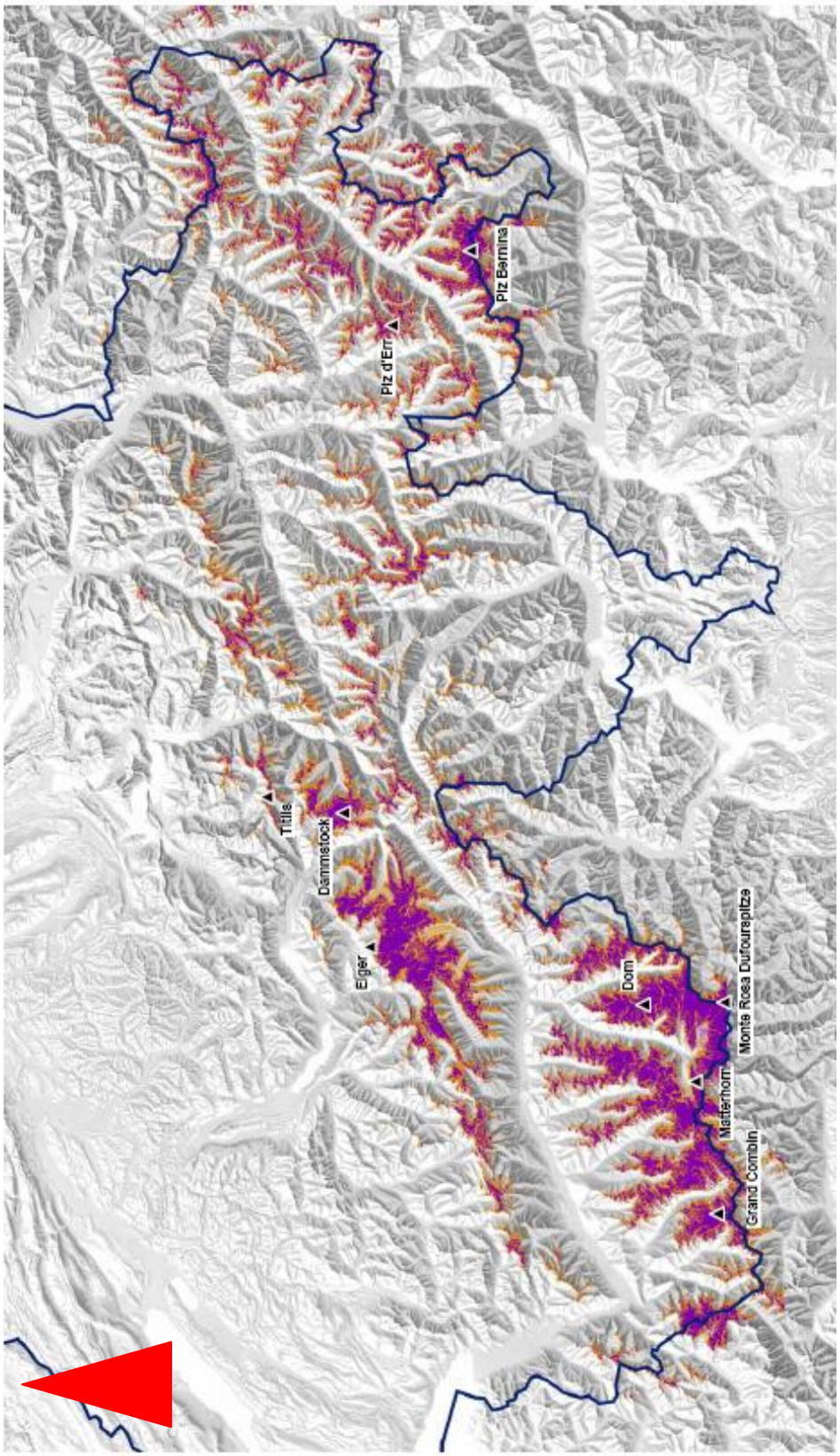

Fig I1. Permafrost map of Switzerland. Areas with a chance of local permafrost are marked yellow, areas where large permafrost zones are highly likely are marked purple. The red arrow indicates north *(Bundesamt für Umwelt, 2010)*.

Appendix J. Research of the *ETHZ* in Randa.

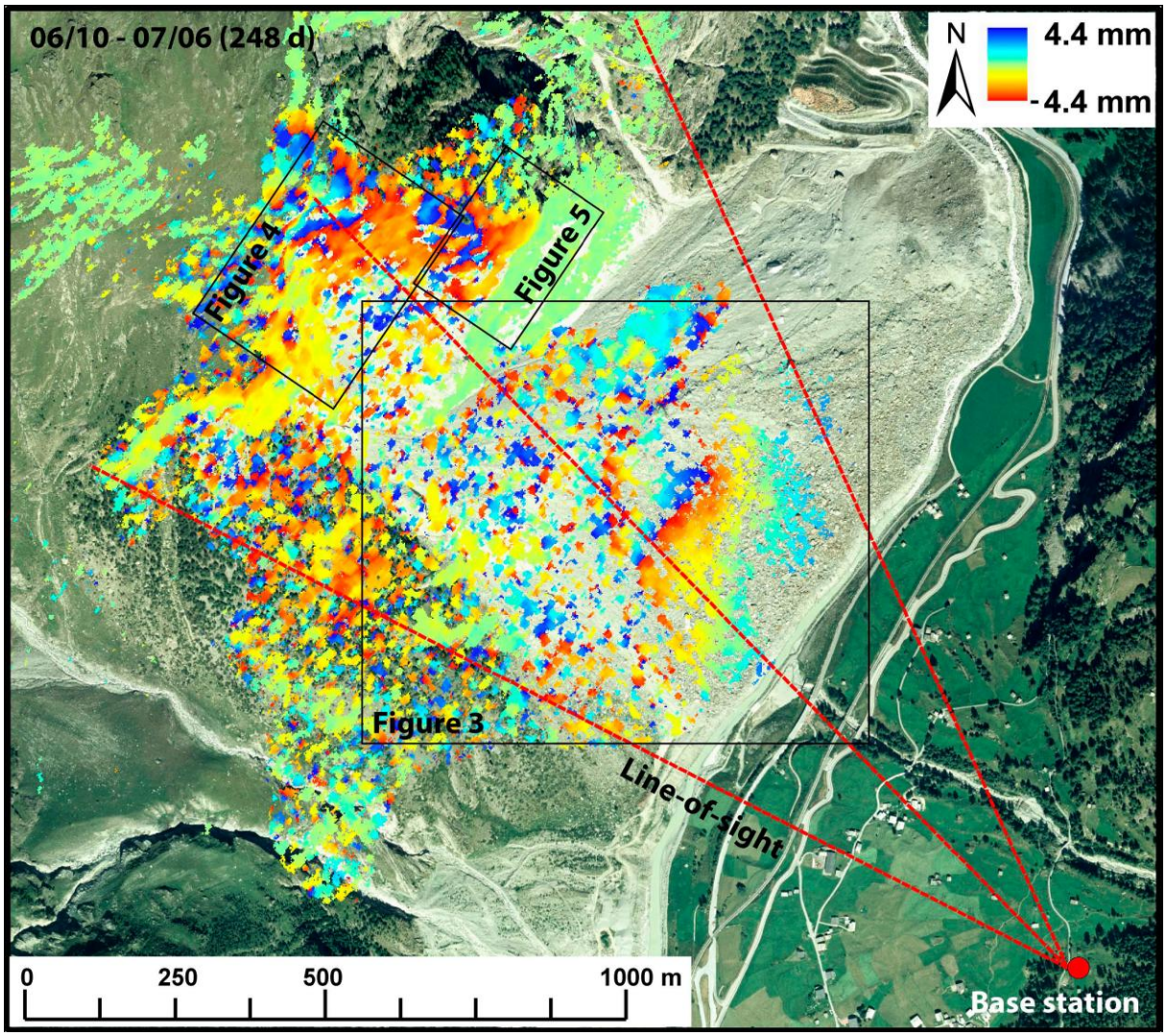

Fig J1. GB-DInSAR monitoring of the rock scarp in Randa. Shown in red are the lines-of-sight and location of the base-station on the opposite valley flank. A GB-DInSAR displacement map is based on two surveys within 248 days. The colour scale shows the displacement rates of individual rock masses, where negative values imply that the masses move towards the base station *(Gischig et al., 2009).*

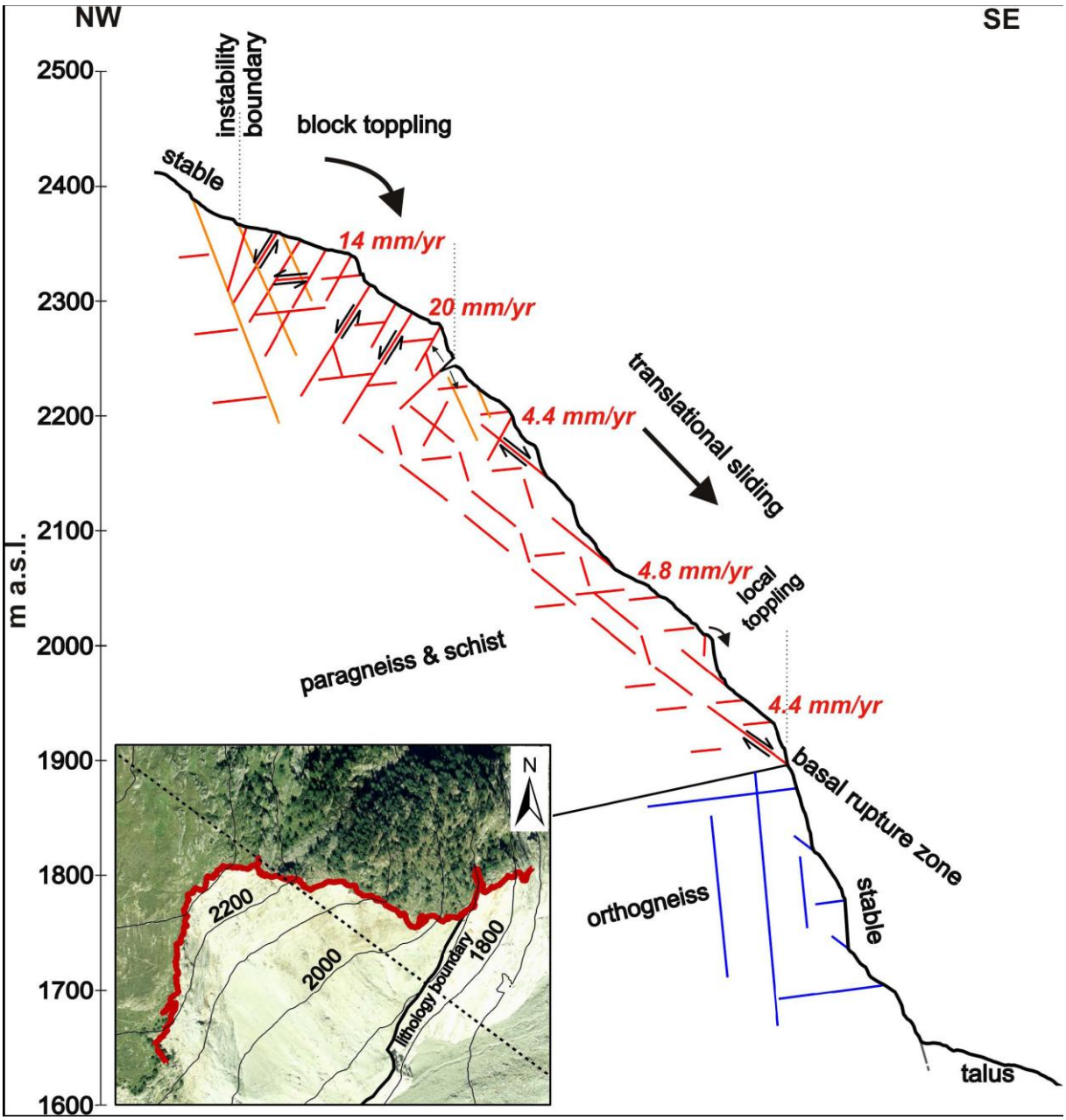

Fig J2. Conceptual 2D kinematic model of the instability. Both the results from Willenberg et al. (2008b) and from Gischig et al. (2009) are included. The velocities indicated are the displacement rates derived from GB-DInSAR *(Gischig et al., 2009).*

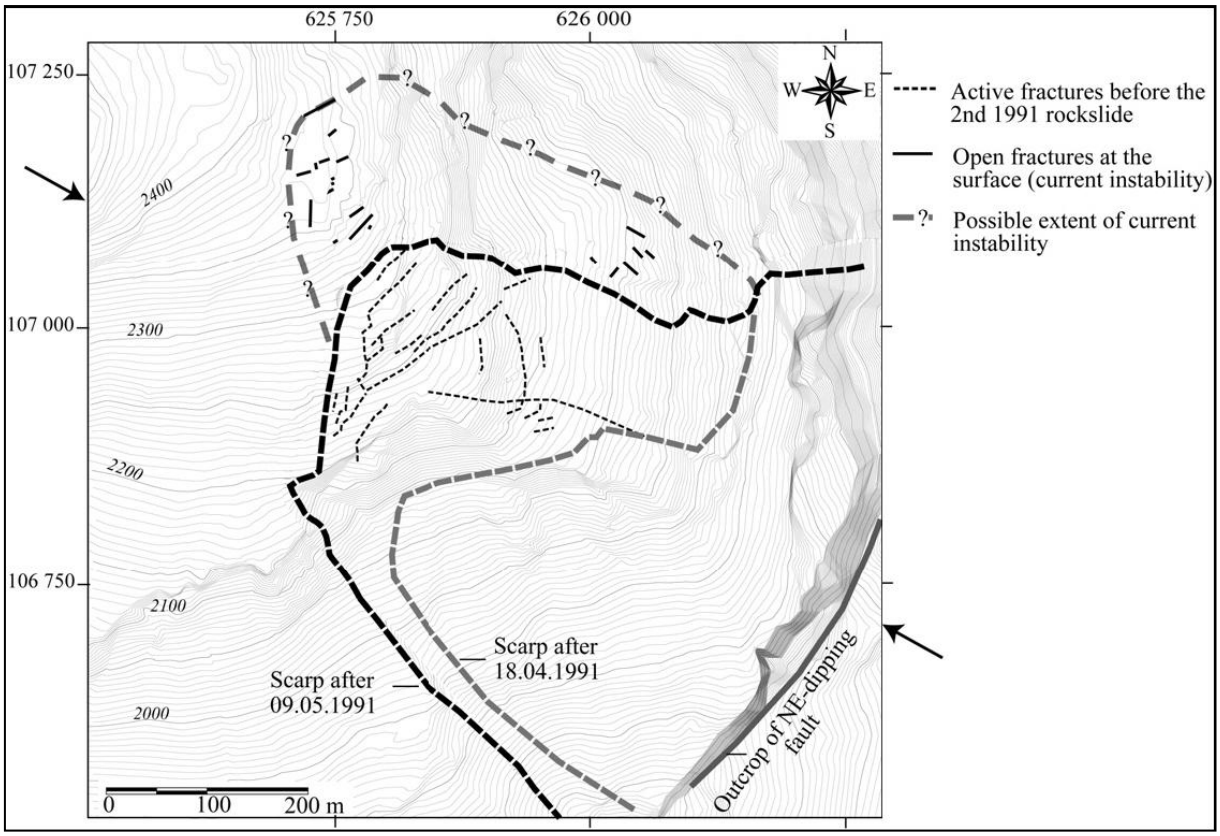

Fig J3. Topographic map of the project area before the 1991 rockslides. The tops of the scarps of the two main rockslide events (April 18 and May 9,1991) are indicated. The thin dotted lines are surface fractures that were seen to be active between the first and second rockslide events. The thin solid lines denote open surface fractures on the currently moving rock mass to the north and northwest of the rockslide scarp. The extent of the current instability NW of the 1991 rockslide scarp is based on geodetic monitoring data. The NE-dipping fault indicated close to the valley floor is proposed to have acted as a basal sliding surface for the first 1991 rockslide event *(Willenberg et al., 2008a)*.

Appendix K. Results of Gasser (1995).

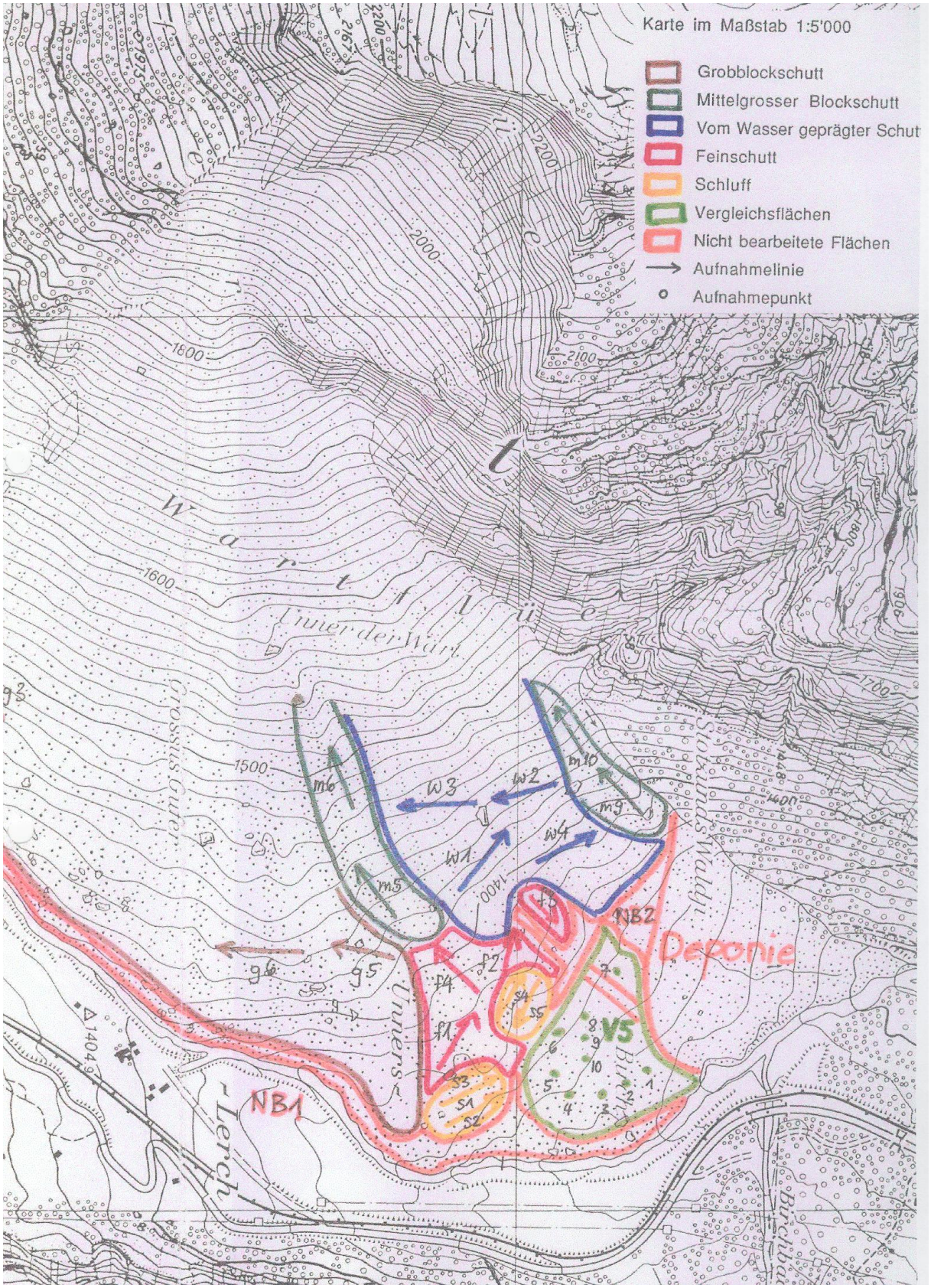

Fig K1. Substratum according to Gasser (1995) *(Gasser, 1995)*.

Gesamtartenliste Grober Blockschutt

MONOCOTYLEDONES

Gramineae
Agrostis rupestris
Agrostis cf. stonolifera
Agrostis tenuis
Calamagrostis arundinacea
Festuca violacea
cf. Festuca rubra
Poa alpina
Poa cf. supina
Poa trivialis
Trisetum distichophyllum

DICOTYLEDONES

Achillea millefolium
Alyssum calycinum
Arabis glabra
cf. Arenaria verna
Artemisia absinthium
Biscutella levigata
Campanula rotundifolia
Carduus defloratus
Cardamine resedifolia
Cerastium strictum
Epilobium angustifolium
Epilobium fleischeri
Epilobium nutans
Erigeron acer
Filago cf. Arvensis (minima?)
Gypsophila repens
cf. Hieracium murorum
Linaria alpina
Saxifraga aizoides
Saxifraga aspera
Saxifraga bryoides
Saxifraga macropetala
Saxifraga oppositifolia
Saxifraga paniculata
Sedum album
Sedum atratum
Sedum dasyphyllum
Sempervivum arachnoideum
cf. Senecio
cf. Silene otites
Taraxacum cf. officinale
Thymus serpyllum
Tussilago farfara
Urtica dioeca
Verbascum lychnitis

<90>
<92> (Cruciferae)

Papilionaceae
Trifolium pratense
Trifolium cf. thalii

Holzgewächse
Betula pendula
Larix decidua
Picea excelsa
Salix sp. I
Salix sp. II (Alnus viridis?)

Fig K2. Species Gasser (1995) found in the “Large blocks”. Marked in red are those of relevance for this study *(Gasser, 1995)*.

Gesamtartenliste Mittelgrosser Blockschutt

MONOCOTYLEDONES

Gramineae
Agrostis rupestris
Agrostis tenuis
Agrostis stonolifera
Anthoxanthum cf. alpinum
Bromus cf. inermis
Bromus tectorum
Calamagrostis varia
Cynosurus cristatus
Dactylis glomerata
Festuca amethystina
Festuca pumila
Festuca rubra
Festuca violacea
Festuca sp.
Helictotrychon versicolor
Koeleria pyramidata
Lolium perenne
Poa alpina
Poa annua
Poa bulbosa
Poa cf. laxa
Poa minor
Poa pratensis
Poa sp.
Trisetum distichophyllum

Juncaceae
Luzula spicata

DICOTYLEDONES

Achillea millefolium
Alyssum calycinum
Arabidopsis thaliana
Arabis alpina
Arabis corymbiflora
Arabis hirsuta
Arenaria multicaulis
Arenaria serpyllifolia
Artemisia absinthium
Artemisia campestris
Artemisia mutellina
Biscutella levigata
Campanula cochleariifolia
cf. Carlina acaulis
Cerastium pedunculatum
Cerastium cf. trigynum
Cerastium strictum
Cerastium sp.
Cirsium cf. eriophorum
Epilobium angustifolium
Epilobium cf. collinum
Epilobium fleischeri
Erigeron alpinus
Erigeron cf. canadensis
Erigeron uniflorus
cf. Filago
Galium cf. pumilum
Gypsophila repens
Herniaria alpina
Herniaria glabra
Hieracium auricula
Hieracium pilosella
Hieracium staticifolium
Hieracium velutinum
Hieracium sp.
Linaria alpina
Minuartia cf. sedoides
Minuartia verna
Moehringia ciliata
Myosotis alpestris
Plantago lanceolata
cf. Ranunculus
Rumex scutatus
Satureja alpina
Saxifraga aizoides
Saxifraga aizoon
Saxifraga cf. oppositifolia
Scabiosa columbaria
Sedum album
Sedum atratum
Sedum dasyphyllum
Sedum rupestre
Silene otites
Silene rupestris
Spergula arvensis
Stachys recta
Taraxacum officinale
cf. Taraxacum
Teucrium montanum
Thymus serpyllum
Verbascum lychnitis
Veronica fruticans
Viola odorata
<25>
<31> Erigeron?
<35>

Papilionaceae
Anthyllis sp.
Astragalus penduliflorus
Lotus pilosus
Trifolium montanum
Trifolium cf. thalii

Holzgewächse
Betula pendula
Larix decidua
Picea excelsa
Rubus idaeus
Salix cf. nigricans
Salix sp.
cf. Sambucus nigra
Solanum dulcamare

PTERIDOPHYTA

Sp. (Farn)

Fig K3. Species Gasser (1995) found in the “Smaller blocks”. Marked in red are those of relevance for this study *(Gasser, 1995)*.

Gesamtartenliste Feinschutt

MONOCOTYLEDONES

Gramineae

Agrostis rupestris
Agrostis stonolifera
Agrostis tenuis
Agrostis sp.
Bromus tectorum
Dactylis glomerata
Deschampsia caespitosa
Festuca amethystina
Festuca arundinacea
Festuca rubra
Festuca sp.
Festuca violacea
Koeleria pyramidata
Phleum alpinum
Phleum hirsutum
Poa alpina
Poa annua
Poa bulbosa
Poa cf. laxa
Poa minor
Poa pratensis
Poa supina
Poa trivialis
Poa sp.
Sesleria disticha
Trisetum distichophyllum
<123>
<130>

DICOTYLEDONES

Achillea millefolium
Alyssum calycinum
Arabis corymbiflora
Arabis glabra
Arabis hirsuta
Artemisia absithium
Artemisia campestris
Cardamine resedifolia
Carduus defloratus
Cerastium strictum
cf. Draba
Epilobium angustifolium
Epilobium cf. collinum
Epilobium fleischeri
Erysimum helveticum
Gypsophila repens
Herniaria glabra
Hieracium murorum
Linaria alpina
Minuartia verna
Rorippa pyrenaica
Rumex scutatus
Saxifraga aizoides
Saxifraga cf. biflora
Saxifraga bryoides
Sedum album
Sedum atratum
Sedum dasyphyllum
Sedum rupestre
Sedum sp.
Silene nutans
Silene rupestris
cf. Taraxacum officinale
Thymus serpyllum
Tussilago farfara
Verbascum crassifolium
Verbascum lychnitis
<128>

Papilionaceae

Trifolium cf. thalii

Holzgewächse

Betula pendula
Larix decidua
Picea excelsa
Salix foetida
Salix sp.

Fig K4. Species Gasser (1995) found in the “Fine-grained debris”. Marked in red are those of relevance for this study *(Gasser, 1995)*.

Gesamtartenliste Vom Wasser geprägter Schutt

MONOCOTYLEDONES

Gramineae
Agrostis stonolifera
Agrostis tenuis
Calamagrostis arundinacea
Dactylis glomerata
Deschampsia caespitosa
Festuca rubra
Festuca violacea
Festuca sp.
Phleum alpinum
Phleum hirsutum
Poa alpina
Poa concinna
<108>

DICOTYLEDONES

Achillea millefolium
Achillea nana
Alyssum calycinum
Arabis corymbiflora
Arabis glabra
cf. Arenaria biflora
Arenaria serpyllifolia
Artemisia absinthium
Artemisia mutellina
Carlina vulgaris
Cerastium strictum
Dianthus carthusianorum
Draba sp.
Epilobium angustifolium
Epilobium fleischeri
Erigeron cf. canadensis
cf. Erigeron neglectus
Gypsophila repens
Herniaria alpina
Linaria alpina
Minuartia verna
Petasites paradoxus
Rumex scutatus
Sagina glabra / Linnaei
Saxifraga aizoides
Saxifraga bryoides
Saxifraga oppositifolia
Taraxacum officinale
Thymus serpyllum
cf. Tussilago farfara
Verbascum lychnitis

Holzgewächse
Acer Pseudoplatanus
cf. Alnus
Betula pendula
Larix decidua
Picea excelsa
Salix cf. nigricans
Salix sp.

Fig K5. Species Gasser (1995) found in the “Water-influenced debris”. Marked in red are those of relevance for this study *(Gasser, 1995).*

Gesamtartenliste Schluff

MONOCOTYLEDONES

Gramineae
Agrostis tenuis
Agrostis sp.
cf. Calamagrostis arundinacea
Calamagrostis varia
Dactylis glomerata
Festuca amethystina
Festuca rubra
Festuca cf. vallesiaca
Festuca violacea
Festuca sp.
Lolium multiflorum
Phleum alpinum
Phleum hirsutum
Poa alpina
Poa annua
Poa pratensis
Poa trivialis
Trisetum distichophyllum

DICOTYLEDONES

Alyssum calycinum
Arabis alpina
Arabis corymbiflora
Arabis hirsuta
cf. Arenaria verna
Artemisia cf. campestris
Artemisia mutellina
cf. Biscutella levigata
Cardamine resedifolia
Cerastium brachypetalum
Cerastium strictum
Dianthus Carthusianorum
Epilobium angustifolium
Epilobium fleischeri
Erysimum helveticum
Euphrasia minima
Gypsophila repens
Herniaria glabra
Hieracium staticifolium
Linaria alpina
Minuartia laricifolia
Minuartia verna
Rumex scutatus
Saxifrage aizoides
Saxifrage cf. aspera
Saxifraga bryoides
Saxifraga oppositifolia
Sedum album
Sedum atratum
Sedum rupestre
Silene nutans
Silene vallesia
Taraxacum cf. officinale

Papilionaceae
Trifolium repens
Trifolium cf. thalii

Holzgewächse
Acer Pseudoplatanus
Betula pendula
Larix decidua
Picea excelsa
Rubus idaeus
Salix cf. nigricans

Fig K6. Species Gasser (1995) found in the “Silt”. Marked in red are those of relevance for this study *(Gasser, 1995)*.

Appendix L. Plot map.

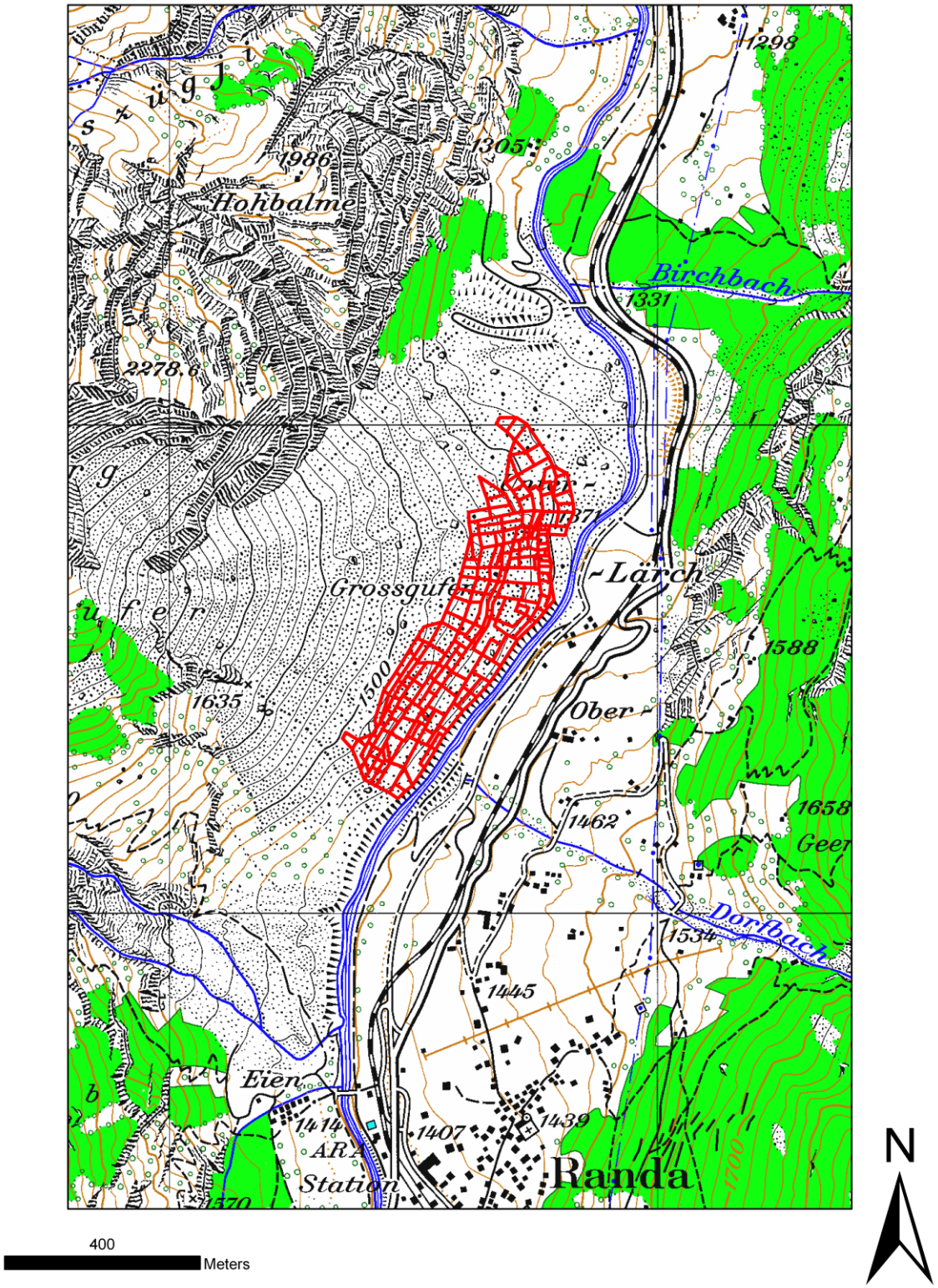

Fig L1. Map of the Randa region. Plots in the surveyed area are marked red *(ArcGIS, 2010)*.

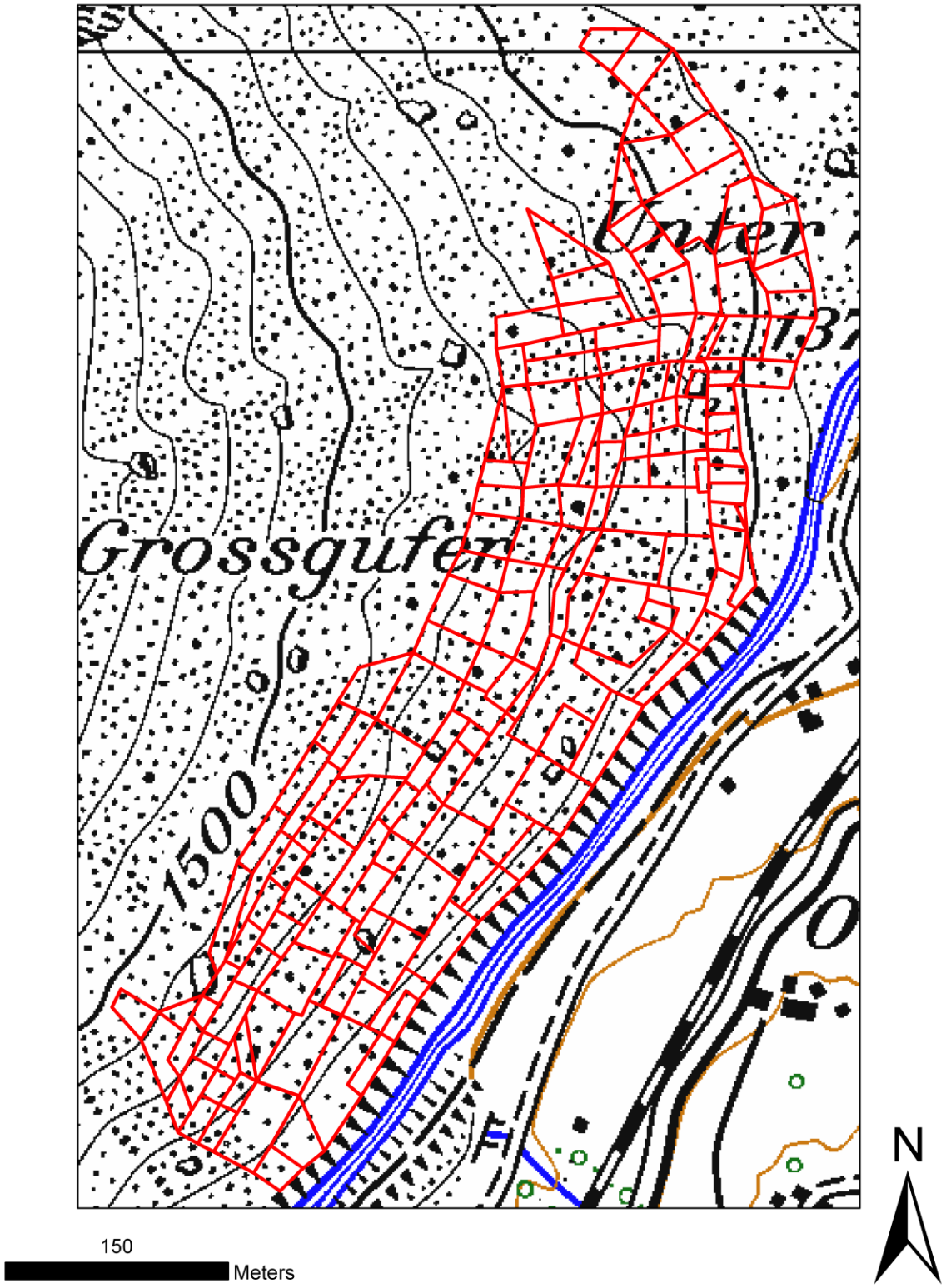

Fig L2. Map of the surveyed area. Plots are marked red *(ArcGIS, 2010)*.

Appendix M. Method schematic.

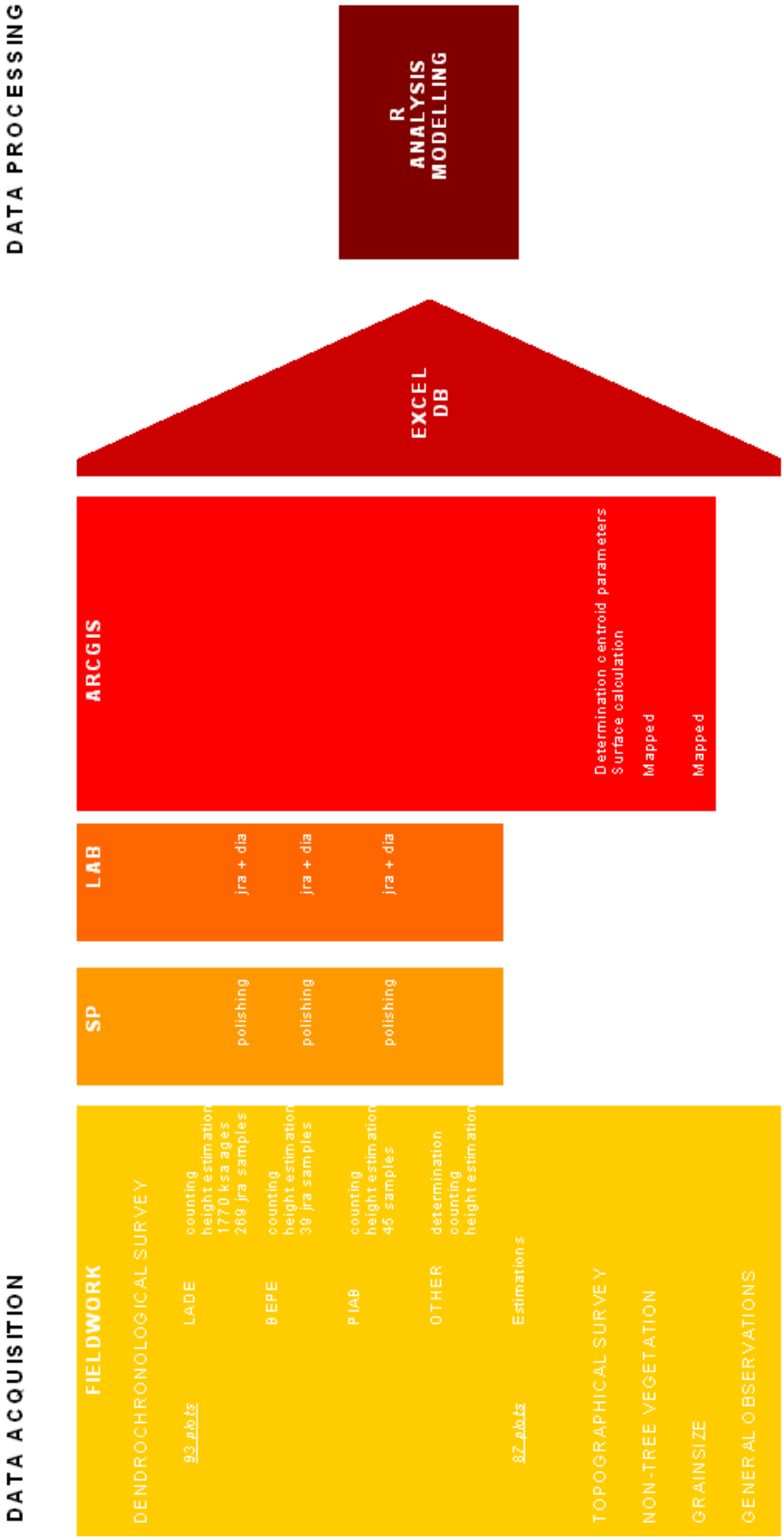

Fig M1. Schematic representation of the working procedure. Used abbreviations: growth-ring determined age (jra), bud-scale scar determined age (ksa), sample preparation (sp), and diameter (dia).

Appendix N. Deposit seen from Chüebodmen.

Fig N1. The rockslide deposit seen from Chüebodmen on the eastern flank of the Matter Valley *(LVdB)*.

Fig N2. The rockslide deposit seen from Chüebodmen on the eastern flank of the Matter Valley *(LVdB)*.

Appendix O. Aspect map.

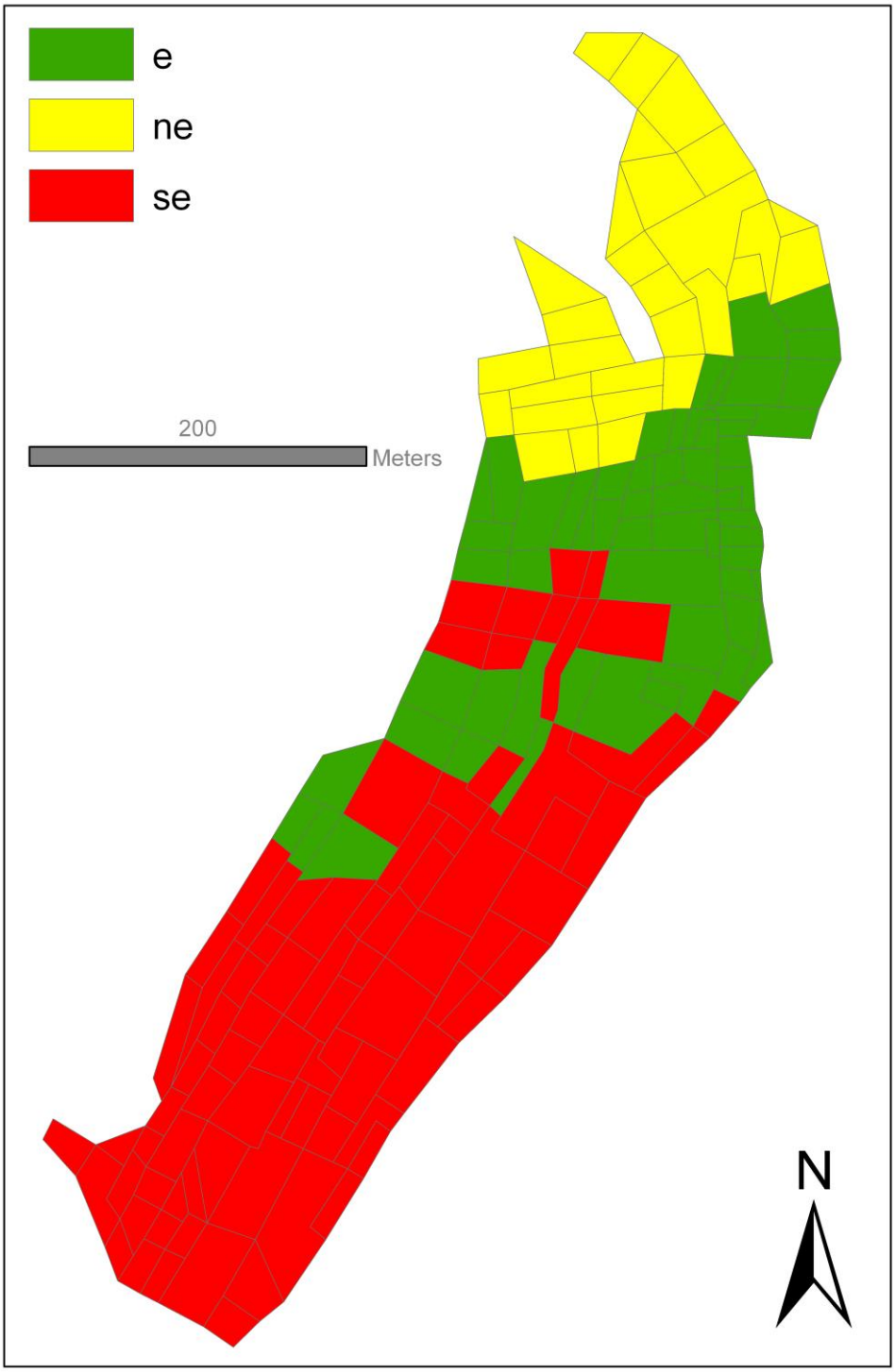

Fig O1. Map showing the aspect per plot: east-facing (e), northeast-facing (ne), and southeast-facing *(ArcGIS, 2010).*